



**Michigan
Technological
University**

Michigan Technological University
Digital Commons @ Michigan Tech

Dissertations, Master's Theses and Master's Reports

2018

Development of Open Source Software and Hardware Tool-Chains for Novel Electronics

Shane Oberloier

Michigan Technological University, swoberlo@mtu.edu

Copyright 2018 Shane Oberloier

Recommended Citation

Oberloier, Shane, "Development of Open Source Software and Hardware Tool-Chains for Novel Electronics", Open Access Master's Thesis, Michigan Technological University, 2018.
<https://digitalcommons.mtu.edu/etdr/675>

Follow this and additional works at: <https://digitalcommons.mtu.edu/etdr>



Part of the [Electrical and Electronics Commons](#)

DEVELOPMENT OF OPEN SOURCE SOFTWARE AND HARDWARE TOOL-
CHAINS FOR NOVEL ELECTRONICS

By

Shane Oberloier

A THESIS

Submitted in partial fulfillment of the requirements for the degree of

MASTER OF SCIENCE

In Electrical Engineering

MICHIGAN TECHNOLOGICAL UNIVERSITY

2018

© 2018 Shane Oberloier

This thesis has been approved in partial fulfillment of the requirements for the Degree of
MASTER OF SCIENCE in Electrical Engineering.

Department of Electrical and Computer Engineering

Thesis Advisor: *Dr. Joshua Pearce*

Committee Member: *Dr. Roger Kieckhafer*

Committee Member: *Dr. Timothy Havens*

Department Chair: *Dr. Daniel Fuhrmann*

Table of Contents

List of figures	4
Preface.....	7
Acknowledgements	8
Abstract	9
1 Introduction.....	10
1.1 Thesis Outline & Motivation.....	10
1.2 References	11
2 General Design Procedure for Free and Open Source Hardware for Scientific Equipment	12
2.1 Abstract	12
2.2 Introduction	12
2.3 Materials and Methods	13
2.3.1 Generalized Procedure	13
2.3.2 Details of Each Procedure Step.....	14
2.3.2.1 Literature review & Proof of concept	14
2.3.2.2 Use of only Free and Open Source Tool Chain	14
2.3.2.3 Minimize complexity	15
2.3.2.4 Minimize material consumption	15
2.3.2.5 Maximize components that can be digitally distributed manufactured	15
2.3.2.6 Create parametric designs	16
2.3.2.7 Off-the-shelf parts	16
2.3.2.8 Validation.....	16
2.3.2.9 Proper documentation	16
2.3.2.10 Share aggressively	17
2.3.3 Case Study: Slide dryer.....	17
2.4 Results and Discussion.....	22
2.4.1 Techno-Economic Comparisons	25
2.4.2 Future Work	27
2.5 Conclusions	27
2.6 References	28
3 Belt Driven Open Source Circuit Mill Using Low Cost 3-D Printer Components ..	34
3.1 Abstract	34

3.2	Introduction	34
3.3	Methods	36
3.3.1	Construction	36
3.3.1.1	D3D Design System	36
3.3.1.2	Custom Adaptions	37
3.3.2	Software – Copper Carve	38
3.3.2.1	Backlash Compensation	39
3.3.2.2	Substrate Distortion Compensation	40
3.3.2.3	Usage of Timers	43
3.3.2.4	Usage of Timers	43
3.3.3	Mill Usage Workflow	43
3.3.3.1	Board Design	43
3.3.3.2	FlatCAM	44
3.3.4	Validation	44
3.3.4.1	Positional Accuracy	44
3.3.4.2	Feature Accuracy	45
3.3.4.3	Distortion Compensation Validation	45
3.4	Results	46
3.4.1	Overall Designs	46
3.4.2	Positional Accuracy	46
3.4.3	Quality of Mill Cut	47
3.4.4	Feature Accuracy	48
3.4.5	Distortion Compensation	50
3.5	Discussion	52
3.5.1	Open Source as Development Platform	52
3.5.2	D3D and Other Applications	52
3.5.3	Software Philosophy	52
3.5.4	Market Comparison	53
3.5.5	Additional Applications & Future Work	54
3.6	Conclusions	54
3.7	References	55
4	Open Source Low-Cost Power Monitoring System	59
4.1	Abstract	59
4.2	Hardware in context	59
4.3	Hardware description.	61
4.3.1	Overall System	62
4.3.2	Main Hub	63
4.3.3	Splitting Hub	68
4.3.4	DUEL NODE	70
4.3.5	Discussion	77

4.4	Design files.....	78
4.5	Bill of Materials.....	79
4.6	Build Instructions	83
4.7	Operation Instructions	88
4.8	Validation and Characterization	89
4.8.1	Validation by Simulation	89
4.8.2	Results from Calibration Procedure.....	91
4.8.3	Validation from physical implementation	93
4.9	Conclusions	95
4.10	References:	95
5	Conclusions and Future Work	100
5.1	Overview	100
5.2	Future Work	100
5.2.1	General Design Procedure for Free and Open Source Hardware for Scientific Equipment	100
5.2.2	Belt Driven Open Source Circuit Mill Using Low Cost 3-D Printer Components.....	100
5.2.3	Open Source Low-Cost Power Monitoring System.....	100
5.3	Conclusions	101
5.3.1	General Design Procedure for Free and Open Source Hardware for Scientific Equipment	101
5.3.2	Belt Driven Open Source Circuit Mill Using Low Cost 3-D Printer Components.....	101
5.3.3	Open Source Low-Cost Power Monitoring System.....	101

List of figures

Figure 1: A rendering of the slide dryer in OpenSCAD.	20
Figure 2: Barrel jack connections and covering.	21
Figure 3: The completed 30 slide capacity open source dryer.....	22
Figure 4: Average surface temperature of slides as a function of time for the open source slide dryer (30 slide version).....	23
Figure 5: The thermal distribution of the wet slides while drying.....	23
Figure 6: Comparing design options for the open source slide dryer: 66 slide dryer behind a 30 slide dryer.....	24
Figure 7: The FreeCAD model of the open source circuit mill.	36
Figure 8: The 3-D printed component models for the D3D design system. (From left to right the rendered designs of the motor mounting block, bearing mount block, and carriage block are shown.	37
Figure 9a: The spindle mount model; Figure 9b: The board holder model	38
Figure 10: The Machine Control Interface of Copper Carve.....	39
Figure 11: An illustration of substrate deformation.....	40
Figure 12: A sketch defining the regions and points used for 3D linear interpolation	41
Figure 13: Setup of dial indicator for measuring backlash on X-axis	44
Figure 14: A test pattern to verify feature repeatability and backlash compensation effectiveness.....	45
Figure 15: An image of the completed circuit mill.....	46
Figure 16: Top row from left to right: (1) Feedrate of 50mm/min, plunge depth of 0.1mm, (2) Feedrate of 100mm/min, plunge depth of 0.1mm, Bottom row: (3) Feedrate of 150mm/min plunge depth of 0.1mm, (4) At 50mm/min, plunge depth of 0.2mm,	48
Figure 17: An image of the octagonal shape used to verify feature accuracy	48
Figure 18: A histogram of feature widths measured on the X axis	49
Figure 19: A histogram of feature widths measured on the Y axis	50

Figure 20: The resultant circuit board which was milled on a 10° incline	51
Figure 21: The rendered tool path in the XY axis	51
Figure 22: The rendered toolpath in the XZ axis.....	51
Figure 23: A simple sustainable house designed by OBI. The proposed system would monitor loads and sources such as the 3000W PV panels, LED lighting, and water pump [16]. Stars denote measurable devices.....	60
Figure 24: An example system setup with 9 DUEL nodes, and 2 splitting hubs	62
Figure 25: An overview of the Main Hub.....	63
Figure 26: The Main Hub	64
Figure 27: The I2C connection standard. The pull-up resistors may be managed internally by the Arduino.	64
Figure 28: The software flow programmed onto the Arduino onto the Arduino in the main hub.....	66
Figure 29: The Main Hub Schematic.....	67
Figure 30: The Main Hub board Layout.....	67
Figure 31: The splitting-hub is used for connecting multiple DUEL nodes to the main-hub.....	68
Figure 32: The splitting-hub	68
Figure 33: Splitting Hub Schematic.....	69
Figure 34: The Splitting Hub Board Layout	70
Figure 35: The DUEL node is capable of customized for fixed power measurement ranges, and outputs the data via I2C	71
Figure 36: The complete schematic for the DUEL node	73
Figure 37: The single layer board of the DUEL node	73
Figure 38: The RJ-45 BOB.....	74
Figure 39: The data packet structure sent from the DUEL node	75
Figure 40: The firmware flow chart for the DUEL node.....	76

Figure 41: The final output from FlatCAM	83
Figure 42: An example uneven 3-D height map of raw PCB material	84
Figure 43: The DUEL node after the smoothing process	85
Figure 44: The illuminated circuit board before cleaning	85
Figure 45: The board after being completely cleaned	86
Figure 46: The bottom side of the DUEL node prototype after assembly	87
Figure 47: The completed DUEL node prototype	87
Figure 48: The completed DUEL node.....	88
Figure 49: The configuration for calibrating the voltage input of the DUEL node	88
Figure 50: The configuration for calibrating the current input of the DUEL node (10 ohm 100W resistance used)	89
Figure 51: The circuit used to simulate an AC current measurement.....	90
Figure 52: The results of placing a simulated 10A AC input to the sensor. Additionally, a frequency response is generated	90
Figure 53: The DUEL node calibration curve for DC current measurement	91
Figure 54: The DUEL node calibration curve for DC voltage measurement	91
Figure 55: The DUEL node calibration curve for DC current measurement (created by varying load)	92
Figure 56: The DUEL node calibration curve for DC voltage measurement (created by varying load)	92
Figure 57: The DUEL node calibration curve for AC current measurement	93
Figure 58: The DUEL node calibration curve for AC voltage measurement	93
Figure 59: DC Current Measurement Error	94
Figure 60: DC Voltage Measurement Error.....	94
Figure 61: AC Current Measurement Error	94
Figure 62: AC Voltage Measurement Error.....	95

Preface

This thesis consists of three journal articles, one of which has been published, and the rest are planned to be submitted. The first article is titled “General Design Procedure for Free and Open Source Hardware for Scientific Equipment” and was published in *Designs*. This article appears in Chapter 2 of this thesis and includes contributions from two authors. The author wrote the code, made the design, and performed the experiments. Joshua M. Pearce conceived and designed the experiments. Both contributors wrote the paper.

The second article is titled “Belt Driven Open Source Circuit Mill Using Low Cost 3-D Printer Components” and can be found in Chapter 3 of this thesis. It is currently under review to be published in *Inventions*. The article is the work of two contributors. The author constructed the hardware, designed the software and designed and performed the experiments. Joshua M. Pearce and the author wrote the paper.

The third article is titled “Open Source Low-Cost Power Monitoring System” and is found in Chapter 4 of this thesis. It is currently under review to be published in *HardwareX*. The article is the work of two contributors. The author designed and constructed the hardware, designed the firmware, and designed and performed the experiments. Joshua M. Pearce also designed experiments. Both researchers wrote the paper.

Acknowledgements

Thank you to my advisor, Dr. Joshua M. Pearce for your patience and guidance during the writing and research for this thesis. Without your help, this would have never been possible.

I also owe great thanks to my wife, Sarah, and our cats Salem and Nara for always being a source of support and comfort.

Lastly, I would like to thank the researchers of Michigan Tech Open Sustainability Technology Lab (MOST). Your assistance and insights during this process were invaluable.

Abstract

3-D printing technologies have become widely adopted and have spurred innovation and efficiency across many markets. A large contributor to the success of 3-D printing are open source, low cost electronics. On-site circuit manufacturing, however, has not become as widely utilized as 3-D printing. This project attempts to address this problem by proposing and demonstrating an open source circuit board milling machine which is inexpensive, easily manufactured, and accurate. In three interdependent sub-projects, this thesis defines a standard method for designing open source hardware, the design of the bespoke circuit mill, and explores an application of the mill for novel circuit manufacturing.

The first sub-project develops a standardized process for designing, prototyping, and distributing open source hardware. Following these steps can help ensure success for each individual part of the project. In order to validate the procedure, a case study is explored of designing low cost parametric glass slide driers.

The second sub-project details the design and construction of a circuit prototyping machine. The open source design procedure is implemented to assure maximum effectiveness. A software interface is also designed to control and carry out processing steps on the milling machine. The mill minimizes lead time and production costs of experimental circuitry. The mill also stands as a strong open source tool that can help foster growth in distributed manufacturing of electronics for a wide array of applications.

The third and final sub-project explores a flexible and scalable power monitoring system. The electronics are designed according to the open source design procedure and are manufacturable with the circuit milling machine. The power meter can be used to monitor and log power consumption of a wide range of loads, including both AC and DC.

1 Introduction

1.1 Thesis Outline & Motivation

Traditionally circuit boards are manufactured using in quantity batches using photolithography to create isolated traces [1]. Though this process is possible to carry out in labs and households, it generates hazardous waste which can be challenging to legally discard [2]. Circuit milling offers a clean, subtractive method to manufacture custom circuitry. Commercial circuit board mills can be considered expensive in that they can cost more than \$3000 [3]. In addition to the high entry price, circuit milling has not seen a high impact in the amateur hobbyist market because of a lack of both clear procedures for inexperienced designers to develop their own circuits and the lack of a unified database of user generated electronics designs. In this project, a comprehensive open-source tool chain is developed to address and solve this problem. First, an overarching set of methods is laid out in Chapter 2, which permeates the following steps in this thesis. Briefly, a parametric and low-cost glass slider drier is designed to validate the effectiveness of the proposed methods. Next, the circuit milling machine is designed using low cost, and low part count 3-D printer components in Chapter 3. Via properly tuned motion control, the mill maximizes the accuracy from low cost 3-D printer components. The machine also meets specifications laid out by Open Circuit Institute, an Open Access Circuit design repository [4]. Chapter 4 then involves a largely scalable energy monitoring device, capable of logging energy data from a variety of loads simultaneously.

Though each step of this thesis can stand alone, each Chapter relies on the work done in preceding Chapters. The open source hardware design methodology was a first step, as it lays a clear foundation, which is used, in every following Chapter. The circuit board mill is a logical next step because it allows for fast, inexpensive, and open source means of device fabrication needed in the next Chapter and in future work. With this circuit board mill, the energy logger system can be manufactured. The methods of designing and fabricating the energy logger can then be used to develop a wide array of novel electronic devices.

1.2 References

1. Burgess, Larry W. "Multilayer circuit board manufacturing." U.S. Patent 4,642,160, issued February 10, 1987.
2. "Ferric Chloride FAQ - Prototyping Guides." MG Chemicals. Accessed April 04, 2018. <https://www.mgchemicals.com/resources/technical-support/prototyping-guides/ferric-faq>.
3. "Bantam Tools Desktop PCB Milling Machine." Bantam Tools. Accessed March 28, 2018. <https://www.bantamtools.com/products/bantam-tools-desktop-pcb-milling-machine>.
4. "Standards." Standards | Open Circuit Institute. Accessed April 04, 2018. <http://opencircuitinstitute.org/content/standards>.

2 General Design Procedure for Free and Open Source Hardware for Scientific Equipment¹

2.1 Abstract

Distributed digital manufacturing of free and open source scientific hardware (FOSH) used for scientific experiments has been shown to reduce the costs of scientific hardware from 90 to 99%. In part from these cost saving, the manufacturing of scientific equipment is beginning to move away from a central paradigm of purchasing proprietary equipment to one in which scientists themselves download open source designs, fabricate components with digital manufacturing technology and then assemble the equipment themselves. This trend creates a need for a new design paradigm, which designers can follow when targeting this scientific audience. This study provides such a ten step generalized design procedure for the development of free and open source hardware for scientific applications. A case study is provided for an open source slide dryer that can be easily fabricated for under \$20, which is more than 300 times less than some commercial alternatives. The bespoke design is parametric and easily adjusted for many applications. By designing using open source principles and the proposed methods, the outcome will be customizable, under control of the researcher, less expensive than commercial options, more maintainable, and many applications will benefit the user since the design documentation is open and freely accessible.

2.2 Introduction

As distributed digital manufacturing of free and open source scientific hardware (FOSH) used for scientific experiments [1] has been shown to reduce the costs of scientific hardware from 90 to 99% [2]. These somewhat shocking cost savings have proven resilient across both standard [3] as well as custom equipment [4]. This has supported the rapid growth of an engineering subfield to develop FOSH for science, which is represented by the annual *Gathering for Open Science Hardware* [5] as well as two new academic journals the *Journal of Open Hardware* [6] and *HardwareX* [7]. There are numerous examples of FOSH scientific equipment in all fields, ranging from syringe pumps [8] to self-assembling robots [9]. Examples exist in the field of biology [10-14], optics [15], and microfluidics [16-18]. Many open tools exist for physics and materials, including radial stretching systems with force sensors [19], a robot-assisted mass spectrometry assay platform [20], a large stage 4-point probe [21], and automated microscope [22]. Simple yet essential devices for health and medical treatment in the developing world include a mobile water quality tester [23], and sample rotator mixer

¹ The material contained in this Chapter was previously published in *Designs* 2018, 2(1), 2; doi:10.3390/designs2010002 This article is an open access article distributed under the terms and conditions of the Creative Commons Attribution (CC BY) license (<http://creativecommons.org/licenses/by/4.0/>)

[24]. Some open hardware platforms mate with extensive open source software, like the GNU radio system [25]. There are open source ventures into IOT energy monitors for buildings [26], energy efficient homes and subsystems [27], and even smart cities [28]. It is easier now than ever to share and collaborate on open source scientific instruments [29]

One of the primary enabling innovations that provides the opportunity for distributed manufacturing of open source hardware [30]–based scientific equipment is the 3-D printing capabilities of the self-replicating rapid prototyper (RepRap) project [31–33]. The RepRap 3-D printers have been used to provide high-quality educational experiences for students in a wide-range of disciplines in the classrooms [34,35] as well as become scientific platforms themselves [36]. A maturing network of peer-production [37] as well as 3-D printing file repositories [38] provide both time and fund savings within scientific labs [39]. Combining 3-D printing with readily off-the-shelf components and open source electronics (e.g. the Arduino prototyping platform [40–41]) has enabled the automation of scientific equipment [1–4,8–29]. As the fabrication of scientific equipment moves away from a central paradigm of purchasing proprietary equipment to one in which scientists themselves download open source designs, fabricate components with digital manufacturing technology and then assemble the equipment themselves there is a need for a new design paradigm, which designers can follow when targeting this audience.

This study provides such a generalized design procedure for the development of free and open source hardware for scientific applications. After laying out and explaining each of 10 steps in the procedure a case study is provided for an open source slide dryer. The case study is discussed as a practical example to the benefits and drawbacks of this approach.

2.3 Materials and Methods

2.3.1 Generalized Procedure

The generalized procedure contains ten core steps:

1. Evaluate existing similar scientific tools for their physical functions and base the design of the FOSH design off of replicating the physical effects, not pre-existing designs. If necessary, evaluate a proof of concept.
2. Use only free and open source software tool chains and open hardware for the fabrication of the device.
3. Attempt to minimize the number and type of parts and the complexity of the tool.
4. Minimize the amount of material and the cost of production.
5. Maximize the use of components that can be distributed digitally manufactured from using widespread and accessible tools such as the RepRap 3-D printer.
6. Create a parametric design to pre-design all of the potential components for different bespoke tools rather than only a single design.

7. All components that are not easily and economically fabricated with existing open hardware equipment in a distributed fashion should be chosen from off-the-shelf parts, which are readily available throughout the world.
8. Validate the design for the targeted function(s).
9. Document the design, manufacture, assembly, calibration, and operation of the device meticulously.
10. Share all of the documentation in the open access literature.

2.3.2 Details of Each Procedure Step

2.3.2.1 Literature review & Proof of concept

A literature review must be undertaken before a new open hardware device is to be designed. This literature review should ensure that there has not been other open source attempts at creating the same device as well as detailing how similar devices are fabricated for commercial applications. In both cases the fundamental concepts that are targeted are the physical effects that the device must perform as well as determining the metrics of success.

In order for open hardware to thrive, there must be cooperation rather than competition. If a literature review reveals that a solution already exists, build off of what has been done, adding improvements or refinements.

In conjunction with this step, it may be useful to generate an as-simple-as-possible proof of concept. If there are even signs of success – the design may be worth pursuing. However if the proof of concept does not work, it may be wise to rethink the approach.

2.3.2.2 Use of only Free and Open Source Tool Chain

Use free and open-source software design tools where possible in the initial design (e.g. open source CAD packages such as OpenSCAD [42], FreeCAD [43], or Blender [44]). For example, with an open source customizer [45] it is possible for even novices to make customizable designs. FOSS should be used for all software whenever possible [46-48]. Finally, the fabrication equipment used to make the targeted device should run free and open source firmware and when possible be FOSH itself (e.g. a RepRap 3-D printer [49]). If that is not feasible, then low-cost and/or widely-used software packages and hardware should be favored. This is to ensure the widest possible accessibility of your designs for remixing by others.

Using FOSH and FOSS should fall in naturally with the scientific method as an important factor in the scientific method is repeatability. However, if an experiment uses high-priced proprietary tools, there is a large barrier for others to replicate the results. By using open source design methodologies for hardware costs can be minimized, allowing for ease of replication and verification.

2.3.2.3 Minimize complexity

In order to support maintenance, upgrading, repair and end of life disassembly [50] and recycling [51], attempt to minimize the number and type of parts (e.g. use all the same type of fastener) and the complexity of the tool overall. This can be done by using identical fasteners wherever feasible. Minimizing dissimilar materials when unnecessary and reducing the part count. It should be noted, however that the individual parts when digitally manufactured can be as complex as the tools (e.g. 3-D printers) allow for with no penalty.

Designers must consider that the users of their instruments may not be engineers or specifically skilled in instrument manufacturing. Therefore, complexity should also be reduced in manufacturing techniques as well as applied theories.

2.3.2.4 Minimize material consumption

By reducing the amount of material used the environmental impact is minimized as the processing and transportation embodied energy are all reduced by the reduced use of material [51-57]. This can be done by eliminating non-functional bulk to designs, and for 3-D printed designs minimizing infill percentage to fulfill mechanical requirements. In addition, material minimization reduces overall economic costs from reduced processing time as well as material costs.

2.3.2.5 Maximize components that can be digitally distributed manufactured

The use of distributed digitally manufactured from using widespread and accessible tools such as the RepRap 3-D printer [49] and open PCB mills [58] help to reduce both the environmental impact [51-57] as well as reduce the economic costs of production [59-61]. Lead times can also be reduced, as well as improving maintainability.

2.3.2.6 Create parametric designs

By making parametric designs rather than solve a specific case all future cases can also be solved while enabling future users simply to alter the core variables to make the device useful for them. For example, a simple 3-D printable syringe pump [8] resulted in thousands of downloads and customizations creating millions of dollars of value for the scientific community in the first year of its release [62,63]. The syringe pumps were used in multi-material 3-D printers [58], wax printing of paper-based microfluidics [64], and as a fluid handling robot for chemical and biological experiments [65]. In addition, the original design was improved and ported from a Raspberry Pi environment to an Arduino environment for in-lab control [66].

The creation of parametric tools allows a large degree of flexibility to the user. Properly parametrized 3-D model designs will allow users to alter critical dimensions for their purposes. In some cases, it will also allow models to be reformatted such that they could be manufactured with a wide and unforeseeable range of tools.

2.3.2.7 Off-the-shelf parts

All customized parts are designed to be digitally manufactured, but often times less expensive components can be found that are mass manufactured (e.g. pipes, tubes, screws, etc.). These should be sourced so they are as widely available as possible throughout the world. Using off the shelf parts allow research labs to stock a minimum of parts, which are widely used. This, once again, reduces lead time, which speeds up research.

2.3.2.8 Validation

In order for the FOSH tool to be used in the scientific community, it must be validated using a clear and transparent procedure and have a low cost effective method of calibration. Again, whenever possible using other digitally manufactured open hardware tools and FOSS to complete the validation and calibration.

2.3.2.9 Proper documentation

The bar to clear to have acceptable documentation for open hardware is much more detailed than normally allowed in the methods sections of peer reviewed writing. The documentation must actively assist a non-specialist in recreating the hardware. The Open Source Hardware Association (OSHW) have extensive guidelines for properly documenting and releasing open source designs [67]. In summary, the guidelines are:

- Share design files in the most universal type
- Include a fully detailed bill of materials, including prices and sourcing information.

- If software is involved make sure the code is clear coherent and understandable by a lay-man.
- Include many photos such that nothing is obscured – and can be used as a reference while manufacturing.
- In the methods section, the entire manufacturing process must be detailed, as these are instructions for users to replicate the design.
- Share on many file hosting sites (see step 10 below), but also be sure to specify a license. This gives users information on what fair use of the design constitutes.

2.3.2.10 *Share aggressively*

Open source hardware can be at a disadvantage when competing with proprietary technology, because proprietary technology is sold through conventional channels and typically will have a marketing budget to pay for advertising. FOSH can be sold and marketed through this model as well, but in some cases this is not appropriate. In order for FOSH to proliferate, designs must be shared aggressively – just to raise awareness of the existence of the option. All of the documentation for a project can be shared on the Open Science Framework [68], which is set up to take any type of file and handle large data sets. Software can be shared on sites like GitHub [69] or SourceForge [70], and should include proper documentation on the inner-workings of the code, as well as a brief summary. 3-D designs can be shared on sites set up by government scientific funders like the NIH 3D Print Exchange [71] or open source companies like Ultimaker’s YouMagine [72] or MyMiniFactory [73] as well as other repositories [74]. Circuit designs can be shared on sites like the Open Circuit Institute [75] or Open Electronics [76].

Designers should consider spreading designs to as many hosting sites as possible, as this will only increase exposure. Regardless of which site, it is important to engage with the community, building personal rapport. Building a reputation of intelligence, reliability and helpfulness will bolster confidence in your designs, and increase usage.

2.3.3 **Case Study: Slide dryer**

In order to demonstrate these ten design steps in the creation of FOSH hardware for science a case study is presented on the development of an open source slide dryer. Slide dryers are designed to warm glass microscope slides gently to decrease drying time for experiments after cleaning steps. Slide dryers allows users to increase their productivity. Slide dryers are available commercially from \$200-5,245 USD [77]. Commercial slide dryers come in many different shape, sizes, and with different capabilities [77]. As a generalization of the design, all slide dryers provide a rack structure and a heat source.

In this case study the target is to design a FOSH slide dryer with an acceptable capacity (30 slides) and a fast drying rate (10 minutes or less). The numbers chosen are some-what arbitrary, but due to the parametric design of the system, design constraints may be

altered to better fit requirements for a specific laboratory. Note that the two target features (capacity and dry time) can not both be optimized – as dry time decreases, slide count must decrease as well for a given amount of power consumption.

In the first step, the existing literature is surveyed for slide dryer designs. There has been some efforts to patent the concept of slide drying [78-80]. One attempt [78] uses an electric current to generate heat, however it has since expired. Another design [79] patented in Russia uses forced air. Yet another design [80] uses gas forced through a tube in order to create heat and has also expired. Next, a search for open source solutions is carried out. There is one design available on the Internet, “Glass Slide Dryer” [81]. Though this design is functional and less costly than commercial systems, it has a few apparent issues:

- Poor documentation and construction notes
- Not scalable
- Overly-complex
- The device is not characterized.

These issues have prevented it from widespread adoption.

Finally, commercialized slide dryers are reviewed. The most expensive option (over \$5,000) [77] is able to heat 57 slides (unless an additional shelf is purchased for \$284) at 70°C. Many other options are available [77,82-86], but all products are expensive considering their function. The lowest-cost design that fits the target specifications comes in at a cost of \$225 [77] and most slider dryers or warmers were several hundred to over \$1,000.

Upon review of the existing options, it is found that the FOSH community is in need of a well-documented, customizable and effective slide dryer. Concepts are generated, some tested, and simplified and refined until an optimal design is found. The simple proof of concept (step 1) that led to this final design was simply aluminum wire wrapped around a box hooked to a variable power supply. The chosen design, which was designed to be parametric in OpenSCAD [42] (step 2 and 6), involves 3-D printing a base with a peg structure on an open source 3-D printer, (step 2 and 5). The 3-D printable parts are designed to minimize filament consumption (step 4). Then readily available wire (step 7) can be woven across the base. When a voltage is applied, electrical energy will be converted to heat due to the resistance of the wire [87] in a simple design (step 3).

20 AWG copper magnet wire is selected for its low cost and resistance to corrosion [88]. The resistance is measured by measuring out a long length of wire, in this case 10m. Then, using a fluke meter [89] the resistance of the length can be found. Simply dividing the measured resistance by the length, the resistivity can be found. For the specific wire used [88], a resistivity of 0.000220 Ohm/mm is found. This value is required to find the minimum length of wire to match the selected power supply.

An off the shelf (step 7) 12V 5A power supply is selected [81] due to both low cost and high availability. Additionally, most off-the-shelf supplies like the one selected have thermal overloads built in to prevent damage due to short circuits. Using Ohm's law [87], the necessary length L can be found, given resistivity ρ , current I and voltage V :

$$L = \frac{V}{I\rho} \dots(1)$$

The wattage, P , consumed is simply defined by [87] :

$$P = IV \dots(2)$$

It should be noted that it is not wise to run a power supply continuously at full capacity [90]. Therefore it is advised to use a fraction of the available I . In this case study, 90% of I is utilized in the design.

Once L has been determined, it is only a matter of distributing the wire among the rack system. The rack is developed in OpenSCAD [42] (step 2). This allows for the design to be entirely parametric (step 6), as well as transferable to customizers [45]. Key parameters that the model depends on are:

- Wire Resistance: The measured resistivity of the heating element (in Ohm/mm).
- Wire Diameter: The diameter of the heating element (in mm).
- Supply V: The voltage of the power supply (in V).
- Supply I: Maximum allowable current from the power supply (in A).
- Slide count: The desired amount of slides to dry (number).
- Slide Dimensions: Width and length of the slides (in mm)
- Printer Dimensions: The 3-D print bed surface area X and Y size of the 3-D printer to be used.

There are many lesser dimensional parameters, which specify features such as winding pegs and rack height, which can be adjusted by the user to make a slide dryer ideal for their application. The SCAD model will optimize the design to fit the user's 3-D printer, while minimizing part counts (step 3). Each rack can be connected together using snap-fit connectors, also generated by the model. As this is a parametric design, it allows for similar results to be achieved via different means. For example, a smaller printer can be used by printing off a larger number of shelves to accommodate the same number of slides as a larger printer can do with less shelves but of greater area. If only a 24V supply is available, simply by changing the parameters, the design can still facilitate the user's desired number of slides. The intension of this design is not necessarily for users to replicate exactly what was used in this case study, rather empower them to use materials and tools readily available in their lab or work place to easily generate a useful and reliable slide dryer for themselves.

The example design based on the desired slide count generated seven shelves for an Lulzbot Taz 5 printer [91]. The design in the OpenSCAD environment can be viewed in Figure 1.

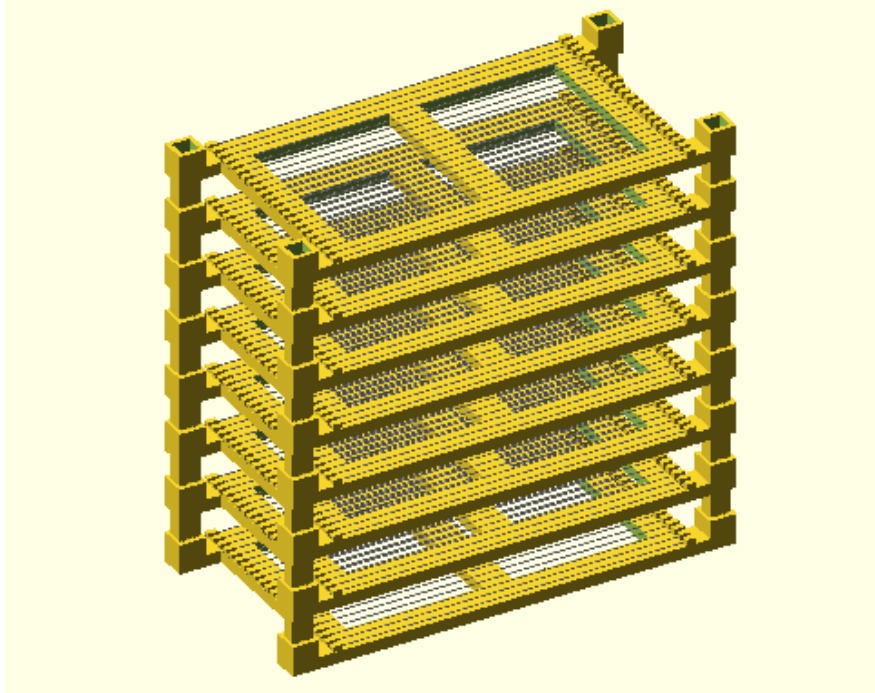


Figure 1: A rendering of the slide dryer in OpenSCAD.

Following guidelines for appropriate documentation (step 9), the bill of materials along with item, number, price and source are shown in Table 1. As can be seen in Table 1 the cost of the materials to build the open source slider dryer for 30 slides is \$16.63.

Table 1: Bill of materials for the 30 slide – open source slide dryer.

Part	Link	Quantity	Cost
HIPS Filament	https://www.lulzbot.com/store/filament/hips	120g	\$4.79
20 AWG Magnet wire	http://a.co/gbuYXLf	10.6 m	\$2.16
12V 5A Power Supply	http://a.co/7YzVkHB	1	\$8.89
Barrel Jack	https://www.digikey.com/short/q7wbrm	1	\$0.76
Shrink Tube	https://www.digikey.com/short/q300mc	30mm	\$0.03

The manufacturing of the device is fairly simple. First, the user must print all necessary components. Then weave wire around the pegs (there should be one strand of wire per each set of pegs). Once one shelf is completed, the user inserts the pegs, and attaches the next shelf, and wraps the wire once around the peg to tension the lower shelf. This process is repeated for all shelves. Once complete, the user strips both ends of the wire with a razor blade and cuts and places 10mm pieces of shrink tube over the wire (do not shrink yet). Then the wire is soldered to the middle tab, and the back tab of the barrel jack (the wire is not polarized, so it does not matter which wire is soldered to which tab). Finally, shrink the shrink tube over the solder joints, as well as the unconnected barrel jack tab (as in Figure 2)

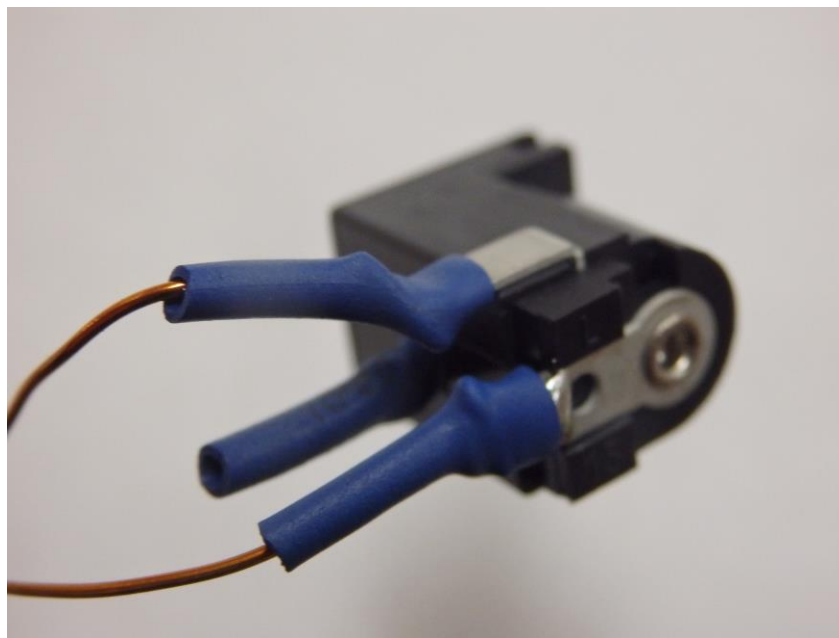


Figure 2: Barrel jack connections and covering.

The slide dryer is sliced using open source Cura [92] using the high-quality default print settings. 120 g of high impact polystyrene (HIPS) filament and 10.6 m of magnet wire is used. A 5.5 mm barrel jack is soldered to the wire ends in order to easily interface with the power supply. The assembled open source slide dryer can be seen in Figure 3.

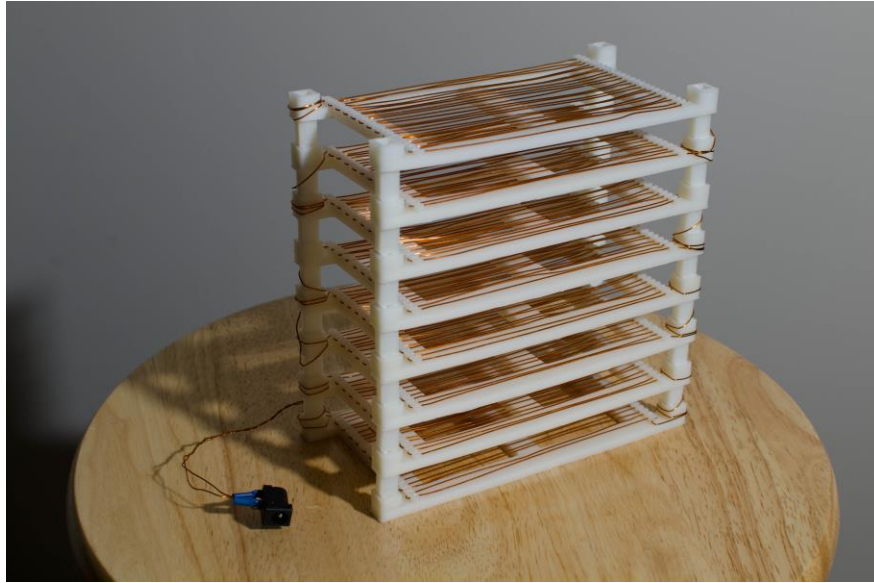


Figure 3: The completed 30 slide capacity open source dryer.

As validation (step 8), 30 slides are washed in water and rinsed in ethanol, and then placed on the open source dryer. The dryer is then powered on, and the time-to-dry is measured while the temperature is being monitored with an open source thermocouple-based data logger (T400, Pax Instruments) [93]. The warming kinetics experiment is repeated three times. Lastly, a FLIR thermal distribution on a single rack is viewed with a thermal camera to demonstrate uniformity of heating.

2.4 Results and Discussion

The open source slide dryer successfully met the design parameters. The amount of time required to dry 30 slides is ~5 minutes (+/- 2 min.), well below the desired 10 minute target limit. The temperature during heat-up is recorded in Figure 4. On average it takes 5 minutes to fully heat up.

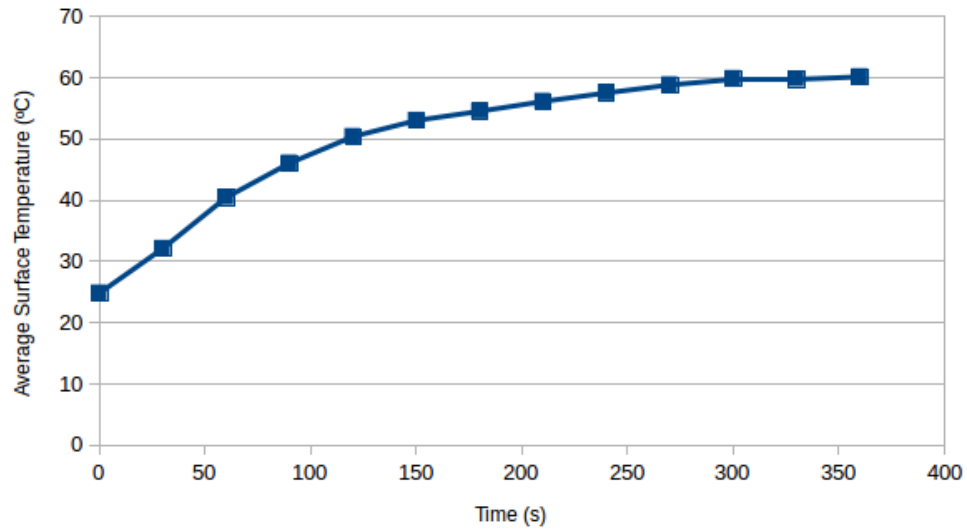


Figure 4: Average surface temperature of slides as a function of time for the open source slide dryer (30 slide version).

As can be seen by Figure 4, the slide temperature at the point of complete dryness is measured with a thermocouple and found to be 60 °C. Lastly, the thermal distribution as viewed with a thermal camera demonstrates heating uniformity as shown in Figure 5.

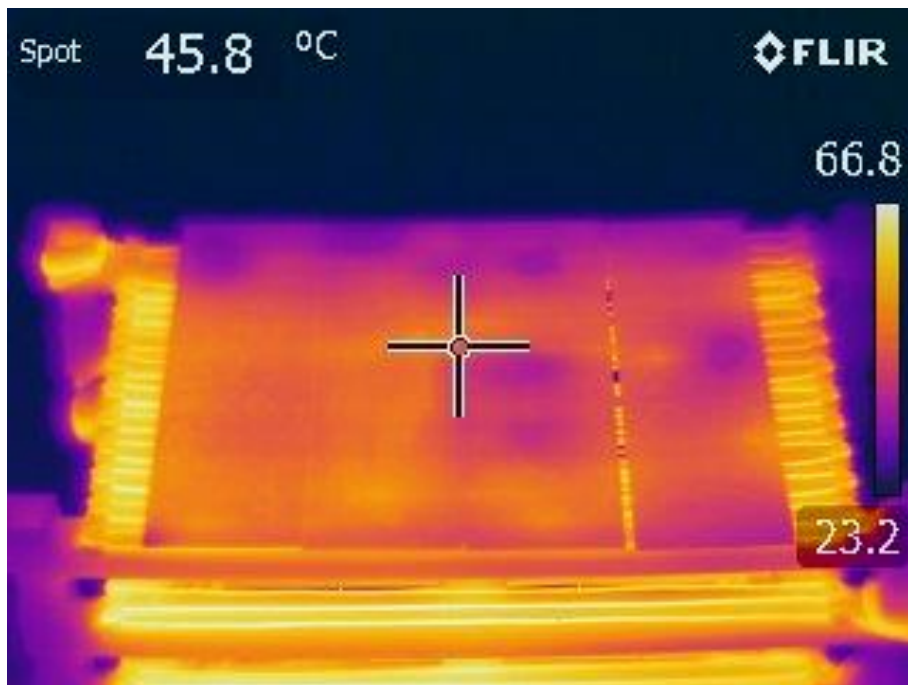


Figure 5: The thermal distribution of the wet slides while drying.

The parametric design of the open source slide dryer allowed for different models to be generated and tested. For example, a slide dryer with a capacity of 66 slides was created using the same methods as the 30-slide system (Figure 6). However using the same power supply will yield insufficient heat to dry slides, and therefore will need a doubled voltage (24V, 5A supply) to have the same density.



Figure 6: Comparing design options for the open source slide dryer: 66 slide dryer behind a 30 slide dryer.

Many different design ideas were explored before arriving at the simple solution of applying current directly to wire. The first iteration was designed base off of a circuit suggested in [2], which involved an open source microcontroller (Arduino [41]) controlling a relay tied to high wattage resistors and a power supply. A thermistor was used as a control feedback, so the dryer could be set to a desired temperature. The resistors were put in a 3-D printed enclosure with a fan, and ventilation shafts. Slides were made to sit on top of the enclosure and have heat from the resistors transferred to them. The test design was prototyped using a breadboard. As this was clearly not a permanent solution, the electronics where put onto a custom circuit board and milled. Two designs were tested, one with utilizing the Arduino and relay, and the other utilizing an Op-Amp and MOSFET. The design ultimately was not selected due to a couple downfalls. First, the heat could not be transferred to the slides quickly enough. The resistors would hit peak heat, and the slides would take an excessive amount of time to dry (more than 30 minutes). The design was also overly complex. In addition, there were a couple unique parts to 3-D print that were not simple-to-print geometry (as was the final design shown in Figure 1). Additionally, a custom circuit board, though convenient once made, is not approachable by all users. The final design is demonstrated to be superior because of its low unique part count (5 parts total via step 3), easy to

manufacture from a minimum of material (step 4) using open source tools (step 5), and highly parametric model (step 6) using readily available off-the-shelf parts (step 7). Another advantage over previously conceived designs is direct thermal contact enabling more efficient energy use. The wire also distributes the heat as proven in Figure 5, ensuring an even and quick dry as validated above (step 8). The complete design is open source and can be found at [94] (step 9). After publication of this article, the design will be shared aggressively on many 3-D printing repositories (step 10) (NIH 3D Print Exchange [71], Youmagine [72], and MyMiniFactory [73], as well as in the PLOS Open Toolbox [95] and Appropedia [96].

2.4.1 Techno-Economic Comparisons

The price of the design is approximately \$16.63, dollars which is significantly less expensive by more than one order of magnitude up to more than 300 times less than commercial alternatives (see [77,82-86]). Previous work has shown that the labor costs [3] in fabricating such open source equipment is small and that moving to open source scientific hardware is easily justified by economics alone. However, as the open source slide dryer can be customized to fit the exact needs of the research group and size can be accommodated by the design, the value to the researcher tends to be larger than simple economics would predict.

Table 2: A comparison of commercial slide driers and the FOSH solution. Times denoted with * indicate experiment-based predictions based on maximum device temperature and not actual measurements from the device.

Name	Cost (US\$)	Capacity	US\$/Slide	Max Temp.	Drying Time
FOSH 30 slide drier	16.63	30 slides	0.55	58	3.21 min
FOSH 66 slide drier	23.82	66 slides	0.36	42	4.58 min
FOSH 66 Slide drier (24 V)	41.12	66 slides	0.62	66	2.16 min
SHUR/Dry Slide Dryer III [56]	5245.00	38 slides	138.03	70	1.00 min *
Large Size Economical Slide Warmer [56]	1274.00	66 slides	19.30	100	1.37 min *
Slide Drying Bench, Electrothermal [61]	1131.21	50 slides	22.62	100	1.37 min *
Scientific Device Slide Heater [62]	1080.00	20 slides	54.00	65	1.66 min *
Slide Warmer [63]	301.00	23 slides	13.09	70	1.63 min *
XH-2002 [64]	350.00	23 slides	15.22	75	1.31 min *
Slide Warmers for 24 slides [65]	317.00	24 slides	13.22	70	1.63 min *
Slide warmer 23 slides [56]	225.00	23 slides	9.78	70	1.63 min *
Slide warmer 66 slides [56]	285.00	66 slides	4.32	70	1.63 min *

From the total costs and the cost per slide data available in Table 2, it is clear that the FOSH solution can be significantly more cost-effective than even the least expensive commercial solution. The advantage commercial slide driers have over the proposed FOSH solution is decreased drying time based on their maximum rated temperature. For the lowest cost per slide drying, the FOSH device is more than 7 times more cost-effective. In general, for a two orders of magnitude reduction in cost, the slide dry time is about doubled. Although the majority of the most cost-effective commercial solutions have rapid drying times, their capacity is less than half (almost a third) that of a solution like the FOSH 66 slide 24 V design. Effectively, this indicates that in large batches, the FOSH solution can outperform in terms of both cost and efficiency. In small batches, the FOSH design has a lower initial cost. The costs of proprietary slide dryers can come with other services (e.g., a warranty) that the user must determine are valuable enough to warrant paying the premium for commercial closed systems. Once again, the advantage the FOSH solution has over all closed-source commercial solutions is that it can be modified and optimized for a given researcher. If the drying times shown in this particular device are not sufficient for a lab's needs, users may simply change the design parameters to increase the power output. If this is done to reach higher temperatures (e.g., 100 °C), then higher temperature thermopolymers are recommended for the 3-D printed

components. For example, polycarbonate (PC) is heat resistant up to 116 °C and would be appropriate to match any commercial slide dryer with a maximum temperature of 100 °C or below. PC costs about twice the HIPS used here, which would increase the cost of the FOSH device by about \$5.00 for plastic in addition to the more powerful power supply. These changes do not alter the overall results of the economic analysis. Lastly, although many of the commercial versions were also open to the environment, a few were enclosed to stop contamination. The FOSH system could also be easily enclosed to reduce contamination.

2.4.2 Future Work

Future work can improve the slide dryer further by 1) building an enclosure for it to protect from drafts and contaminants as well as dry the slides in an inert atmosphere, 2) change the geometry to dry different types of objects, 3) provide controls and temperature feedback for variable temperatures or for custom warming sequences to be followed, and 4) adjust the corners of the 3-D printable design to enable better wire management. In addition, the open source slide dryer design can be easily altered for many different applications far outside of the narrow scoped focused on here. For example, this design could be altered into a parametric space heater, a part shelf, or a parametric load resistor. Submitting this design to popular 3-D printing sites such as [69-71] (step 10) will give the design exposure and could potentially spawn unconceivable permutations of the design.

In this case study, the slide dryer has become the property of the open source community, and will empower researchers, teachers and hobbyists alike to accelerate their own research when a slide dryer is appropriate. The cost of conventional scientific hardware is expensive because of a relatively low demand, making research-grade equipment prohibitively expensive [97]. By designing using open source principles based of the proposed methods, the outcome will be less expensive than commercial options, more maintainable, and many applications will benefit the user since the design documentation is open and free of proprietary information. As many scientists begin to use this design methodology in their own equipment it will enable more rapid progress as we all have the opportunity to “stand on the shoulders of giants” [98].

2.5 Conclusions

This chapter successfully demonstrated the use of a ten step method to develop open source hardware designs for scientific equipment. In this case study the open source slide dryer, which can be fabricated to have equivalent functionality for a small fraction of the cost of commercial systems has become the property of the open source community, and will empower researchers, teachers, citizen scientists and hobbyists alike. The custom design is parametric and easily adjusted for many laboratories and other applications. By designing using open source principles and the proposed methods, the outcome will be customizable, under control of the researcher, less expensive than commercial options,

more maintainable, and many applications will benefit the user since the design documentation is open and freely accessible.

2.6 References

1. Pearce, J. M. Building Research Equipment with Free, Open-Source Hardware. *Science* **2012**, 337 (6100): 1303–1304. DOI: 10.1126/science.1228183
2. Pearce, J. Open-Source Lab: How to Build Your Own Hardware and Reduce Research Costs. 1st ed. Elsevier: Waltham, MA, USA, 2014.
3. Trivedi, D.K; Pearce. J.M. Open Source 3-D Printed Nutating Mixer. *Applied Sciences*, **2017**, 7(9), 942; doi:10.3390/app7090942
4. L iardon, J. L., & Barry, D. A. Adaptable Imaging Package for Remote Vehicles. *HardwareX* **2017**,2. Doi: 10.1016/j.ohx.2017.04.001
5. Dosemagen, S., Liboiron, M. & Molloy, J., (2017). Gathering for Open Science Hardware. *Journal of Open Hardware* **2016**. 1(1), p.4. [10.5334/joh.5](https://doi.org/10.5334/joh.5)
6. Journal of Open Hardware. Available online: <https://openhardware.metajnl.com/> (accessed 29 Nov 2017)
7. HardwareX. Available online: <https://www.journals.elsevier.com/hardwarex/> (accessed 29 Nov 2017)
8. Wijnen, B., Hunt, E.J., Anzalone, G.C. and Pearce, J.M., Open-source syringe pump library. *PloS One* **2014**, 9(9), p.e107216.
9. Zykov, V., Chan, A., & Lipson, H. (2007, March). Molecubes: An open-source modular robotics kit. In *IROS-2007 Self-Reconfigurable Robotics Workshop* **2007** (pp. 3-6).
10. Baden, T.; Chagas, A.; Marzullo, T.; Prieto-Godino, L.; Euler, T. Open Laware: 3-D Printing Your Own Lab Equipment. *PLoS Biology* **2015**, 13 (3).
11. Damase, T.R.; Stephens, D; Spencer, A.; Allen, P.B. Open source and DIY hardware for DNA nanotechnology labs. *Journal of Biological Methods*, **2015**. 2(3), p.e24.
12. Oh, J.; Hofer, R.;Fitch, W.T., An open source automatic feeder for animal experiments. *HardwareX* **2017**, 1:13-21.
13. McMunn, M.S. A time-sorting pitfall trap and temperature datalogger for the sampling of surface-active arthropods. *HardwareX*, **2017**, 1:38-45.
14. Gali, H. An Open-Source Automated Peptide Synthesizer Based on Arduino and Python. *SLAS TECHNOLOGY: Translating Life Sciences Innovation*, **2017**. p.2472630316685844.
15. Zhang, C.; Anzalone, N.C.; Faria, R.P.; Pearce, J.M., Open-source 3D-printable optics equipment. *PloS One* **2013**, 8(3), p.e59840.
16. Fobel, R.; Fobel, C.; Wheeler, A.R. DropBot: an open-source digital microfluidic control system with precise control of electrostatic driving force and instantaneous drop velocity measurement, *Appl. Phys. Lett.* **2013**, 102 (19), 193513.

17. Pearce, J.M.; Anzalone, N.C.; Heldt, C.L. Open-Source Wax RepRap 3-D Printer for Rapid Prototyping Paper-Based Microfluidics. *Journal of Laboratory Automation* **2016**, 21(4):510-516.
18. Mista, C.; Zalazar, M.; Peñalva, A.; Martina, M.; & Reta, J. M. Open Source Quartz Crystal Microbalance with dissipation monitoring. In *Journal of Physics: Conference Series* (Vol. 705, No. 1, p. 012008). **2016** IOP Publishing.
19. Schausberger, S.E.; Kaltseis, R.; Drack, M.; Cakmak, U.D.; Major, Z. ; Bauer, S. Cost-Efficient Open Source Desktop Size Radial Stretching System With Force Sensor. *IEEE Access* **2015**, 3:556-561.
20. Chiu, S.H.; Urban, P.L. Robotics-assisted mass spectrometry assay platform enabled by open-source electronics. *Biosensors and Bioelectronics* **2015**, 64:260-268.
21. Chandra, H.; Allen, S.W.; Oberloier, S.W.; Bihari, N.; Gwamuri, J.; Pearce, J.M. Open-source automated mapping four-point probe. *Materials* **2017**, 10(2), p.110 ; doi:10.3390/ma10020110
22. Wijnen, B.; Petersen, E. E.; Hunt, E. J.; Pearce, J. M. Free and open-source automated 3-D microscope. *Journal of Microscopy* **2016**, 264(2), 238-246.
23. Wijnen, B., Anzalone, G.C. and Pearce, J.M. Open-source mobile water quality testing platform. *Journal of Water Sanitation and Hygiene for Development* **2014**, 4(3):532-537.
24. Dhankani, K.; Pearce , J. M. Open Source Laboratory Sample Rotator Mixer and Shaker. *HardwareX* **2017**, 1, 1-12.
25. Valerio, D. Open source software-defined radio: A survey on gnuradio and its applications. *Forschungszentrum Telekommunikation Wien, Vienna* **2008**, *Technical Report FTW-TR-2008-002*.
26. Pocero, L.; Amaxilatis, D.; Mylonas, G.; Chatzigiannakis, I. Open source IoT meter devices for smart and energy-efficient school buildings. *HardwareX*, **2017**, 1:54-67.
27. Thomson, C. C., & Jakubowski, M. (2012). Toward an Open Source Civilization:(Innovations Case Narrative: Open Source Ecology). *Innovations* **2012**, 7(3), 53-70.
28. Jiang, J.; Claudel, C. A high performance, low power computational platform for complex sensing operations in smart cities. *HardwareX* **2017**,1:22-37.
29. Harnett, C. Open source hardware for instrumentation and measurement. *IEEE Instrumentation & Measurement Magazine* **2011**, 14(3). DOI: 10.1109/MIM.2011.5773535
30. Gibb, A.; Abadie, S. *Building open source hardware: DIY manufacturing for hackers and makers*, 1st ed; Addison-Wesley Professional: Boston, MA, USA, 2014.
31. Sells, E.; Bailard, S.; Smith, Z.; Bowyer, A.; Olliver, V. RepRap: The Replicating Rapid Prototyper-Maximizing Customizability by Breeding the Means of Production. *Proceedings in the World Conference on Mass Customization and Personalization*, Cambridge, MA, USA. 2010.
32. Jones, R.; Haufe, P.; Sells, E.; Iravani, P.; Olliver, V.; Palmer, C.; Bowyer, A. RepRap-the Replicating Rapid Prototyper. *Robotica* **2011**, 29 (01): 177–91.

33. Bowyer, A. 3D Printing and Humanity's First Imperfect Replicator. *3D Printing and Additive Manufacturing* **2014**, 1 (1): 4–5.
34. Kentzer, J.; Koch, B.; Thiim, M.; Jones, R.W.; Villumsen, E. An open source hardware-based mechatronics project: The replicating rapid 3-D printer. In *Mechatronics. Proceedings of the 4th International Conference; IEEE*, pp. 1-8.
35. Schelly, C.; Anzalone, G.; Wijnen, B.; Pearce, J.M. Open-source 3-D printing technologies for education: Bringing additive manufacturing to the classroom. *Journal of Visual Languages & Computing* **2015**, 28, pp.226-237.
36. Zhang, C.; Wijnen, B.; Pearce, J.M., Open-source 3-D platform for low-cost scientific instrument ecosystem. *Journal of Laboratory Automation* **2016**, 21(4):517-525.
37. Moilanen, J.; Vaden, T. 3D Printing Community and Emerging Practices of Peer Production. *First Monday*. 2013. doi:10.5210/fm.v18i8.4271.
38. Coakley, M.F.; Hurt, D.E.; Weber, N.; Mtingwa, M.; Fincher, E.C.; Alekseyev, V.; Chen, D.T.; Yun, A.; Gizaw, M.; Swan, J. ; Yoo, T.S. The NIH 3D print exchange: a public resource for bioscientific and biomedical 3D prints. *3D Printing and Additive Manufacturing* **2014**, 1(3), pp.137-140.
39. Coakley, M.; Hurt, D.E., 3D Printing in the Laboratory: Maximize Time and Funds with Customized and Open-Source Labware. *Journal of Laboratory Automation*, **2016**, 21(4):489-495.
40. Banzi, M., & Shiloh, M. *Getting started with Arduino: the open source electronics prototyping platform*. Maker Media, Inc.. 2014. 978-1449363338
41. Arduino. Available online: <https://www.arduino.cc/> (accessed 29 Nov 2017)
42. OpenSCAD. Available online: <http://www.openscad.org/> (accessed 29 Nov 2017)
43. FreeCAD. Available online: <https://www.freecadweb.org/> (accessed 29 Nov 2017)
44. Blender. Available online: <https://www.blender.org/> (accessed 29 Nov 2017)
45. Nilsiam, Y., & Pearce, J. M. Free and Open Source 3-D Model Customizer for Websites to Democratize Design with OpenSCAD. *Designs*, **2017**, 1(1), 5.
46. Feller, J., & Fitzgerald, B. (2002). *Understanding open source software development (pp. 143-159)*. London: Addison-Wesley.
47. Lakhani, K. R.; Wolf, R. G. Why hackers do what they do: Understanding motivation and effort in free/open source software projects. *Perspectives on free and open source software* **2005**, 1, 3-22.
48. Hippel, E. V.; Krogh, G. V. Open source software and the “private-collective” innovation model: Issues for organization science. *Organization Science* **2003**, 14(2), 209-223.
49. RepRap. Available online: <http://reprap.org/> (accessed 29 Nov 2017)
50. Harjula, T., Rapoza, B., Knight, W. A., & Boothroyd, G. (1996). Design for disassembly and the environment. *CIRP Annals-Manufacturing Technology*, **1996**, 45(1), 109-114.
51. Zhong, S.; Pearce, J.M.. Tightening the loop on the circular economy: Coupled distributed recycling and manufacturing with recyclebot and RepRap 3-D printing, *Resources, Conservation and Recycling* **2018**, 128, pp. 48–58. doi: 10.1016/j.resconrec.2017.09.023

52. Kreiger, M., & Pearce, J. M. (2013). Environmental life cycle analysis of distributed three-dimensional printing and conventional manufacturing of polymer products. *ACS Sustainable Chemistry & Engineering*, **2013**, 1(12), 1511-1519.
53. Kreiger, M. A., Mulder, M. L., Glover, A. G., & Pearce, J. M. (2014). Life cycle analysis of distributed recycling of post-consumer high density polyethylene for 3-D printing filament. *Journal of Cleaner Production*, **2014**, 70, 90-96.
54. Kreiger, M., & Pearce, J. M. (2013). Environmental impacts of distributed manufacturing from 3-D printing of polymer components and products. *MRS Online Proceedings Library Archive*, **2013**, 1492, 85-90.
55. Kreiger, M., Anzalone, G. C., Mulder, M. L., Glover, A., & Pearce, J. M. (2013). Distributed recycling of post-consumer plastic waste in rural areas. *MRS Online Proceedings Library Archive*, **2013**, 1492, 91-96.
56. Gebler, M., Uiterkamp, A. J. S., & Visser, C. A global sustainability perspective on 3D printing technologies. *Energy Policy*, **2014**, 74, 158-167.
57. Faludi, J., Bayley, C., Bhogal, S., & Iribarne, M. (2015). Comparing environmental impacts of additive manufacturing vs traditional machining via life-cycle assessment. *Rapid Prototyping Journal*, **2015**, 21(1), 14-33.
58. Anzalone, G.C.; Wijnen, B.; Pearce, J.M. Multi-material additive and subtractive prosumer digital fabrication with a free and open-source convertible delta RepRap 3-D printer. *Rapid Prototyping Journal*, **2015**, 21(5), 506-519.
59. Wittbrodt, B. T., Glover, A. G., Laureto, J., Anzalone, G. C., Oppliger, D., Irwin, J. L., & Pearce, J. M. Life-cycle economic analysis of distributed manufacturing with open-source 3-D printers. *Mechatronics*, **2013**, 23(6), 713-726.
60. Petersen, E.E.; Pearce, J. Emergence of Home Manufacturing in the Developed World: Return on Investment for Open-Source 3-D Printers. *Technologies*, **2017**, 5(1), 7; doi:10.3390/technologies5010007
61. Petersen, E. E., Kidd, R. W., & Pearce, J. M. Impact of DIY Home Manufacturing with 3D Printing on the Toy and Game Market. *Technologies*, **2017**, 5(3), 45.
62. Pearce, J. Quantifying the Value of Open Source Hardware Development. *Modern Economy*, **2015**, 6, 1-11, [10.4236/me.2015.61001](https://doi.org/10.4236/me.2015.61001).
63. Pearce, J. M. Return on investment for open source scientific hardware development. *Science and Public Policy*, **2015**, 43(2), 192-195, 10.1093/scipol/scv034.
64. Pearce, J.M.; Anzalone, N.C.; Heldt, C.L. Open-Source Wax RepRap 3-D Printer for Rapid Prototyping Paper-Based Microfluidics. *Journal of Laboratory Automation*, **2016**, 21(4):510-516.
65. Zhang, C.; Wijnen, B.; Pearce, J.M., Open-source 3-D platform for low-cost scientific instrument ecosystem. *Journal of Laboratory Automation*, **2016**, 21(4):517-525.
66. Lynch open source syringe pump modifications. Available online: http://www.appropedia.org/Lynch_open_source_syringe_pump_modifications (accessed 29 Nov 2017)
67. Best Practices for Open-Source Hardware 1.0. Available online: <https://www.oshwa.org/sharing-best-practices/> (accessed 29 Nov 2017)

68. Open Science Framework. Available online: <https://osf.io/> (accessed 29 Nov 2017)
69. GitHub. Available online: <https://github.com/> (accessed 29 Nov 2017)
70. SourceForge. Available online <https://sourceforge.net/> (accessed 29 Nov 2017)
71. NIH 3D Print Exchange. Available online: <https://3dprint.nih.gov/> (accessed 29 Nov 2017)
72. Youmagine. Available online: <https://www.youmagine.com/> (accessed 29 Nov 2017)
73. MyMiniFactory. Available online: <https://www.myminifactory.com/> (accessed 29 Nov 2017)
74. Printable part sources. Available online: http://reprap.org/wiki/Printable_part_sources (accessed 29 Nov 2017)
75. Open Circuit Institute. Available online: <http://opencircuitinstitute.org/> (accessed 29 Nov 2017)
76. OpenElectronics Available online: <https://www.open-electronics.org/> (accessed 29 Nov 2017)
77. Slide Warmers and Oven / Incubators. Available online: <https://www.emsdiasum.com/microscopy/products/histology/heaters.aspx> (accessed 29 Nov 2017)
78. Microscopic-slide drier. Available online: <https://patents.google.com/patent/US1170739A> (accessed 29 Nov 2017)
79. Шахтная аэрожёлобная сушилка. Available online: <https://patents.google.com/patent/RU2589894C1> (accessed 29 Nov 2017)
80. Slide staining and heating rack. Available online: <https://patents.google.com/patent/US2101161A> (accessed 29 Nov 2017)
81. Glass Slide Dryer. Available online: <https://3dprint.nih.gov/discover/3dpx-004001> (accessed 29 Nov 2017)
82. VWR slide warmers dryers Available online: <https://us.vwr.com/store/product/3617131/slide-warmers-dryers> (accessed 29 Nov 2017)
83. Fischer Scientific slide warmers Available online: <https://www.fishersci.com/us/en/products/I9C8KUA7/slide-warmers.html> (accessed 29 Nov 2017)
84. Thomas Scientific Slide warmers Available online: <https://www.thomassci.com/search/go?ThomasDomain=www.thomassci.com&w=slide+warmers> (accessed 29 Nov 2017)
85. Lab Scientific Slide warmers Available online: <https://labscientific.com/Cytology/Tissue-Floating-Bath-and-Slides-Warmer/Slide-Warmers/> (accessed 29 Nov 2017)
86. Agar Scientific Slide warmers Available online: <http://www.agarscientific.com/slide-warmers-for-24-slides-and-56-slides.html> (accessed 29 Nov 2017)
87. Irwin, J. D.; Nelms, D. I. *Basic Enineering Circuit Analysis*, 10th ed.; Wiley: New Jersey, USA, 2011; pp. 27, 978-0-470-63322-9

88. Remington Industries. 20H200P 20 AWG Magnet Wire, Enameled Copper Wire, 200 Degree, 1.0 lb., 0.0343" Diameter, 314' Length, Natural. Available online: <http://a.co/gbuYXLf> (accessed 29 Nov 2017)
89. Fluke. Model 187 & 189 True RMS Multimeter. Available online: http://assets.fluke.com/manuals/187_189_umeng0200.pdf (accessed 29 Nov 2017)
90. LEDMO Power Supply, Transformers, LED Adapter, 12V, 5A Max, 60 Watt Max, for LED Strip. Available online: <http://a.co/2FwKrqr> (accessed 29 Nov 2017)
91. LulzBot TAZ 5. Available online: <https://www.lulzbot.com/store/printers/lulzbot-taz-5> (accessed 29 Nov 2017)
92. Cura Lulzbot Edition. Available online: <https://www.lulzbot.com/cura> (accessed 2 Dec 2017)
93. Pax Instruments. T400 Temperature Datalogger Set. Available online: <http://paxinstruments.com/products/sku927/> (accessed 29 Nov 2017)
94. Open source slide dryer. OSF. Available online: <https://osf.io/rm2ah/> (accessed 4 Dec 2017)
95. PLOS Open Toolbox. Available online: <http://collections.plos.org/open-source-toolkit-hardware/> (accessed 29 Nov 2017)
96. Appropedia. Available online: <http://www.appropedia.org/> (accessed 2 Dec 2017)
97. Pearce, J.M. Impacts of Open Source Hardware in Science and Engineering. *The Bridge*, 2017. 47(3) 24-31.
98. Dryden, M. D.; Fobel, R.; Fobel, C.; Wheeler, A. R. Upon the Shoulders of Giants: Open-Source Hardware and Software in Analytical Chemistry. *Analytical Chemistry* **2017**, 89(8), 4330-4338.

3 Belt Driven Open Source Circuit Mill Using Low Cost 3-D Printer Components

3.1 Abstract

Barriers to inventing electronic devices involve challenges of iterating electronic designs due to long lead times for professional circuit board milling or high-costs of commercial milling machines. To overcome these barriers this study provides open source (OS) designs for a low-cost circuit milling machine. First, design modifications for mechanical and electrical sub-systems of the OS D3D Robotics prototyping system are provided. Next, Copper Carve, an OS custom graphical user interface, is developed to enable circuit board milling by implementing backlash and substrate distortion compensation. The performance of the OS D3D circuit mill is then quantified and validated for: positional accuracy, cut quality, feature accuracy and distortion compensation. Finally, the return on investment is calculated for inventors using it. The results show by properly compensating for motion inaccuracies with Copper Carve, the machine achieves a motion resolution of 10 microns, which is more than adequate for most circuit designs. The mill is at least five times less expensive than all commercial alternatives and the material costs of the D3D mill are repaid from fabricating 20-43 boards. The results show that the OS circuit mill is of high-enough quality to enable rapid invention and distributed manufacturing of complex products containing custom electronics.

3.2 Introduction

Domestic commerce started in the U.S. as household-level distributed manufacturing (DM) [1,2]. However, standardized high-volume, centralized mass production overtook it with the first industrial revolution and has made up the majority of domestic production until the present [3-8]. Recently many authors have argued that DM with 3-D printing can reduce costs for consumers for a wide range of products [9-13]. This can be accomplished with 3-D printing businesses manufacturing and selling products to consumers or other businesses [14-17]. As examples of the growing prevalence of this trend, 3-D printing stations are being added to commercial chains such as Home Depot [18] and the United Postal Service [19]. However, free and open source hardware (FOSH) development [20,21], provides a profitable investment for household-level DM with self-replicating rapid prototyper (RepRap) 3-D printers [22-24]. RepRap-centered DM of high-end products (e.g., scientific tools) has been shown to significantly reduce costs [25-30] and provides a high return on investments (ROIs) for science funders [31,32]. In addition, this model is being adopted by the average American consumer and the number of free pre-designed 3-D products of all kinds is also growing rapidly because of the economic benefits of DM for both DIY kits [33] as well as plug-and-play commercial 3-D printers [34]. Most strikingly, a recent study showed commercial 3-D

printers were economically viable even when used for only fabricating hard plastic toys [35] or flexible products from relatively-expensive specialty 3-D printing filament [36].

However, currently DM has matured primarily in mechanical products and components because of widespread cost declines in the open sourcing of 3-D printing [37]. Open source electronics has created many successful companies, because various open hardware business models work well with hobbyist electronics [38], however, DM of electronics is not as mature. For example, the fabrication stations at Home Depot [18] and the US Postal service [19] only include mechanical prototyping, but do not offer electronics. The lack of maturity in DM of open source electronics is a limiting factor in the complexity of products. There are two primary reasons for the slow adoption of DM circuit boards. First, there is a lack of unified sources for pre-designed projects, equivalent to sources for 3-D printable models like MyMiniFactory [39], Thingiverse [40], and YouMagine [41] or the search engine Yeggi [42]. There are some sources of FOSH circuitry such as Open Circuit Institute [43] and Open Circuits [44], though they have not been widely adopted. Most importantly, there are no widely recognized low-price FOSH circuit milling machines equivalent to the RepRap 3-D printers that can be built by consumers or purchased from companies like Lulzbot [45], re:3D [46] and Ultimaker [47]. The existing mills on the market are either prohibitively expensive [48], or lack proper documentation and are difficult to tune due to reliance on closed source designs [49]. The current traditional methods of circuit board procurement (ordering from fabrication shops) can be improved on in terms of both lead time and cost [50] with a low-cost FOSH circuit board mill.

This study provides open source designs for a low-cost circuit milling machine in order to overcome these limitations and enable DM of complex products containing custom electronics. The goal of the design is to provide an enabling device for inventors to make novel electronic designs by leveraging the same open source and peer to peer (P2P) methodologies found to be so successful in 3-D printing. The mill is thus designed around the open source D3D Robotics prototyping system [51], because of a low part count, scalability, and ability to be DM. First, this study provides the design modifications for the mechanical and electrical system of the D3D system. Next, a custom graphical user interface (GUI) open source software called Copper Carve is developed to enable circuit board milling. Copper Carve is minimalist in nature and made to be easily modified for other applications although here the implementations of two critical features, backlash compensation, and substrate distortion compensation are discussed for their importance to circuit board milling. The mathematics of these features are detailed and discussed. The performance of the open source circuit mill is quantified and validated for 1) positional accuracy, 2) quality of cut, 3) feature accuracy and 4) distortion compensation. Finally, the cost of the machine is considered, as well as a return on investment (ROI) analysis for using it.

3.3 Methods

First, the design (Figure 7) and construction of the device is discussed, as well as adaptations that must be made to customize D3D to this new application. Next, the major components of the software will be explained. Lastly, a standard operation procedure will be defined, as well as a validation procedure to characterize the machine and test for proper operation.

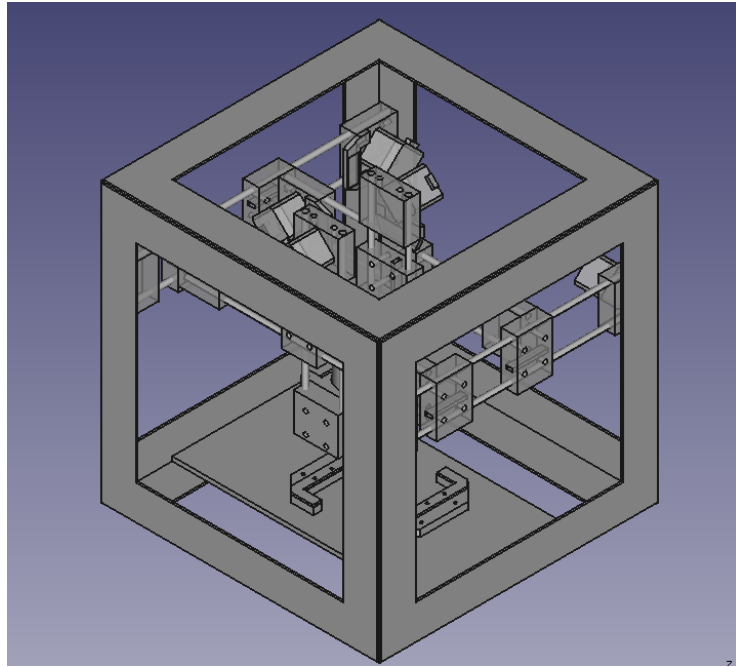


Figure 7: The FreeCAD model of the open source circuit mill.

3.3.1 Construction

3.3.1.1 D3D Design System

The D3D construction has already been proven by Open Source Ecology (OSE) [52], as an effective FFF 3-D printer [51]. The system itself consists of few original components for motion axes; motor pieces, idler pieces, and carriage pieces (Figure 8). A breakdown of the quantities of each piece used can be found in the machine bill of materials (BOM) available <https://osf.io/mf78v/>.

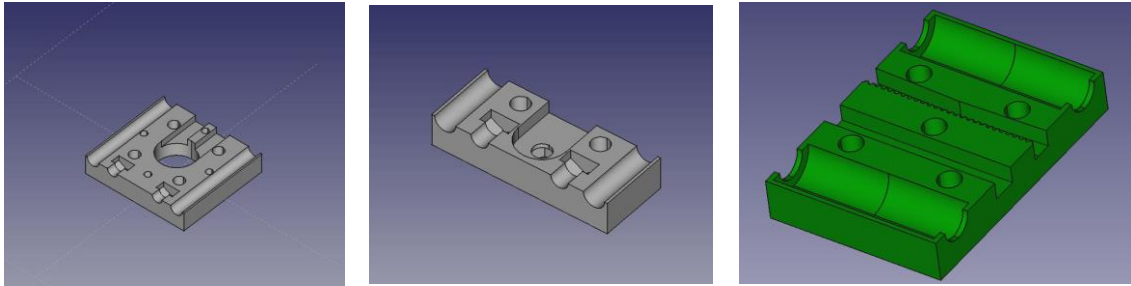


Figure 8: The 3-D printed component models for the D3D design system. (From left to right the rendered designs of the motor mounting block, bearing mount block, and carriage block are shown.

The mill is built inside of a 406.4 mm (16 inch) cubic space frame for rigidity, and ease of mounting. The D3D building blocks are all designed with short sockets for 10 pound neodymium magnets [54], which are used to easily connect and reconfigure components like the end stop interfaces. Magnets are also used to fixture the movement axes to the space frame.

Though it is not necessarily a D3D requirement, OSE recommends the utilization of the open source Arduino Mega [54], paired with a RAMPS motor control board [55]. The firmware used is a slight variation on the Marlin 3-D printer firmware [56]. A 12V DC power supply is used for motors [57], and a 0-50V DC supply is used for powering the spindle [58].

3.3.1.2 Custom Adaptions

A few custom components must be designed to facilitate the tool spindle (Figure 9a), and board holder (Figure 9b). In addition, each axis must be driven by two stepper motors to facilitate the loads associated with carrying the tool spindle, as well as milling into material. In addition, the Z axis requires a higher current supply than is on the RAMPS driver board, so a TB6600 based driver [59] is selected and split to two stepper motors.

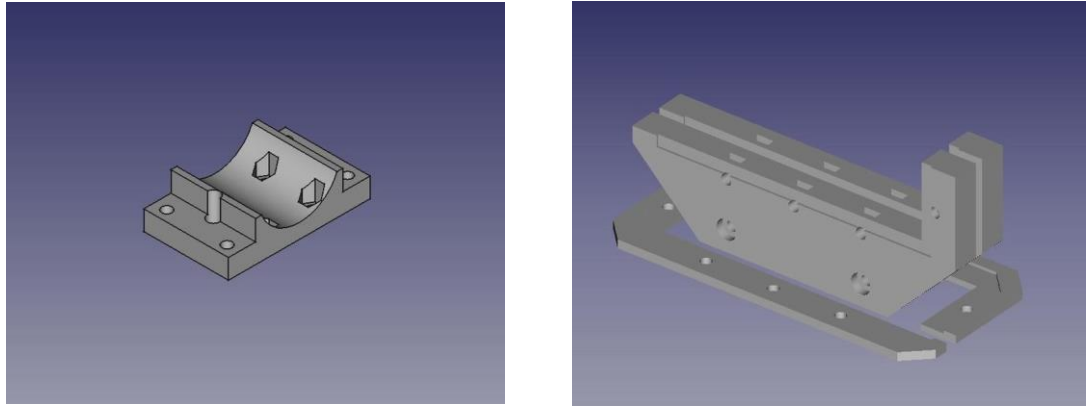


Figure 9a: The spindle mount model; Figure 9b: The board holder model

The last modifications are to add four compression springs to the Z axis linear rails. They are used to cancel the 1 kg of weight associated with the tool spindle. Since D3D is based around belt driven axes, the failure mode of the loaded Z axis would be to fall until it collides with the cutting surface – effectively breaking cutting tools or ruining the work piece. The addition of the springs mitigates this issue and changes the failure mode to lift the spindle or, at least maintain its position (when friction in the belt matches the forces caused by compressed springs).

3.3.2 Software – Copper Carve

Copper Carve (Figure 10) is programmed in C++ using the community edition of QT Creator [60]. The software is designed specifically to communicate with Marlin firmware and utilize the RAMPs board hardware configuration. Since Copper Carve is also intended to be used for other D3D based projects, it is designed to be a minimalistic backbone that can be expanded for other applications. Copper Carve is released under the open source license GNU GPL [61]. In order to maintain flexibility, the software is made to be as modular as possible. There are a few key required features that are described below.

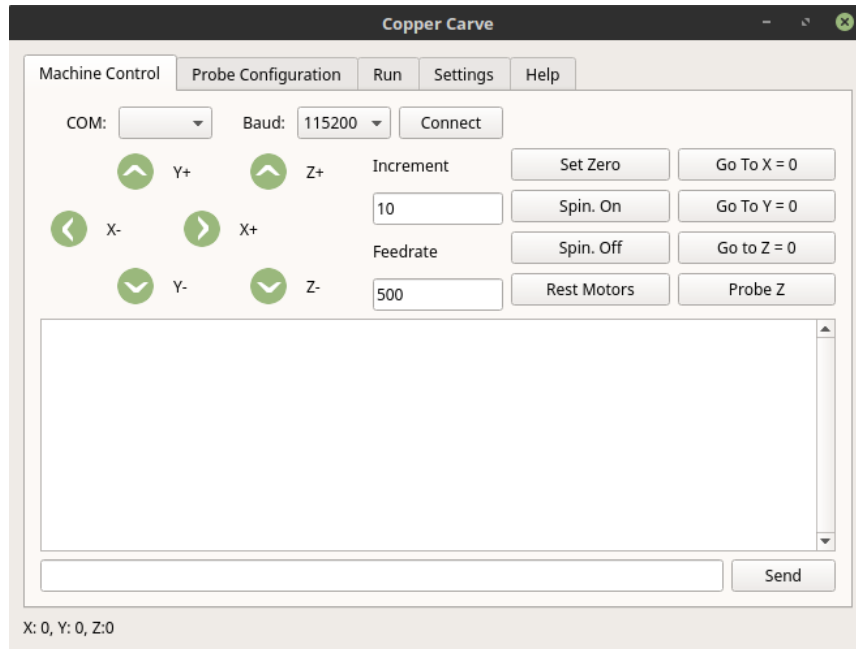


Figure 10: The Machine Control Interface of Copper Carve

3.3.2.1 Backlash Compensation

The first critical feature needed for PCB milling implemented in Copper Carve is backlash compensation. Mechanical backlash is a phenomenon caused when a movement axis changes direction. It is the maximum distance through which a mechanical component can be moved in one direction without applying appreciable force [62]. For example, as the drive belt and pulley have tolerances between their teeth, the pulley will “slip” a finite and predictable amount when moving to push against the reverse sides of the belt teeth. Backlash causes movement axes to move slightly smaller distances than commanded. This error can cause significant cutting errors when milling fine features such as completely removing 0.5 mm circuit traces.

There are two necessary steps to compensate for backlash: 1) detecting backlash, and 2) injecting movement instructions to accommodate the physical limitations of the system. Since all motion commands are sent through Copper Carve, backlash can be predicted by examining the sequence of sent G-Code commands. The algorithm is straightforward and detailed in pseudocode below.

```

If Motion Command
  For Each Direction
    If Direction != Previous Direction
      Call Compensate for Backlash
    End If
    Store Direction
  End For
End If

```

Once backlash has been detected, all other operation must be put on hold to allow the serial port to become available for compensation G-Code. This is detailed below in pseudocode.

```

Store Location
SendGCode(G91)//Relative Movement
For Each Direction
  If Backlash Present
    Move by backlash increment
  End If
End For
SendGCode(G90)//Absolute Movement
SendGCode(G92 Location)//Reset to Measured Location

```

3.3.2.2 Substrate Distortion Compensation

Commonly, inexpensive copper clad fiberglass used as a circuit board base material has a large degree of warpage as illustrated in Figure 11 (e.g. may vary in height by 2 mm). This warpage is considerable relative to the isolation routing cut depth of 0.1 mm. Because of this distortion, a lack of compensation will cause a failure to cut, or an increased cut depth – both of which will render the work piece unusable.



Figure 11: An illustration of substrate deformation

This warpage can be compensated for by adjusting G-Code files to follow the measured Z axis topology. This topology can be measured automatically using the cutting tool as a continuity probe for the digital input on the RAMPS board. An alligator clamp is used to

connect positive voltage to the cutting tool, and another clamp is used to connect the substrate to the digital input. By default, Marlin reports the location that the digital input is triggered (the digital input is configured as a Z end stop) and halts motion. Using this concept, paired with automated movement, height data can be collected for a grid of points of resolution and size determined automatically by Copper Carve (although it can still be modified by the user).

Once the topology is measured, the G-Code file can be transformed to conform to the measured mesh. This is accomplished by applying 3-D linear interpolation [63]. To start, assume a 2-D array of measured Z height data evenly spaced by ΔX and ΔY . Four points P , Q , R_I , and R_{II} define a rectangular region (visualized in Figure 12) that is offset from the reference origin (i.e. if P is $(0,0,Z)$, then X_{offset} and Y_{offset} will be 0).

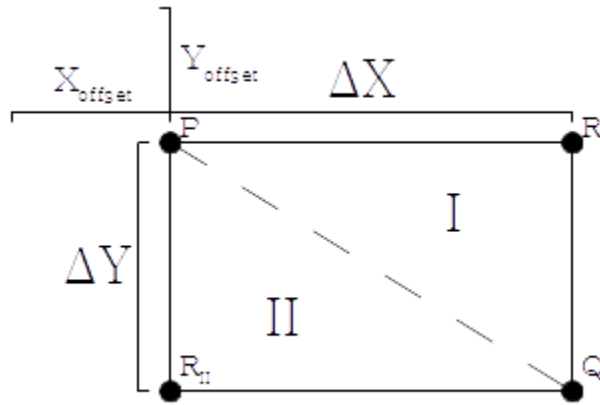


Figure 12: A sketch defining the regions and points used for 3D linear interpolation

First, confirm that a given point from the g-code falls in the region currently being examined. Assume an arbitrary point (X, Y) . In order for this point to fall in the region of concern, the following inequalities must be true:

$$X_{offset} \leq X \leq X_{offset} + \Delta X \dots (3)$$

$$Y_{offset} \leq Y \leq Y_{offset} + \Delta Y \dots (4)$$

Once a point is confirmed to be within the rectangular region, it must next be in sub region I or II. This is important because a plane can only be constrained by 3 points. The interpolation will always use P and Q , but it must be determined whether R_I or R_{II} is to be used. The point is in sub region I if the following inequality is true. This will indicate that R_I must be used for the interpolation.

$$\frac{X}{\Delta X} > \frac{Y}{\Delta Y} \dots (5)$$

If the above inequality is not satisfied, then the point is in sub region II, and satisfies the following relation. R_{II} must be used.

$$\frac{X}{\Delta X} \leq \frac{Y}{\Delta Y} \dots (6)$$

Once the location of the point in the height array is determine, the interpolation process can begin. First, define the points used for interpolation:

$$P = (X_1, Y_1, Z_1) \dots (7)$$

$$Q = (X_2, Y_2, Z_2) \dots (8)$$

$$R = (X_3, Y_3, Z_3) \dots (8)$$

From these three points, two vectors can be defined:

$$\overrightarrow{PQ} = \langle X_2 - X_1, Y_2 - Y_1, Z_2 - Z_1 \rangle \dots (10)$$

$$\overrightarrow{PR} = \langle X_3 - X_1, Y_3 - Y_1, Z_3 - Z_1 \rangle \dots (11)$$

Now it is possible to find the normal vector formed by \overrightarrow{PQ} and \overrightarrow{PR} . This can be done by carrying out the cross product:

$$\vec{n} = \overrightarrow{PQ} \times \overrightarrow{PR} = \begin{vmatrix} \vec{i} & \vec{j} & \vec{k} \\ X_2 - X_1 & Y_2 - Y_1 & Z_2 - Z_1 \\ X_3 - X_1 & Y_3 - Y_1 & Z_3 - Z_1 \end{vmatrix} \dots (12)$$

The value of this determinate is found to be:

$$\vec{n} = (Y_2 - Y_1)(Z_3 - Z_1)\vec{i} + (Z_2 - Z_1)(X_3 - X_1)\vec{j} + (X_2 - X_1)(Y_3 - Y_1)\vec{k} - (Y_2 - Y_1)(X_3 - X_1)\vec{k} - (Z_2 - Z_1)(Y_3 - Y_1)\vec{i} - (X_2 - X_1)(Z_3 - Z_1)\vec{j} \dots (13)$$

In order to keep equations orderly, short hand representations are defined for \vec{i} , \vec{j} , and \vec{k} components of the above equation:

$$L = [(Y_2 - Y_1)(Z_3 - Z_1) - (Z_2 - Z_1)(Y_3 - Y_1)]\vec{i} \dots (14)$$

$$M = [(Z_2 - Z_1)(X_3 - X_1) - (X_2 - X_1)(Z_3 - Z_1)]\vec{j} \dots (15)$$

$$N = [(X_2 - X_1)(Y_3 - Y_1) - (Y_2 - Y_1)(X_3 - X_1)]\vec{k} \dots (16)$$

A 3-D plane can now be defined given the normal vector and a point on the plane, which is assumed to be our point undergoing adjustment (X, Y, Z) , where X and Y are known, and Z is a known value that will be modified.

$$L(X - X_1) + M(Y - Y_1) + N(Z - Z_1) = 0 \dots (17)$$

Finally, solving for Z , a solution is attained:

$$Z = \frac{-L(X-X_1)-M(Y-Y_1)}{N} - Z_1 \dots (18)$$

Using equation 18, each G-Code position can be modified to conform to the measured height mesh.

3.3.2.3 Usage of Timers

In an attempt to keep the code of Copper Carve as comprehensible as possible, QT timers are implemented to handle long or continuing processes such as G-Code streaming or the auto leveling procedure. The timers are used to break up the execution of a sub process and allows for multiple processes to be executed in a parallel and scheduled manner. These same processes could be handled with multi-threading methods, however the implementation in QT would not be easily comprehensible by the lay user.

3.3.2.4 Usage of Timers

Though Copper Carve is made to directly interface with the D3D mill, some considerations have been made. Each G-Code command feeds through an auto-replace function that references a file “substitutions.txt”. This can be used to alter G-Code based on which CAM software is being used, or which firmware the target machine contains.

3.3.3 Mill Usage Workflow

The mill has a specific set of constraints that define minimum specifications of the designed circuit board. In this section, a process is detailed to insure manufacturing that meets these specifications.

3.3.3.1 Board Design

It is recommended that circuit boards are designed in KiCAD [64], since the software is FOSS and fits well with the toolchain. It is required to have a minimum trace spacing of 0.2 mm and a minimum trace width of 0.5 mm. Any smaller trace width will result in the trace being cut completely off of the board.

Once the board is designed, the auxiliary axis must be placed near the circuit board (preferably in the bottom left corner of the edge.cuts layer) in order to reduce any large locational offset from the origin.

3.3.3.2 FlatCAM

The Gerber files are converted to machine readable G-Code files. This is done with the open source PCM CAM package, FlatCAM [65]. Tool settings may vary depending on the specific tool selected. However, a typical cut depth for traces and pads is 0.1 mm. Feed rate for V shaped engraving bits [66] should be 50 mm/minute, and end mills should be 100 mm/minute.

3.3.4 Validation

Circuit board milling requires tight tolerances, otherwise the board will likely malfunction. Because of this, the machine must be tightly calibrated and characterized.

3.3.4.1 Positional Accuracy

First, the positional accuracy of each axis must be measured. This can be done with a dial indicator set up similar to Figure 13.

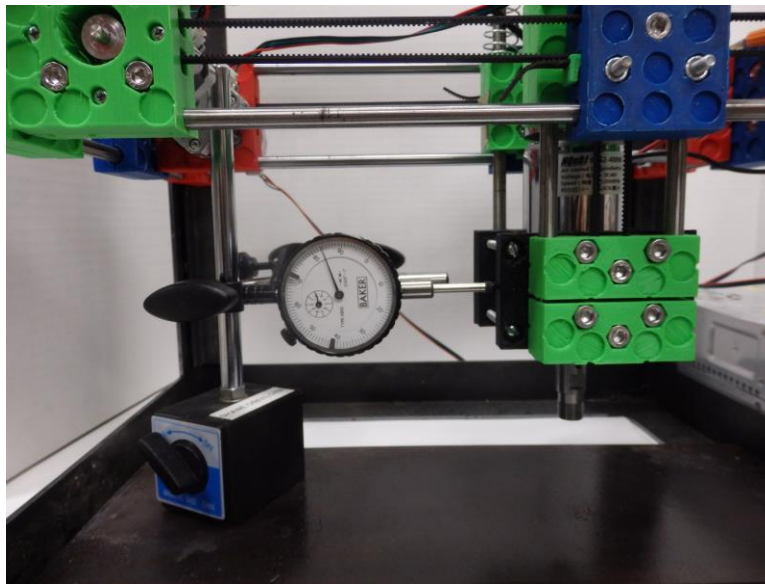


Figure 13: Setup of dial indicator for measuring backlash on X-axis

First, the axis is jogged a small value (1 mm) in the positive direction. The indicator is zeroed, then another positive movement is called of a known value. The actual movement is measured and compared. If there is a discrepancy between the two, the steps per mm value for that axis must be adjusted using the M92 command.

Using the same dial indicator setup, the backlash can be measured; but only after the steps per mm value has been validated. To measure backlash, the position is moved in the negative direction a small value (1 mm). The indicator is then zeroed, and the axis is

jogged in the positive direction. The difference between command and the measured distance is the backlash value. This value is placed in Copper Carve's option screen for each axis. With these values updated, the same test can be performed, and if the compensation is successful, there should be no difference between the movement command and the measured movement.

Quality of Mill Cut

A quality cut is defined as a non-destructive cut in the substrate with minimum burring on the copper edges. This is observed both visually, and with an Olympus PME3 optical microscope, using 50X magnification.

3.3.4.2 Feature Accuracy

Trace width can be a critical dimension, so it is important that their parameters appear on the board as designed. Using an optical microscope, a known trace width can be measured and compared with the intended value. If the measurement is off this can indicate that either the steps per mm, or backlash values were not properly calibrated.

As an additional test, the pattern in Figure 14 is milled out 20 times in both the X and Y axis. This pattern is designed such that the left most rectangle's width will not be affected by backlash errors. The right rectangle will be affected by backlash in movement 3, causing the width of the rectangle to be thinner than the left rectangle. Data gathered from this experiment will show both feature variation, and compensation effectiveness.

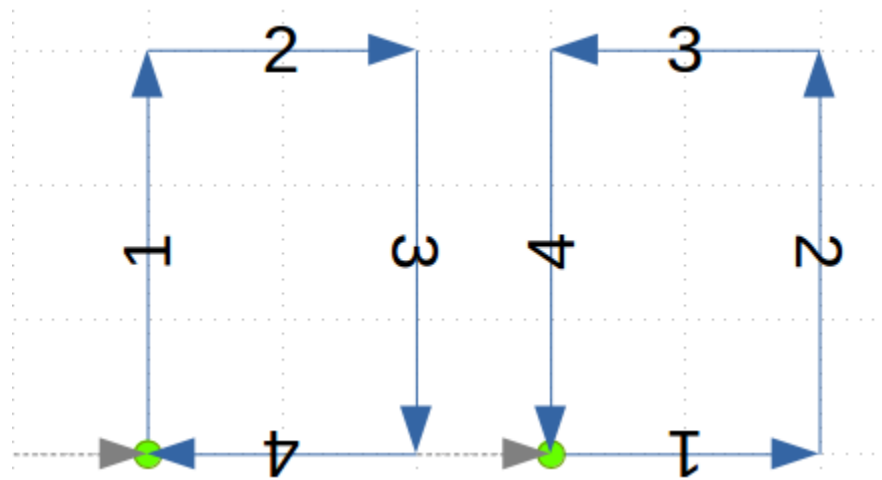


Figure 14: A test pattern to verify feature repeatability and backlash compensation effectiveness.

3.3.4.3 Distortion Compensation Validation

The distortion compensation can be observed by introducing an extreme situation. The copper clad fiber glass is fastened to a piece of wood, cut to set the board at a 10 degree

angle to the cutting surface. A test pattern is then milled, and observed for Z axis accuracy (i.e. under or over-cutting)

3.4 Results

3.4.1 Overall Designs

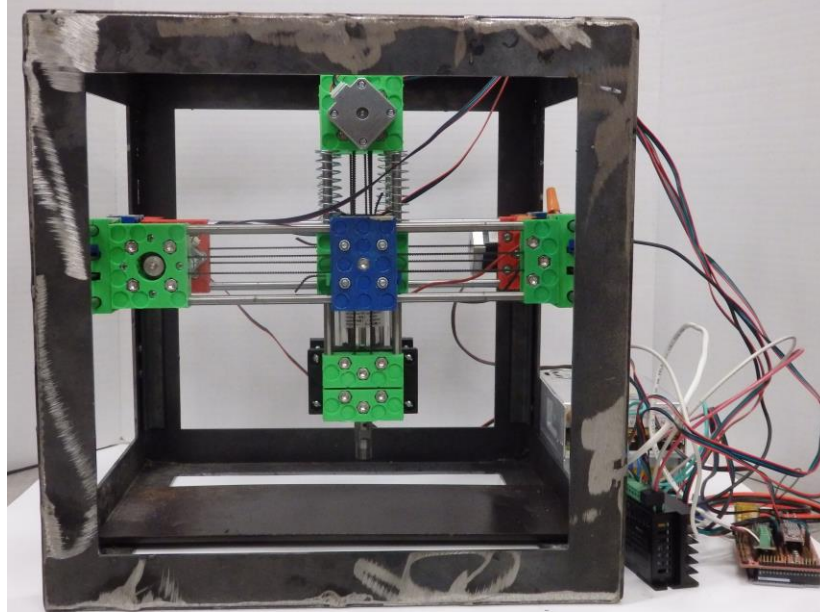


Figure 15: An image of the completed circuit mill

The completed design has been proven to be robust and suitably accurate. The D3D design system has proven itself as a framework for creating low-cost, minimalist, and scalable machines. The machine itself can be constructed during a small 8 hour build time. A comprehensive bill of materials (see <https://osf.io/mf78v/>) shows that the mill costs US\$500 in parts.

3.4.2 Positional Accuracy

The positional accuracy of the machine is found to be suitable for the purpose of cutting most circuit board designs. Thanks to properly implemented motion compensation techniques, the machine step resolution is at the hard limit of 0.01 mm for the X and Y axis, and 0.008 mm for the Z axis. The overall machine characteristics are shown in Table 3.

When measuring machine backlash, a dial indicator can allow for accurate measurements up to 0.0254 mm. This value cannot be directly input into Copper Carve, however. Instead, the value must be some multiple of the resolution. This is because the stepper

motors cannot physically make a “fraction” of a step. Once the values are measured to the fullest accuracy of the dial indicator, they are fine-tuned incrementally by cutting the test pattern in Figure 14, until the rectangles have identical widths.

Table 3: Motion specifications for the circuit mill

Motion Parameter	X Axis (mm)	Y Axis (mm)	Z Axis (mm)
Resolution	0.01	0.01	0.01
Backlash	0.252	0.075	0.01
Rounded Backlash	0.25	0.08	0.01

3.4.3 Quality of Mill Cut

It is desirable to minimize post processing of the boards. One large post processing step is sanding the circuit board to rid the copper cut edges of burrs. By sweeping different cutting feed rates and depth, an optimal configuration can be found. The following samples in Figure 16 are all analyzed visually for the amount and size of burrs present. In this case, it appears operating at a feed rate of 50 mm/min and a cutting depth of 0.2 mm yields the fewest, and smallest burrs.

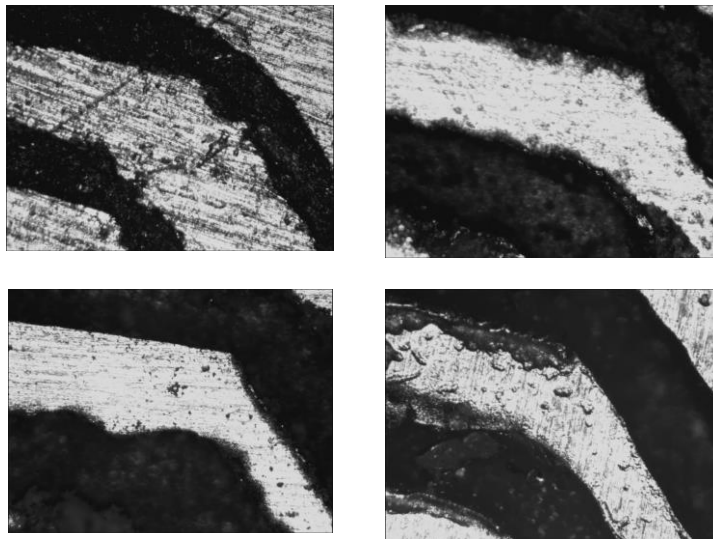


Figure 16: Top row from left to right: (1) Feedrate of 50mm/min, plunge depth of 0.1mm, (2) Feedrate of 100mm/min, plunge depth of 0.1mm, Bottom row: (3) Feedrate of 150mm/min plunge depth of 0.1mm, (4) At 50mm/min, plunge depth of 0.2mm,

3.4.4 Feature Accuracy

A semi-octagonal shape is cut into the copper with a copper trace of widths 0.5 mm and 1 mm. An octagonal shape is chosen to view all common cutting orientations (Figure 17). The minimum width of each feature is measured and compared with the target in Table 4. The width of the cut is also measured and used to adjust the error percentage. This adjustment is made by subtracting the error of the nominal cut width (0.2 mm). This shows that if proper adjustments are made in the CAM software, the indicated error can be achieved.

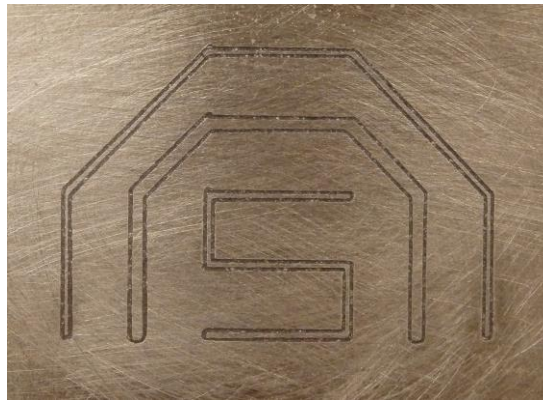


Figure 17: An image of the octagonal shape used to verify feature accuracy

Table 4: A comparison of feature accuracies at different cutting speeds.

Cutting Speed	Width of 0.5mm Trace	Percent Error of 0.5mm Trace	Width of 0.2mm Cut	Percent Error of 0.5mm Trace Adjusted
50 mm/min	0.40mm	20%	0.25mm	10%
100 mm/min	0.35mm	30%	0.35mm	0%
150 mm/min	0.20mm	60%	0.40mm	20%

The 20 patterns for X and Y are milled according to Figure 14. The widths of both the control (right rectangle) and variable (left rectangle) are measured in ImageJ [73] by analyzing a photograph taken with an Olympus Stylus digital camera and a reference scale. The results are displayed in a histogram to demonstrate the distribution of widths of the control and variable rectangles.

Figure 18 suggests that the X axis follows a Gaussian distribution, with a standard deviation of 0.03 mm. This measured deviation is well below the threshold for significant error. Additionally, comparing the means of the distributions for no-back-lash shapes with back-lash induced shapes, there is an offset of 0.045 mm. This indicates that the backlash compensation used during this test is off by 0.045 mm. Ideally the two distributions should be overlapped completely.

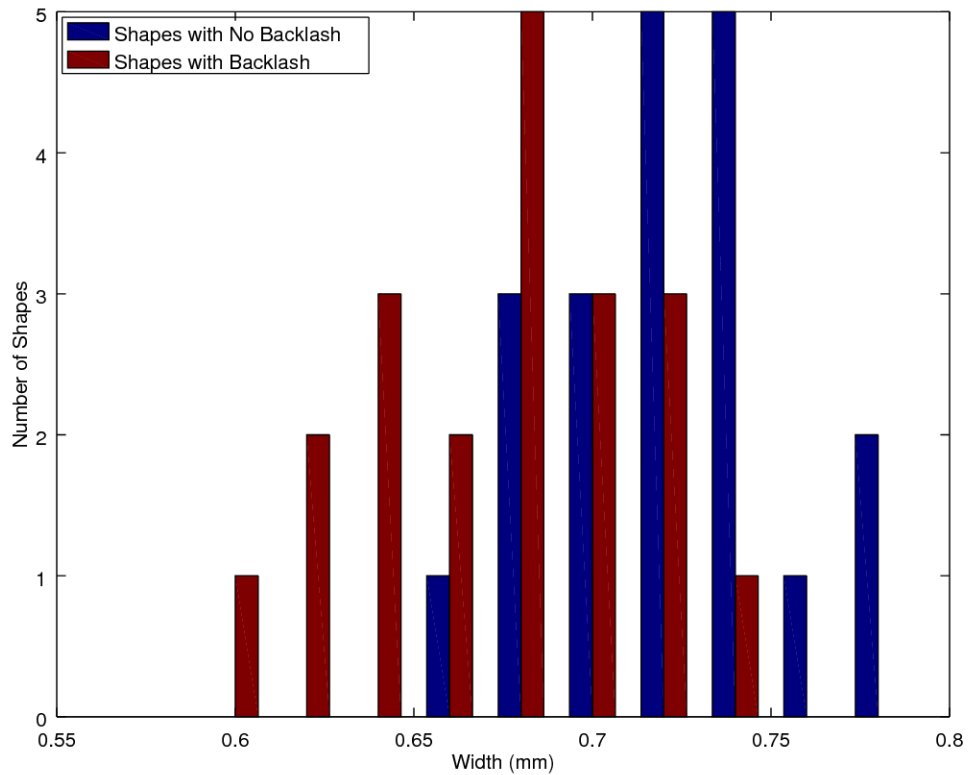


Figure 18: A histogram of feature widths measured on the X axis

Figure 19 shows the two distributions for shapes cut with respect to the Y axis. Unlike Figure 18, the distributions do not follow any apparent trend. However, the standard deviation of the back-lash induced rectangles have a standard deviation of 0.02 mm. The means of each distribution have a space of 0.253 mm, indicating that the backlash compensation used to cut these patterns was not properly selected.

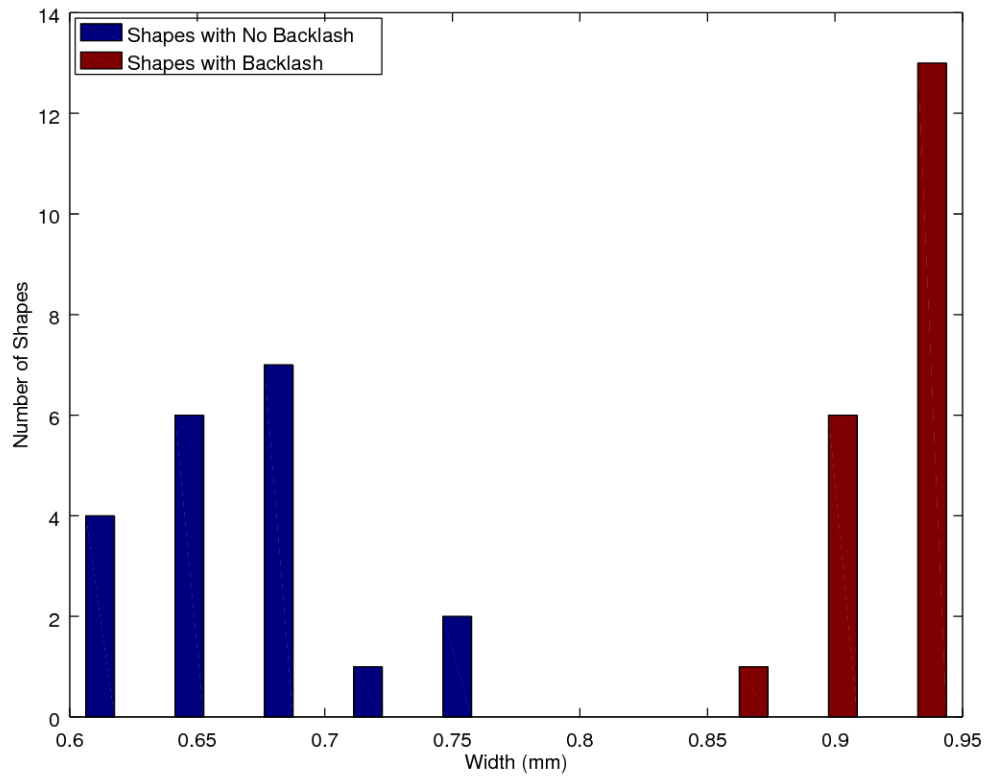


Figure 19: A histogram of feature widths measured on the Y axis

3.4.5 Distortion Compensation

The milling on an incline is executed successfully. The cut board can be viewed in Figure 20. The board is inspected using a flashlight to verify full cuts at all necessary areas. The inspection revealed one error – a failed cut (indicated by the red circle in Figure 20). This error can be remedied by increasing the cut depth by a small increment (0.01 mm). Additionally, the G-Code tool path is rendered in Figure 21 and 22, and visually inspected to follow the expected incline. The code successfully follows the angle, and the error likely occurred from slight measurement error, or a too-shallow cut depth.

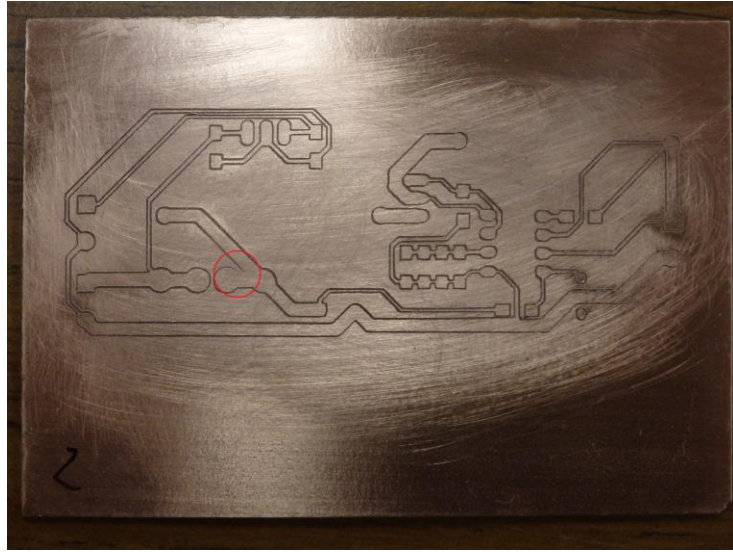


Figure 20: The resultant circuit board which was milled on a 10° incline

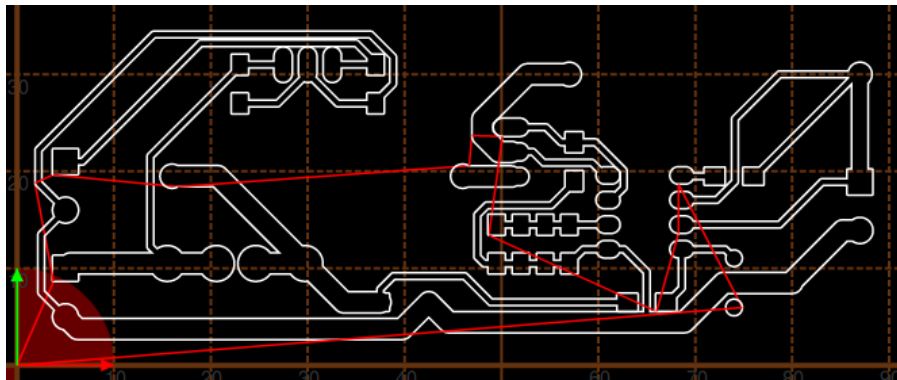


Figure 21: The rendered tool path in the XY axis



Figure 22: The rendered toolpath in the XZ axis

3.5 Discussion

3.5.1 Open Source as Development Platform

This study joins several others [21,25,67] and stands as a testament to the effectiveness of open source technology as a hardware development platform. Very few components to this mill were designed from scratch thanks to contributions like D3D [51], RAMPS [55], Marlin [56], and communities, such as OSE and Arduino that provide helpful support groups and openly welcome contributions back to their library of work. Open source is typically modular and scalable, which maximizes its potential applications [67]. Because of open source emphasis on DM, this machine was capable of being manufactured with a minimum number of tools, or knowledge of manufacturing processes. Now the mill explored in this paper can act as an enabling device for encouraging electronics-based invention and the proliferation of DM of open source electronics.

3.5.2 D3D and Other Applications

Copper Carve is built around the philosophy that open source software should be coded in a way that the target audience can make meaningful modifications to the software. This philosophy requires a skilled programmer to prefer lower level (potentially more complex) solutions, than efficient solutions that invoke obscure or higher-level functions. For example, Copper Carve works for an electronics mill. Typical users of the mill will be electrical engineers, students, inventors and hobbyists. Therefore, it makes sense to consider what kind of modifications the target audience may be making, and what level of programming they may be familiar with. That is why it why Copper Carve does not utilize multi-threaded process, as they require a relatively high knowledge of computer science to properly utilize and modify. A core group of hardy functions, such as `SendGCode()` are established so they can easily be implemented for purposes such as scripted buttons, or custom processes by the target audience.

3.5.3 Software Philosophy

Copper Carve is built around the philosophy that open source software should be coded in a way that the target audience can make meaningful modifications to the software. This philosophy requires a skilled programmer to prefer lower level (potentially more complex) solutions, than efficient solutions that invoke obscure or higher-level functions. For example, Copper Carve works for an electronics mill. Typical users of the mill will be electrical engineers, students, and hobbyists. Therefore, it makes sense to consider what kind of modifications the target audience may be making, and what level of programming they may be familiar with. That is why it why Copper Carve does not utilize multi-threaded process, as they require a relatively high knowledge of computer science to properly utilize and modify. A core group of hardy functions, such as `SendGCode()` are established so they can easily be implemented for purposes such as scripted buttons, or custom processes.

3.5.4 Market Comparison

Commercial circuit board milling machines can cost as much as 3,199 USD [69], which is comparatively expensive in regard to the D3D mill explored in this study. All mills have identical resolutions, and though the maximum speeds seen in commercial systems can improve cutting times, they are limited by the maximum feed rate allowed by the cutting tool, which is well below 1,000 mm/min. Thus the maximum travel speeds are not a major advantage in real-world milling. The final category compared in Table 5, max milling speed, is thus a non-issue when considering the maximum allowable speeds used while milling. This high speed found in other devices is only useful in manual jogging operations, which is a small part of the overall operation. Commercial alternatives are often shipped assembled and ready to use, but because of that, are not scalable nor easily maintainable in cases of a part breakage. The cost of the D3D mill is for the materials only.

Table 5: A comparison of commercial circuit mills to the D3D mill

Name	Price (USD)	Resolution (mm)	Working Area	Max Travel Speed (mm/min)
D3D Mill*	500	0.01	140x200	500
Othermill [69]	3,199	0.01	140x114	2600
Prometheus [70]	1,799	0.01	160x100	3,800
DWR-0906 [71]	1,495	0.01	220x160	2,500
3D Nomad [72]	2,499	0.01	203x203	2,500

*Material Cost only

The mill can be constructed in 10 hours and requires only a 3D printer, a chop saw, a power sander, and a soldering iron. This time does not include time spent 3D printing axis components. The machine construction requires minimal knowledge of electrical wiring, and mechanical assembly. Once the mill is assembled, basic knowledge of mechanical measurements is required in order to validate axial motion.

The price of each mill also weighs heavily on their respective return on investment (ROI). For this analysis, it assumed that unique 100 mm X 80 mm single layer circuit boards are being manufactured. Based on quotes generated from many PCB fabrication sources [50], a board can be ordered for 12.22 USD, if 27 day shipping is selected. From the same source, a board can be ordered for 25.36 USD if 10 day shipping is selected. The labor costs in using the D3D system are relatively trivial and the system does not need to be monitored during fabrication of a circuit. The energy use during the milling of

a standard board was 0.5 kWh, and therefore the energy costs were also ignored. Thus, the only consumable material for the D3D circuit mill is the copper-clad fiber glass, which can cost as low as 0.42 USD [74]. Simply dividing the cost of the mill by the cost per board less the cost to produce on the D3D mill, 43 boards (27 day shipping) or 20 boards (10 day shipping) must be produced in order to recoup the investment for the material costs of the D3D Mill. Compared to commercial alternatives, this can be as 6 times as many boards (258 27-day boards, 120 10-day boards). Although, the use of DM for circuit manufacture will cost less with any of the systems in Table 5, the most valuable asset of DM is the quick turnaround delivered by circuit mills: 2 to 3 hours compared to a minimum of 10 days. This allows inventors and circuit designers to quickly iterate on designs of new boards.

Milling 43 boards is a highly achievable feat during the lifetime of the mill. For example, the base power meter used to monitor an open source home includes 11 boards [75]. With this single project, the mill has already paid for a quarter of its BOM cost. Also, the design process itself for perfecting a new invention is likely to go through multiple iterations and revisions. There are also many cases where the mill could be used as a communal tool, such as research laboratories, fablabs or makerspaces. In all cases, the 43 board threshold can be met in a very short span of time.

3.5.5 Additional Applications & Future Work

The D3D circuit mill has added utility that has not yet been explored. The mill can be used to cut out 2-D components from wood, or plastics. Additionally, the mill can be used to engrave many materials from wood, plastic, and most metals. Due to the relatively low torques the mill is designed for, it is likely that these tasks can be achieved by using small cut depths, and lower feed rates.

In addition to exploring additional applications of the milling machine, Copper Carve can be modified to have many desirable features; such as tool path preview, motion optimization, height map output, and multi-machine communication (for large production systems).

3.6 Conclusions

The open source D3D based circuit mill has proven to be a fully-functional circuit board mill that is constructed entirely on open source platforms. By properly compensating for motion inaccuracies with the open source Copper Carve, the machine has achieved a motion resolution of 0.01 mm, which corresponds to the step size of the stepper motor. The mill is at least five times less expensive than all commercial alternatives, with manufacturing capabilities that can fabricate by most design standards. This allows the materials costs of the D3D mill to be recouped in as little as 20 boards while offering users several hours turnaround time between design iterations for inventors instead of 10 days.

3.7 References

1. Tryon, R.M. Household Manufactures in the United States 1640–1860: A Study in Industrial History; University of Chicago Press: Chicago, IL, USA, 1917.
2. Sokoloff, K.; Villaflor, G. The Market for Manufacturing Workers. In *The Market for Manufacturing Workers during Early Industrialization: The American Northeast, 1820 to 1860*; Goldin, C., Rockoff, H., Eds.; University of Chicago Press: Chicago, IL, USA, 1992.
3. Hounshell, D. *From American System to Mass Production, 1800–1932*; Johns Hopkins University Press: Baltimore, MD, USA, 1984.
4. Fine, C.; Freund, R. *Economic Analysis of Product-Flexible Manufacturing System Investment Decisions*; Massachusetts Institute of Technology: Cambridge, MA, USA, 1986; pp. 1757–1786.
5. Wilson, J. Henry Ford vs. Assembly Line Balancing. *Int. J. Prod. Res.* **2013**, *52*, 757–765.
6. Kravis, I.; Lipsey, R. *Towards an Explanation of National Price Levels*; Working Paper Series 1034; National Bureau of Economic Research: Cambridge, MA, USA, 1982.
7. Lipsey, R. Challenges to Home- and Host-Country Effects of Foreign Direct Investment. In *Challenges to Globalization: Analyzing the Economics*; Baldwin, R.E., Winters, A., Eds.; University of Chicago Press: Chicago, IL, USA, 2004.
8. Bain, J. Economies of Scale, Concentration and the Condition of Entry in Twenty Manufacturing Industries. *Am. Econ. Rev.* **1954**, *44*, 15–39.
9. Scan, B. How to Make (almost) Anything. *The Economist*, 2005. Available online: <http://www.economist.com/node/4031304> (accessed on 11 October 2017).
10. Gershenfeld, N. How to Make almost Anything: The Digital Fabrication Revolution. 2012. Available online: <http://cba.mit.edu/docs/papers/12.09.FA.pdf> (accessed on 28 October 2017).
11. Markillie, P. A Third Industrial Revolution. *The Economist*, 2012. Available online: <http://www.economist.com/node/21552901> (accessed on 11 October 2017).
12. Gwamuri, J.; Wittbrodt, B.; Anzalone, N.; Pearce, J. Reversing the Trend of Large Scale and Centralization in Manufacturing: The Case of Distributed Manufacturing of Customizable 3-D-Printable Self-Adjustable Glasses. *Chall. Sustain.* **2014**, *2*, 30–40.
13. Wittbrodt, B.; Laureto, J.; Tymrak, B.; Pearce, J. Distributed Manufacturing with 3-D Printing: A Case Study of Recreational Vehicle Solar Photovoltaic Mounting Systems. *J. Frugal Innov.* **2015**, *1*, 1–7.
14. Wohler, T. *Wohlers Report 2016: 3D Printing and Additive Manufacturing State of the Industry Annual Worldwide Progress Report*; Wohlers Associates Inc.: Fort Collins, CO, USA, 2016.
15. Anderson, P.; Sherman, C.A. A discussion of new business models for 3D printing. *Int. J. Technol. Mark.* **2007**, *2*, 280–294.
16. Laplume, A.; Petersen, B.; Pearce, J. Global value chains from a 3D printing perspective. *J. Int. Bus. Stud.* **2016**, *47*, 595–609.

17. Laplume, A.; Anzalone, G.; Pearce, J. Open-source, self-replicating 3-D printer factory for small-business manufacturing. *Int. J. Adv. Manuf. Technol.* **2015**, *85*, 633–642.
18. HOME DEPOT | DIY MEETS MIY (MAKE IT YOURSELF). Available online: <https://www.makerbot.com/media-center/2014/07/14/home-depot-diy-meets-miy-make> (accessed on 22MAR2018)
19. Ariel Bogle. Can UPS Help Make 3-D Printing Mainstream?. Available online: http://www.slate.com/blogs/future_tense/2013/08/02/ups_plans_to_test_3_d_printing_services_in_u_s_stores.html (accessed on 22MAR2018)
20. Weber, S. *The Success of Open Source*; Harvard University Press: Cambridge, MA, USA, 2004.
21. Gibb, A.; Abadie, S. *Building Open Source Hardware: DIY Manufacturing for Hackers and Makers*, 1st ed.; Addison-Wesley Professional: Boston, MA, USA, 2014.
22. Sells, E.; Bailard, S.; Smith, Z.; Bowyer, A.; Olliver, V. RepRap: The Replicating Rapid Prototyper-Maximizing Customizability by Breeding the Means of Production 2010. In *Proceedings of the World Conference on Mass Customization and Personalization*, Cambridge, MA, USA, 7–10 October 2007.
23. Jones, R.; Haufe, P.; Sells, E.; Iravani, P.; Olliver, V.; Palmer, C.; Bowyer, A. RepRap-the Replicating Rapid Prototyper. *Robotica* **2011**, *29*, 177–191
24. Bowyer, A. 3D Printing and Humanity's First Imperfect Replicator. *3D Print. Addit. Manuf.* **2014**, *1*, 4–5.
25. Pearce, J. Building Research Equipment with Free, Open-Source Hardware. *Science* **2012**, *337*, 1303–1304.
26. Pearce, J. *Open-Source Lab: How to Build Your Own Hardware and Reduce Research Costs*, 1st ed.; Elsevier: Waltham, MA, USA, 2014.
27. Baden, T.; Chagas, A.; Marzullo, T.; Prieto-Godino, L.; Euler, T. Open Laware: 3-D Printing Your Own Lab Equipment. *PLoS Biol.* **2015**, *13*, e1002086.
28. Blua, A. A New Industrial Revolution: The Brave New World of 3D Printing. Radio Free Europe/Radio Liberty. 2013. Available online: <http://www.rferl.org/content/printing-3d-new-industrial-revolution/24949765.html> (accessed on 11 October 2017).
29. Zhang, C.; Anzalone, N.C.; Faria, R.P.; Pearce, J.M. Open-source 3D-printable optics equipment. *PLoS ONE* **2013**, *8*, e59840.
30. Coakley, M.; Hurt, D.E. 3D Printing in the Laboratory: Maximize Time and Funds with Customized and Open-Source Labware. *J. Lab. Autom.* **2016**, *21*, 489–495.
31. Pearce, J. Quantifying the Value of Open Source Hardware Development. *Mod. Econ.* **2015**, *6*, 1–11.
32. Pearce, J.M. Return on investment for open source scientific hardware development. *Sci. Public Policy* **2016**, *43*, 192–195.
33. Wittbrodt, B.; Glover, A.; Laureto, J.; Anzalone, G.; Oppliger, D.; Irwin, J.; Pearce, J. Life-Cycle Economic Analysis of Distributed Manufacturing with Open-Source 3-D Printers. *Mechatronics* **2013**, *23*, 713–726

34. Petersen, E.E.; Pearce, J. Emergence of Home Manufacturing in the Developed World: Return on Investment for Open-Source 3-D Printers. *Technologies* **2017**, *5*, 7.
35. Petersen, E.E.; Kidd, R.W.; Pearce, J.M. Impact of DIY Home Manufacturing with 3D Printing on the Toy and Game Market. *Technologies* **2017**, *5*, 45.
36. Woern, A. L., & Pearce, J. M. (2017). Distributed Manufacturing of Flexible Products: Technical Feasibility and Economic Viability. *Technologies*, *5*(4), 71
37. Rundle, Guy. A Revolution in the Making. Simon and Schuster, 2014.
38. Pearce, Joshua M. Emerging business models for open source hardware. *Journal of Open Hardware* *1*, no. 1 (2017).
39. MyMiniFactory. Available online: <https://www.myminifactory.com/> (accessed 22MAR2018)
40. Thingiverse. Available online: <https://www.thingiverse.com/> (accessed 22MAR2018)
41. Youmagine. Available online: <https://www.youmagine.com/> (accessed 22MAR2018)
42. Yeggi. Available online: <http://www.yeggi.com/> (accessed 22MAR2018)
43. Open Circuit Institute Available online: <http://opencircuitinstitute.org/> (accessed 22MAR2018)
44. Open Circuits. Available online: http://www.opencircuits.com/Main_Page (accessed 22MAR2018)
45. Lulzbot. Available online: <https://www.lulzbot.com/> (accessed 22MAR2018)
46. Re:3D. Available online: <https://re3d.org/> (accessed 22MAR2018)
47. Ultimaker. Available online: <https://ultimaker.com/> (accessed 22MAR2018)
48. Bantam Tools Desktop PCB Milling Machine. Available online: <https://www.bantamtools.com/products/bantam-tools-desktop-pcb-milling-machine> (accessed 22MAR2018)
49. Konmison DIY CNC Router Kits Wood Carving Milling Engraving Machine. Available online: <http://a.co/geXc8sF> (accessed 22MAR2018)
50. PCBShopper. Available online: <https://pcbshopper.com/> (accessed 22MAR2018)
51. D3D. Available online: <http://opensourceecology.org/wiki/D3D> (accessed 22MAR2018)
52. Open Source Ecology. Available online: <https://www.opensourceecology.org/> (accessed 22MAR2018)
53. N42 12mm x 3mm Super Strong Round Magnets Disc Rare Earth Neodymium Magnet. Available online: <http://r.ebay.com/8zLeQR> (accessed 22MAR2018)
54. Arduino MEGA 2560. Available online: <https://www.arduino.cc/en/Main/ArduinoBoardMega2560?setlang=en> (accessed 22MAR2018)
55. RAMPS 1.4. Available Online: http://reprap.org/wiki/RAMPS_1.4 (accessed 22MAR2018)
56. Open Source 3D Printer Firmware. Available Online: <http://marlinfw.org/> (accessed 22MAR2018)
57. 2v 30a Dc Universal Regulated Switching Power Supply. Available Online: <http://a.co/hGDIMnD> (accessed 22MAR2018)

58. Adjustable DC Power Voltage Converter AC 110V-220V to DC 0-48V. Available Online: <http://a.co/er5nsEW> (accessed 22MAR2018)
59. TB6600 4A 9-42V Stepper Motor Driver CNC Controller. Available Online: <http://a.co/hc05ezE> (accessed 22MAR2018)
60. QT. Available Online: <https://www.qt.io/> (accessed 22MAR2018)
61. GNU General Public License. Available Online: <https://www.gnu.org/licenses/gpl.html> (accessed 22MAR2018)
62. Bagad, V. S. "Mechatronics. Pune." (2009).
63. Stewart, James. Multivariable Calculus. Australia: Brooks/Cole, 2012.
64. KiCAD EDA. Available Online: <http://kicad-pcb.org/> (accessed 22MAR2018)
65. FlatCAM. Available Online: <http://flatcam.org/> (accessed 22MAR2018)
66. EnPoint Engraving Bit. Available Online: <http://a.co/eMNTd7l> (accessed 22MAR2018)
67. Oberloier, Shane, and Joshua M. Pearce. General Design Procedure for Free and Open-Source Hardware for Scientific Equipment. Designs 2, no. 1 (2017): 2.
68. Wijnen, Bas, Emily J. Hunt, Gerald C. Anzalone, and Joshua M. Pearce. "Open-source syringe pump library." PloS one 9, no. 9 (2014): e107216.
69. "Bantam Tools Desktop PCB Milling Machine." Bantam Tools. Available Online: <https://www.bantamtools.com/products/bantam-tools-desktop-pcb-milling-machine>. (accessed 22MAR2018)
70. "Prometheus PCB Milling Machine and Accessories." Zippy Robotics, Inc. Available Online: <https://shop.zippyrobotics.com/>. (accessed 22MAR2018)
71. "Desktop CNC Router Table - DWR-0906." Baileigh Industrial. Available Online: <https://www.baileigh.com/desktop-cnc-router-table-dwr-0906>. (accessed 22MAR2018)
72. "Carbide 3D Nomad 883 Pro CNC Machine." MatterHackers. Available Online: <https://www.matterhackers.com/store/l/carbide-3d-nomad-883-pro-desktop-cnc-machine/sk/MN617RF0>. (accessed 22MAR2018)
73. "ImageJ." Accessed June 13, 2018. <https://imagej.nih.gov/ij/>
74. "Copper Clad Laminate PCB Circuit Board (50pcs)" Available Online: <http://a.co/b396EOq> (accessed 22MAR2018).
75. Oberloier, Shane, and Joshua M. Pearce. Open Source Low-Cost Power Monitoring System (In Review)

4 Open Source Low-Cost Power Monitoring System

4.1 Abstract

This study presents an entirely open-source, low-cost power monitoring system capable of many types of measurements including both loads and supplies such as solar photovoltaic systems. In addition, the system can be fabricated using only open source software and hardware. The design revolves around the Digital Universal Energy Logger (DUEL) Node, which is responsible for reading and properly scaling the voltage and current of a particular load, and then serializing it via an on-board ATtiny85 chip. The configuration of the DUEL node allows for custom sensitivity ranges, and can handle up to 50 A and 300V. Up to 127 DUEL nodes communicate via Inter-Integrated Circuit (I2C) on a bus, which can be monitored and logged through an Arduino Uno, or other compatible microcontroller. Using accessible equipment, the DUEL node can be calibrated to a desirable accuracy with an error of less than 1%. The DUEL nodes are also completely customizable, making them fit for any input range, where all commercially-available products are fixed range. The open source solution out performs commercial solutions as the price per measurement (\$18.25) is significantly smaller, while the number of serviceable channels (127) is significantly higher.

Table 6: Specifications table

Hardware name	Open Source Low Cost Power Measurement System
Subject area	Engineering and Material Science
Hardware type	Electrical Engineering and Computer Science
Open Source License	GNU GPL v3
Cost of Hardware	\$155.34
Source File Repository	Open Science Framework: https://osf.io/8keau/

4.2 Hardware in context

As the open source method of technological development [1] has moved aggressively into technically-sophisticated scientific hardware [2-8], there has been another push towards open source appropriate technology (OSAT) for sustainable development [9-11]. One leading example of OSAT is the work by Open Source Ecology (OSE) to fabricate the tools needed for civilization itself [12]. OSE has identified the top 50 most relevant machines to comfortably sustain civilization [13]. OSE uses a model where the design is global and open source, but the manufacturing is distributed, local peer production

[14,15]. One of the main pillars of OSE's plan is distribution on every level: distributed agriculture, manufacturing, and energy production [12].

The OSE mindset has fostered the development of the Open Building Institute (OBI), which was created to design and build comfortable and highly functional homes, such as their first model shown in Figure 23 [16]. OBI houses can be built using OSE's Open Village Construction Set and are designed to be ecologically responsible, scalable, and replicable in the fully open source sense. Ideally these houses are constructed and powered using a sustainable source of electric power such as solar photovoltaic (PV) technology [17], which converts sunlight directly into electricity. Thus, the current designs of OBI all utilize building integrated photovoltaics (BIPV) for energy generation as it has distinct advantages in reducing ecological impact [18], net energy [19] and cost [20]. The OBI building is optimized to supply multiple different configurations of power (i.e. 5V, 12V, 24V, 48V, and 120VAC), in order to cut down on conversion losses (energy conversion processes always result in energy loss [21]). In order to fully understand the designs, and provide valuable feedback in order to enable the OBI design to evolve technically there is a need for a low-cost, flexible an open source monitoring system to log the consumption and generation of electricity.

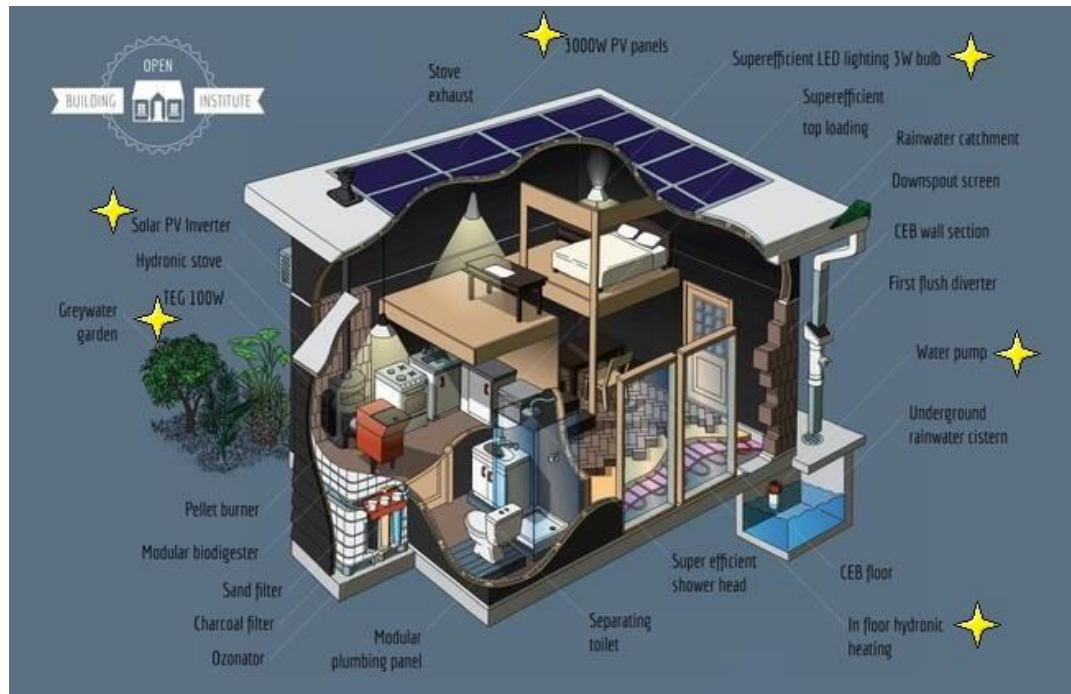


Figure 23: A simple sustainable house designed by OBI. The proposed system would monitor loads and sources such as the 3000W PV panels, LED lighting, and water pump [16]. Stars denote measurable devices.

Some commercial solutions exist for an energy monitoring systems, including the Neurio [22], the Eyedro EHWEM1 [23], the Smappee [24], and CURB [25]. These cost of these

solutions range from \$200 to \$400 [22,25]. The designs are all proprietary, and are capable of taking very few measurements [22] (e.g. the Neurio can only measure 2 AC currents).

There are also many designs for energy monitoring published in the literature. Some of these designs rely on commercially available industrial components [26,27], which severely drive up costs, minimize customization, and decrease accessibility. Others rely on software packages such as LabVIEW which is not open source, and has a non-trivial license cost (e.g. \$399-\$4,999)[28,29]. Furthermore, some designs do not provide permanent hardy solutions and lack integration [30].

Lastly, some relevant academic designs only report on results, and do not share details to pertinent components, which limit their utility [31,32]. Finally, there is an open source alternative commercially available, called the OpenEnergyMonitor [33]. The design consists of multiple modules with a relatively high cost of \$150 per channel (2 AC current measurements, 1 AC voltage measurement). The solution does not appear to be able to be used for custom DC measurements, which can be a major pitfall for this system for some applications such as solar photovoltaic systems.

In order to overcome these limitations of existing energy monitoring systems this study presents an entirely open-source, low-cost power monitoring system, which is capable of many types of measurements for both loads and generation sources such as solar photovoltaic systems, wind power, microhydro, biomass, or fuel cells.

4.3 Hardware description.

The design revolves around the Digital Universal Energy Logger (DUEL) node, which is responsible for reading and properly scaling the voltage and current of a particular load and then serializing it via an on board ATtiny85 chip. The configuration of the DUEL node allows for design-able sensitivity ranges, and can handle up to 50 amps and 400V. DUEL nodes communicate via Inter-Integrated Circuit (I2C), which allows up to 127 nodes on a bus [34]. The bus can be monitored and logged through an Arduino Uno, or any other I2C compatible microcontroller. All designs are made such that they can be manufactured using OSE's proposed tool-set. The proposed design is simple, automatic, and meets the requirements of OBI. Equipped with this system, OBI or other users can make informed decisions on optimization of their power systems for a given building or home.

- This hardware, although specifically designed for OBI can be used for the following:
- Monitoring electricity generation systems (e.g. a PV system of virtually any size)
- Measuring energy converter efficiency
- High channel count, high precision measurement platform for Arduino

- Measuring power consumption of individual devices

4.3.1 Overall System

The system is split into two sets of components: 1) the main hub, and 2) the DUEL nodes. The main hub consists of an Arduino UNO with a small display and SD card breakout, a power supply, and a custom RJ-45 breakout board. The main hub communicates with the sensor nodes via I2C. Because of this, it is necessary to introduce a splitting-hub to facilitate multiple sensors. An example configuration can be seen in Figure 24.

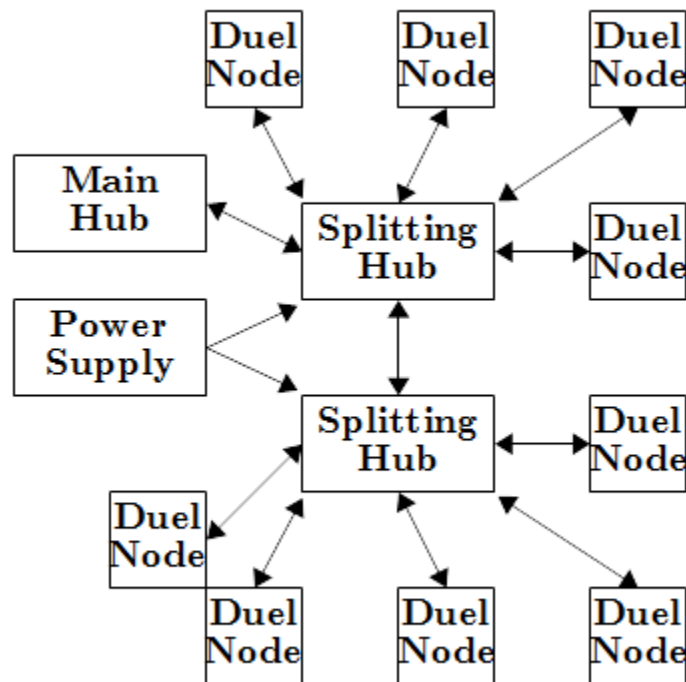


Figure 24: An example system setup with 9 DUEL nodes, and 2 splitting hubs

The DUEL node is a custom circuit implementing an ATTiny85 used for measurement and I2C serialization. The DUEL node is a universal node for virtually any power range. The node measures voltage directly through a single diode rectifier and 10 K Ω potentiometer. Current is measured using a CQ2334 Hall effect current sensor [35], amplified by an operational amplifier circuit. Though the standard DUEL nodes utilize the CQ2334, it is possible to construct the node without the Hall effect sensor, and instead break out signals with header pins, and hook up an external Hall effect, or current transformer for non-invasive sensing [36]. This functionality allows the DUEL node to be configured for a wide range of current and voltage measurements.

All electrical designs are carried out in KiCAD EDA [37] and follow the general design procedure for free and open source scientific hardware [38].

4.3.2 Main Hub

The measurement hub is designed around the Arduino Mega. There are a few justifications for this choice. First, there is a well-established support community for open source Arduino technology, as well as many open-source programs available for reference [39,40]. Second, the Arduino is a component used in many other OSE designs (e.g. The Compressed Earth Brick Press and Micro-Inverter [41,42]), so this will prevent more on-stock back up components. Lastly, the Arduino Mega will have more than enough spare input and outputs (IO) that may be used for future expansion and enhancements. The system is equipped with peripherals in order to handle debugging, power and communication, with the rest of the system, human machine interface (HMI) and data storage, as shown in Figure 25 and 26.

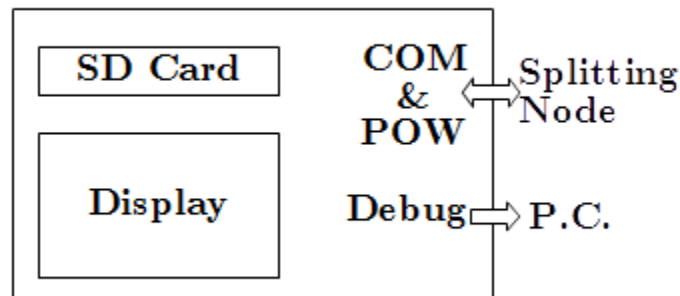


Figure 25: An overview of the Main Hub

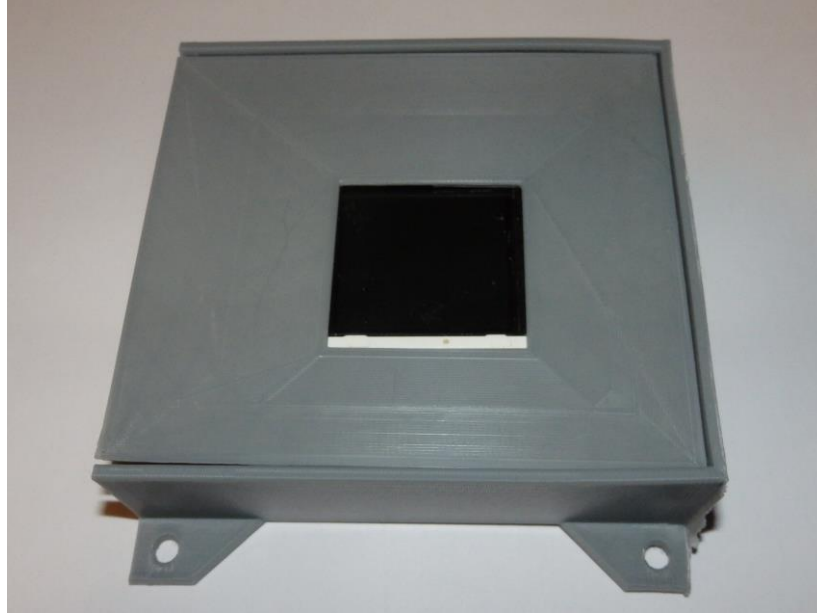


Figure 26: The Main Hub

I2C is chosen as the method of communication with DUEL nodes due its single bus connection style, as seen in Figure 27, which allows for a 7 bit address field that in turn allows for 127 addressable nodes [34]. Serial communication has the benefit of being much more noise tolerant [43], which prevents transmitted analog signals from the DUEL nodes from being flawed by noise, and forcing an overly complex multiplexing circuit [44]. Although the max sampling rate will be significantly reduced because of the serialization, it is important to note that the system is designed for long term analysis and high-resolution data is not the objective.

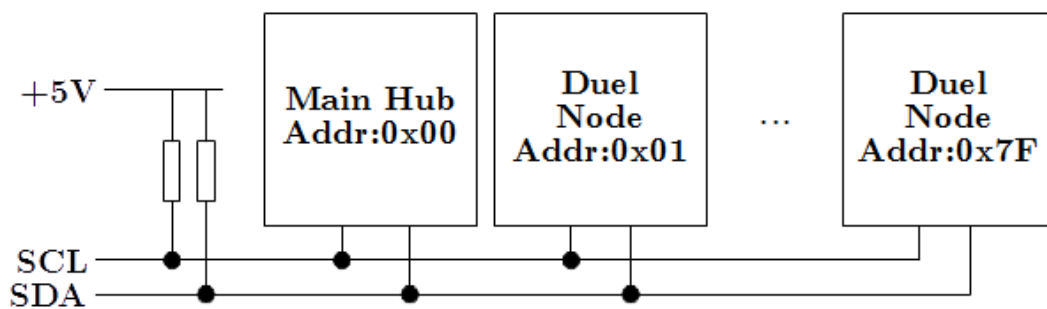


Figure 27: The I2C connection standard. The pull-up resistors may be managed internally by the Arduino.

The RTC module is connected to the Arduino Mega via I2C. With each power measurement, the RTC is polled and the current date and time is recorded. This will be used for synchronization during the data analysis. In order to cut costs, a delay function can be used to time sample intervals, however data may become out of synchronization without a reference.

A small 128x128 TFT display with a micro-SD card [45] is attached to the system. The module can communicate to the Arduino via serial peripheral interface (SPI) [45]. The display and SD card are selectable by respective chip select pins. This module is used to display system status, as well as log information. The details to be listed are:

- RTC Time / Date
- Sampling = True / False
- Current Reading Values
- #Errors Detected
- SD card fill percentage

The Arduino is also connected to an RJ-45 female connector, in order to allow inter-communication with the DUEL nodes. The wiring of the display/SD and RJ-45 is condensed into a circuit board “shield” and can be easily plugged into the board.

The software for the main hub is developed in the Arduino IDE [46]. The IDE is chosen for its capability for rapid development, and large community support, as well as its compatibility with multiple designs [39]. The firmware utilizes Wire.h for I2C communication, as well as Arduino's stdio (which is not syntactically included in the firmware, as the IDE includes it as a default) for serial debugging. The software is designed from the logic in Figure 28. To clarify, the firmware waits a predetermined amount of time and will begin polling each DUEL node for measurements once it is time.

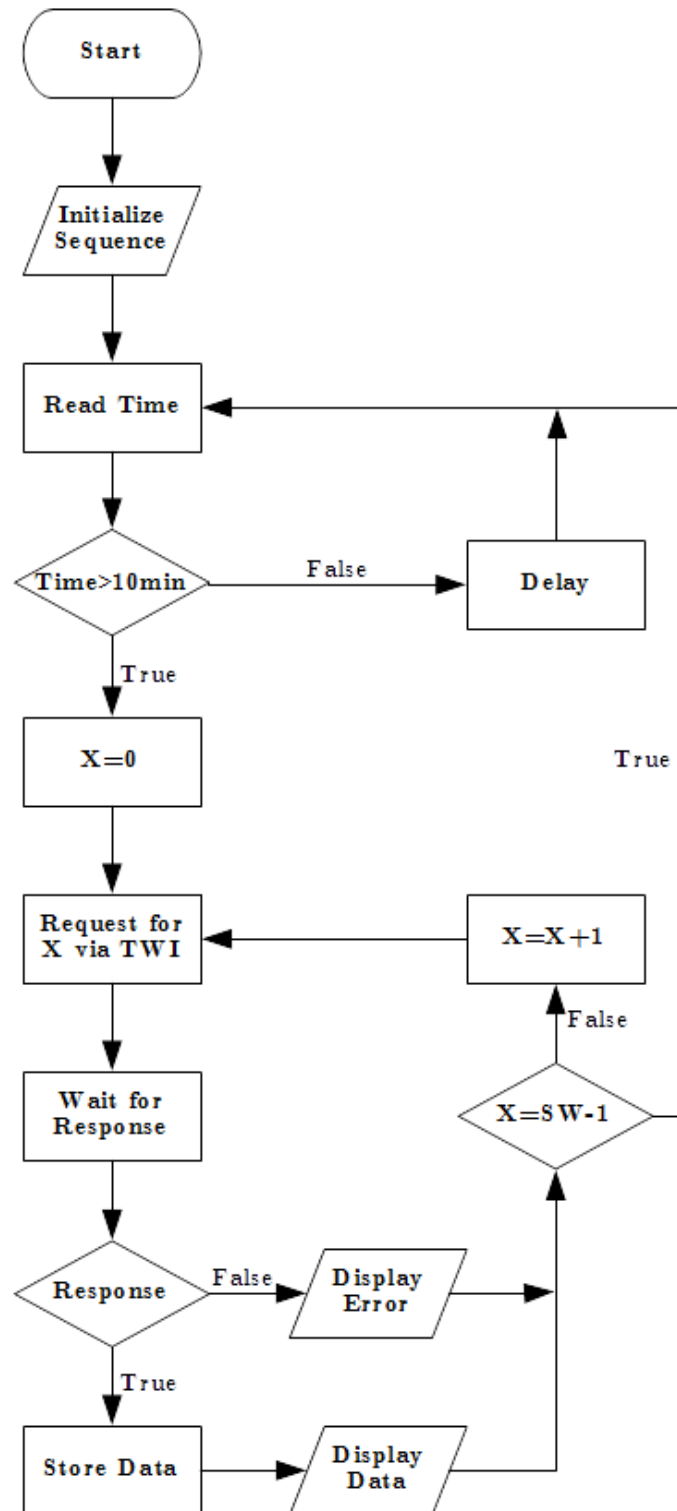


Figure 28: The software flow programmed onto the Arduino onto the Arduino in the main hub

The entire main-hub costs a total of US\$62.37 in materials to produce. The design is made using entirely open source components, and has potential to be completely integrated as a means of cost savings. However, it should be noted that integration will cut down on the modulated design, decreasing maintainability. A cost breakdown of the design can be seen in the Bill of Materials section. Additionally, the schematic and board layout can be viewed in Figures 29 and 30 respectively.

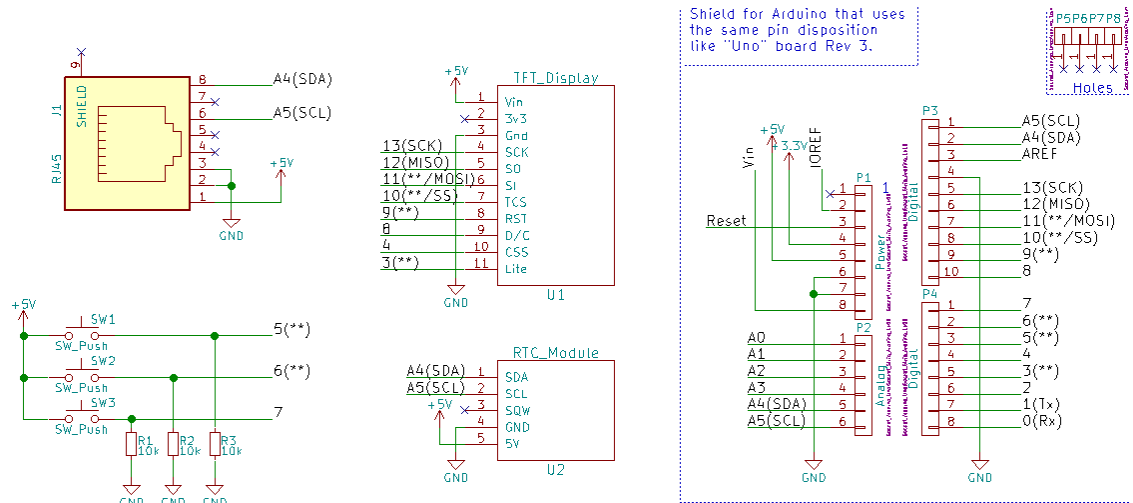


Figure 29: The Main Hub Schematic

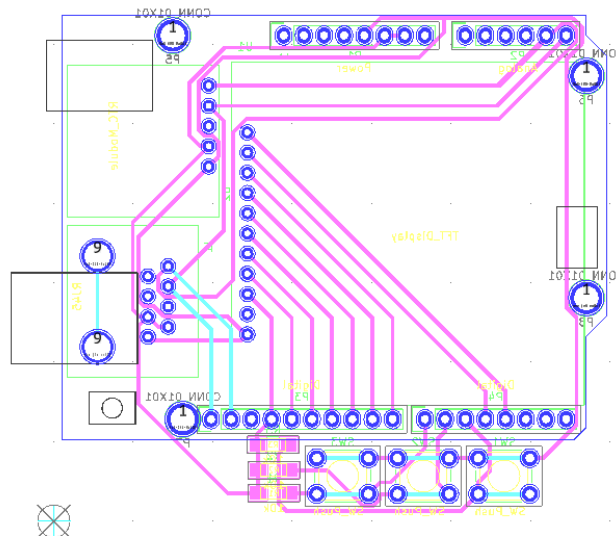


Figure 30: The Main Hub board Layout

4.3.3 Splitting Hub

The splitting-hub (Figure 31 and 32) is a simple distribution board for the I2C, as well as power. Each port has identical connections (meaning that no port is unique or intended for a main host). Each port is connected to an LED which is enabled and disabled by the connected node. This LED can be used as a debug mechanism to indicate proper connection and communication.

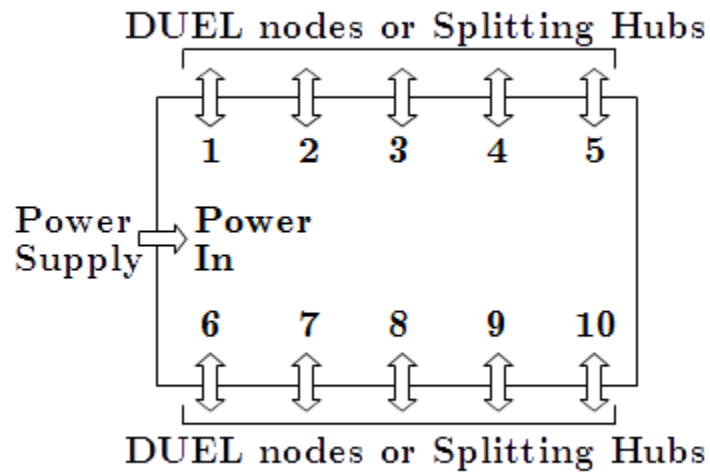


Figure 31: The splitting-hub is used for connecting multiple DUEL nodes to the main-hub

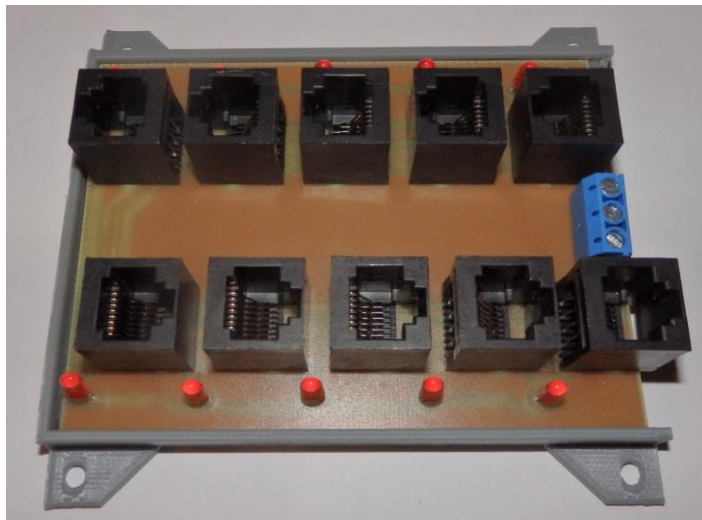


Figure 32: The splitting-hub

Splitting-hubs can be daisy-chained in order to further expand channel availability. Though power can be distributed through the RJ45 connection from one splitting-hub to the next, it is not recommended, as ground loops can be created, as well as resistive losses may compound [44]. The daisy chain should be configured in a star formation to reduce noise potential [47]. Lastly it should be noted that only a DUEL node is capable of controlling LED's. Therefore that indication will not propagate through splitting node inter-connections. Only the LED at the connection point of the DUEL node will be controllable.

The design consists of a milled circuit board with a 3-D printed enclosure and costs a total of \$7.17 to manufacture. The cost breakdown can be seen in the Bill of Materials section. The schematic and board layout can be viewed in Figures 33 and 34, respectively.

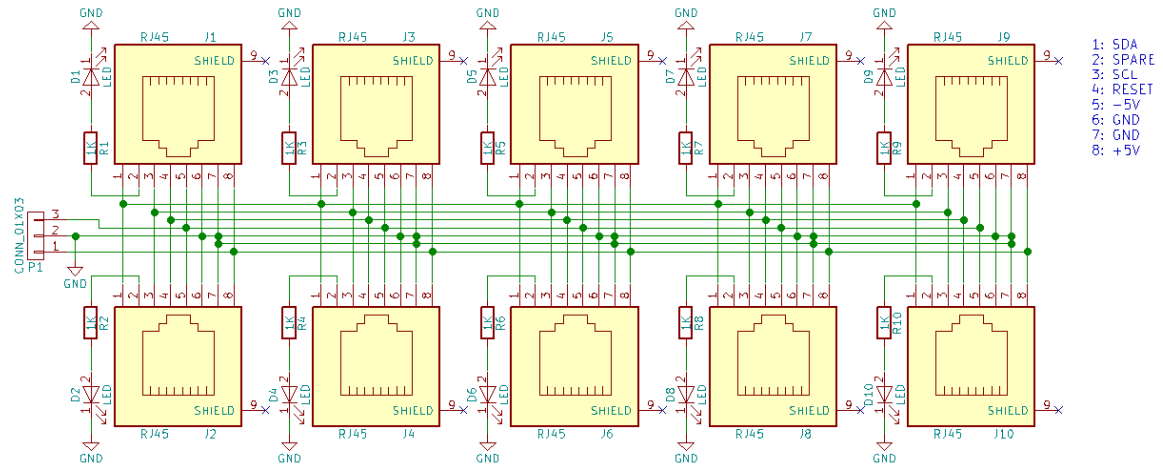


Figure 33: Splitting Hub Schematic

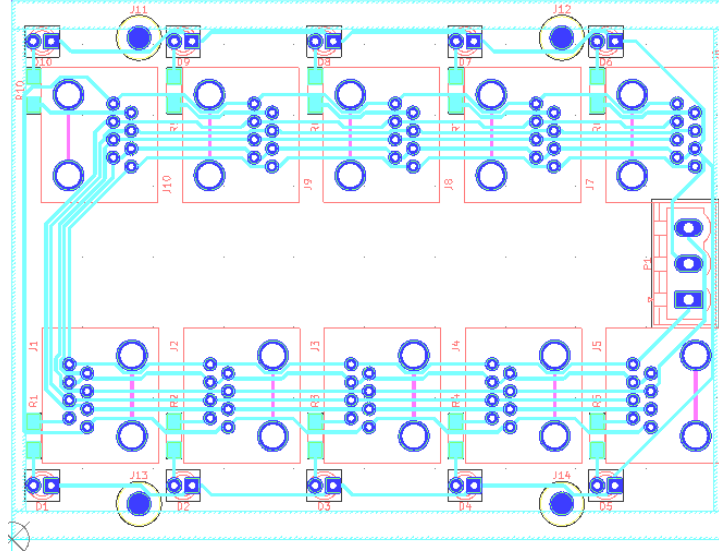


Figure 34: The Splitting Hub Board Layout

4.3.4 DUEL NODE

The measurement node (Figure 35) is designed as a non-specialized circuit with room for nearly endless customization. This customization is made possible by the dual op-amp signal conditioning circuit, as well as the ability to replace the on-board sensor with an external larger ranged device. The conditioning circuit applies a gain and offset to the signal coming from the current sensor. This allows for full utilization of the 10 bit 0-5V range of the ATtiny analog to digital converter (ADC) [48]. Voltage is simply rectified by a diode, and divided by a 10 K potentiometer. The potentiometer can be adjusted to divide any input range to the ADC max of 5V. Additionally, each signal (both current and voltage) is fed through a low-pass filter to remove noise.

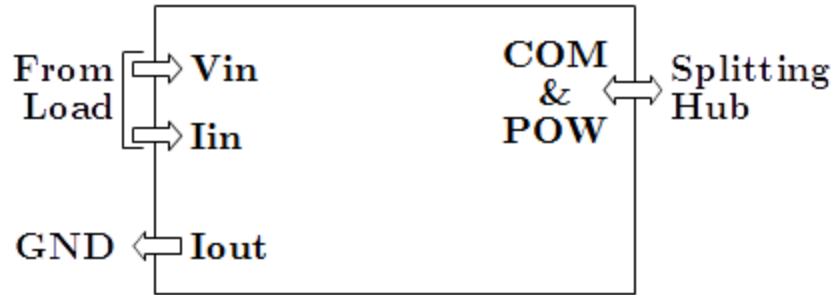


Figure 35: The DUEL node is capable of customized for fixed power measurement ranges, and outputs the data via I2C

The output of the current conditioning circuit is determined by equation 1. Where R_P is the position of the potentiometer, R_g is determined from Table 8, and R_f is 10 k Ω . If using the on board Hall effect sensor, typically R_P will be set to 50%, in order to have an input offset of -2.5V. The reason for this is the CQ2334 outputs on a 0 to 5V scale, where 0V indicates -50A, 2.5V indicates 0A, and 5V indicates 50A [36]. The -2.5V offset allows for measurement positive current only, though, at a higher resolution.

$$V_{out} = (V_{in} - 5R_P)(\frac{R_g}{R_f} - 1) \dots (19)$$

The voltage input circuit can be adjusted simply by changing the position of the 10 k Ω potentiometer. The potentiometer acts as a voltage divider and brings the input voltage down to the 5V range. Additionally, there is a 0.7V drop across the rectifying diode, which must be accounted for. In Table 7, potentiometer positions are calculated for various common voltage ranges.

Table 7: Potentiometer configuration for voltage conditioning

Voltage Conditioning		
Range (V)	Pot Position (%)	Accuracy ($\pm V$)
5	100	.004
12	44	.011
20	26	.019
24	21	.023
48	10	.046
120	4	.117

Table 8: Resistor selection for current conditioning

Current Conditioning (With Hall Effect Sensor)					
Range (A)	Gain	Offset	Pot Position	Rg	Accuracy ($\pm A$)
0.5	200	-500	50	50	.0004
1	100	-250	50	100	.0009
5	20	-50	50	520	.0048
10	10	-25	50	1.1K	.0097
25	4	-10	50	3.3K	.0244
50	2	-5	50	10K	.0488

The aforementioned Hall effect sensor is rated for 50A [36]. However for high current applications, it is recommended that this feature is not used (not soldered in place) and an external current transform or Hall effect sensor is used. If an external sensor is used, the excitation and signal pins can be broken out using header pins placed at the signal pins used for the Hall effect sensor.

After the signals are conditioned, they are fed into the ADC input of the ATTiny. The ATTiny is set to constantly acquire data and keep a cumulative average using Equation 2 [43]. The DUEL node continues to make measurements in between data requests from the master hub. This insures a more accurate representation of the power consumption over the sample interval. The code can be easily reconfigured to only measure and reply with data as requested.

$$V_{avg} = V_{avg\text{-previous}} + \frac{V_{meas} - V_{avg\text{-previous}}}{\text{Sample Count}} \dots (20)$$

The final design for the DUEL node can be seen in Figure 36. The total cost is acquired in the Table below, and is found to be \$18.25.

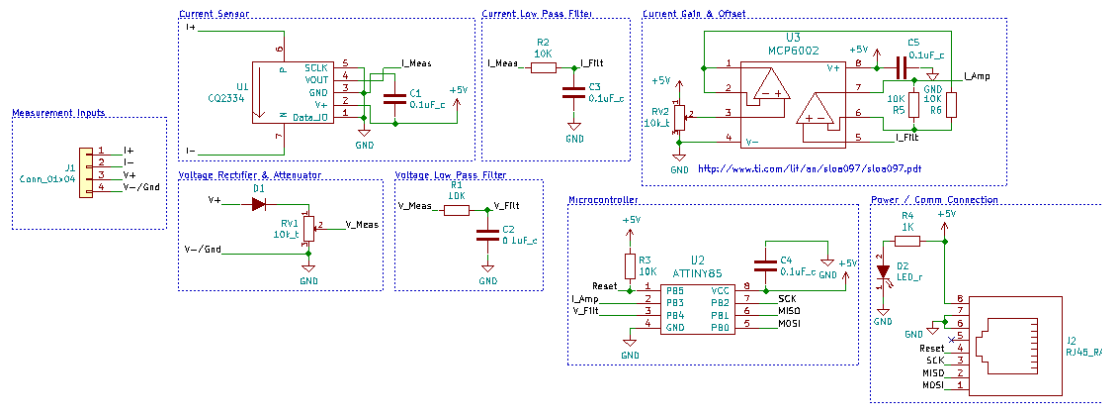


Figure 36: The complete schematic for the DUEL node

The design is placed onto a 9x4cm single layer board, seen in Figure 37.

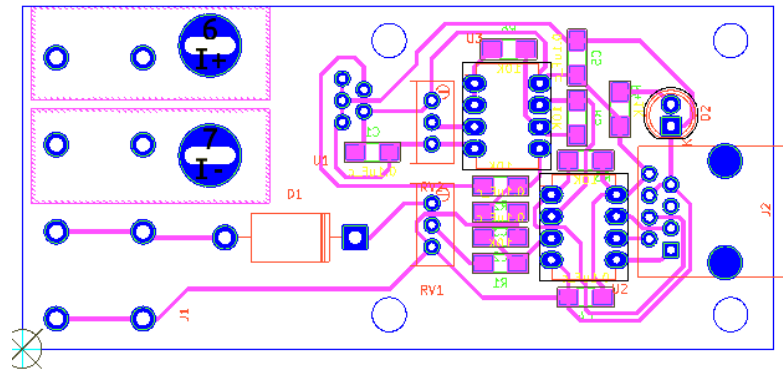


Figure 37: The single layer board of the DUEL node

Much like the main-hub, the firmware for the DUEL node is developed in the Arduino IDE. IDE cannot program the Attiny85 in the default configuration, and multiple

configuration steps must be gone through in order to program the chip [50]. The ATTiny can be programmed by configuring an Arduino Uno as an ISP, and then connecting it to an RJ-45 breakout board (BOB) (a custom one has been designed and is shown in Figure 38).

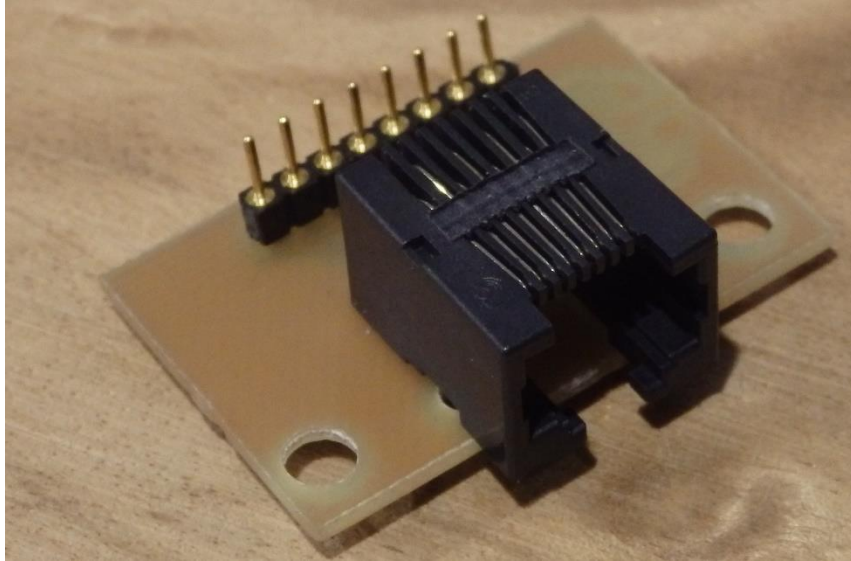


Figure 38: The RJ-45 BOB

The necessary connections from the Arduino UNO to the BOB are detailed in the Table 9 below.

Table 9: Connections to program DUEL with Arduino UNO

Arduino Pin	BOB Pin	Connection Description
5V	Pin 8	Power
GND	Pin 7	Ground
Pin 13	Pin 3	SCL
Pin 12	Pin 2	MISO
Pin 11	Pin 1	MOSI
Pin 10	Pin 4	Reset

The designed firmware utilizes the tinyWireS.h library in order to send signals via I2C to the measurement node. The data packet structure can be seen in Figure 39. The final firmware design follows the flowchart in Figure 40.

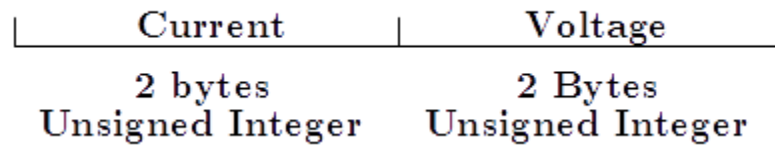


Figure 39: The data packet structure sent from the DUEL node

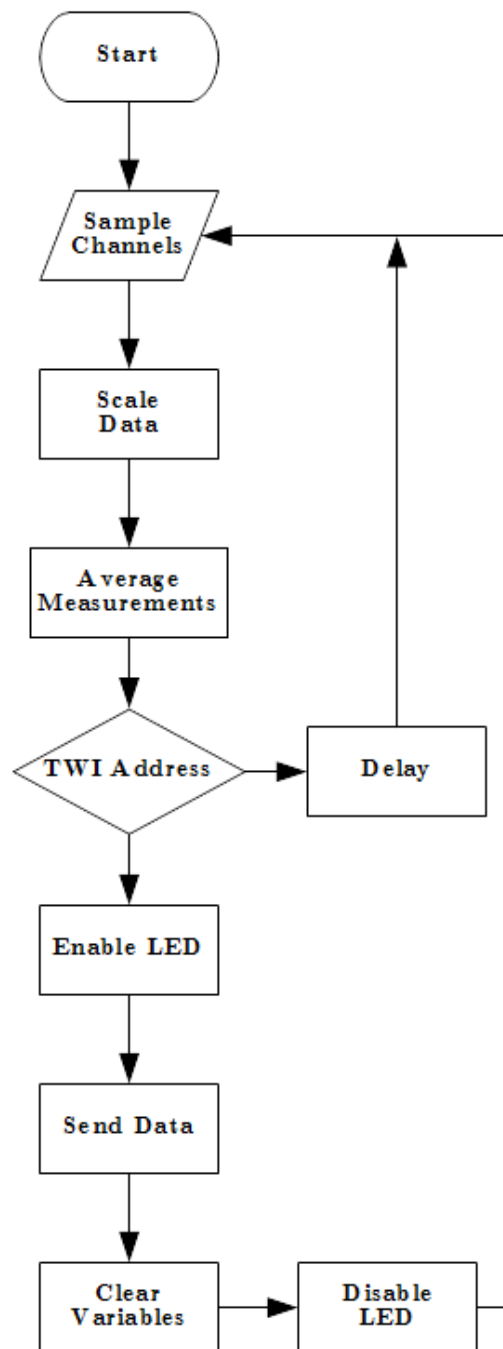


Figure 40: The firmware flow chart for the DUEL node

4.3.5 Discussion

A comparison of some available commercial units to the open source system provided here based on total price, channel type, price per measurement and storage can be seen in Table 10. As can be seen in Table 10, the open source solution proposed in this study outperforms commercial solutions as the price per measurement is significantly smaller, while the number of serviceable channels is significantly higher. The primary limitation of the proposed system is the amount of rewiring required (namely provisions made for invasive current sensors). However if this system is installed at the time of power system construction, the extra effort to install it is minimalized. The DUEL nodes also have an advantage in that they are completely customizable, making them fit for any input range, where all competitors are fixed range. This solution also is capable of advertising a known error, making it more suitable for precision and scientific applications.

Table 10: Comparison of commercially available power monitoring solutions

Name	Price	Channels - Type	Price Per Measurement	Storage
Neurio Solar Monitor [22]	\$289.00	2 – current	\$144.50	Cloud
Eyedro Wired [23]	\$129.00	2 – current	\$64.50	Cloud
Smappee Solar Energy Monitor [24]	\$349.00	2 – voltage 4 – current 1 – appliance AC	\$58.16	Cloud
CURB Home Energy Monitoring System [25]	\$399.00	18 – current	\$22.16	Cloud
Open Source Solution (Basic)	\$158.94	9 – voltage 9 – current	\$8.83	SD card
Open Source Solution (extreme)	\$2,356.04	127 – voltage 127 – current	\$9.27	SD card

The accuracy of both the voltage and current channel is less than 2% error for AC measurements and 1% error for DC measurements, which for the intentions of solar power monitoring systems is satisfactory. It should be noted that the accuracy is only as good as the accuracy of the multimeter used for calibration. The DUEL nodes can be used to monitor individual panel output, bulk array output, power converter efficiency, load draw, and any other current drawing (or producing) application. It is highly scalable

design and CAT-IV compatibility allow for the system to easily be wired throughout a building, recording draws on all appliances.

The system is also able to be fabricated on single layer circuit boards, using only open source software and hardware. This and the open source nature reduces the complexity and the barrier of acquiring this scientific equipment, and will help further science and society as a whole – but most specifically in the areas of renewable energy and energy conservation.

The open source system has achieved the project goal of being inexpensive, at a cost of \$158.94 for a basic system. Using widely available equipment, the DUEL node can be calibrated to a desirable accuracy of less than 1%. The proposed system is also infinitely flexible, as it can be used in multiple configurations, including a sufficiently large amount of connected nodes. The system has a heightened advantage over most competing systems due to the measurement of both current and voltage. The DUEL node also has the advantage of endless customization to meet any measurement need and thus has a wide range of applications as listed (but not limited to) below:

- TIG welder power usage
- Automotive power usage
- Multi-node computing power usage
- Automated assembly line power usage
- Redundant home power meter to test utility meter accuracy
- General purpose expandable data logger for voltage or current based sensors

4.4 Design files

Design Files Summary

All files are available at [51] and are described in Table 11.

Table 11: A description of project files available on the repository

Design file name	File type	Open source license	Location of the file
Main_Hub.Pro	KiCAD Project	GNU GPL v3	https://osf.io/9rts5/
Main_hub.csv	CSV	GNU GPL v3	https://osf.io/9rts5/

Main_hub_encl.scad	CAD Model	GNU GPL v3	https://osf.io/9rts5/
Main_hub.ino	Firmware	GNU GPL v3	https://osf.io/9rts5/
BOB.pro	KiCAD Project	GNU GPL v3	https://osf.io/9rts5/
BOB.csv	CSV	GNU GPL v3	https://osf.io/9rts5/
hub_board.pro	KiCAD Project	GNU GPL v3	https://osf.io/9rts5/
hub_board.csv	CSV BOM	GNU GPL v3	https://osf.io/9rts5/
hub_board_encl.scad	CAD Model	GNU GPL v3	https://osf.io/9rts5/

Main_Hub, BOB, and Duel.pro can be edited in KiCAD. They reference to the schematic, and PCB for each respective component. Duel.ino and Main_Hub.ino contain the Arduino based firmware for the DUEL and Main-hub, respectively. Enclosures is the generic location for all design files for the component enclosures and in separate 3-D printing files folder.

The enclosures are printed using a \$17.99, 1 kg spool of PLA on a Creality Ender 3 3-D printer. A layer height of 0.2mm and infill of 30% is used.

4.5 Bill of Materials

Table 12: Bill of material for the Main-Hub

Designator	Component	Number	Cost per unit US\$	Total cost US\$	Source of materials	Material type
NA	Arduino Uno	1	\$24.95	\$24.95	Arduino.cc	NA

U1	128x128 TDT Display w/ uSD Card	1	\$14.95	\$14.95	Adafruit.co m	NA
U2	Real Time Clock Module	1	\$14.95	\$14.95	Sparkfun.c om	NA
NA	8 GB micro- SD card	1	\$5.99	\$5.99	Amazon.co m	NA
NA	Single layer copper clad fiberglass	1	\$0.42	\$0.42	Amazon.co m	NA
J1	RJ-45 Jack	1	\$0.45	\$0.45	Digikey.co m	NA
J2-J4	Header Pins	32	\$0.0175	\$0.56	Digikey.co m	NA
NA	3-D Printed enclosure	1	\$0.47	\$0.47	In House	PLA
			Total:	\$62.74		
Designator	Component	Number	Cost per unit US\$	Total cost US\$	Source of materials	Material type

Table 13: Bill of material for the Splitting Hub

Designator	Component	Number	Cost per unit US\$	Total cost US\$	Source of materials	Material type
NA	Single layer copper clad fiberglass	1	\$0.42	\$0.42	Amazon.com	NA
J1-J10	RJ-45 Jack	10	\$0.45	\$4.50	Digikey.com	NA
D1-D10	Red LED	10	\$0.11	\$1.19	Digikey.com	NA
R1-R10	1K Resistor	10	\$0.01	\$0.16	Digikey.com	NA
J11-J12	2 Pin Screw Terminal Block	2	\$0.40	\$0.80	Digikey.com	NA
NA	3-D Printed enclosure	1	\$0.37	\$0.37	In House	PLA
			Total	\$7.44		
Designator	Component	Number	Cost per unit US\$	Total cost US\$	Source of materials	Material type

Table 14: Bill of material for the DUEL node

Designator	Component	Number	Cost per unit (US\$)	Total cost - (US\$)	Source of materials	Material type
NA	Single layer copper clad fiber-glass	1	\$0.42	\$0.42	Amazon.com	NA

C1, C2, C3, C4, C5	.1uF Cap	5	\$0.15	\$0.75	Digikey.co m	NA
D2	Red LED	1	\$0.13	\$0.13	Digikey.co m	NA
D1	Rectifier Diode	1	\$0.32	\$0.32	Digikey.co m	NA
J1	4 Pos High Current Connector	1	\$6.53	\$6.53	Digikey.co m	NA
J2	RJ45 Connector	1	\$0.64	\$0.64	Digikey.co m	NA
R1, R2, R3, R5, R6	10K Resistor	5	\$0.01	\$0.05	Digikey.co m	NA
R4	1K Resistor	1	\$0.01	\$0.01	Digikey.co m	NA
RV1, RV2	10K Potentiomet er	2	0.88	1.76	Digikey.co m	NA
U2	ATTiny85 Microcontrol ler	1	1.27	1.27	Digikey.co m	NA
U1	CQ2334 50A Hall Effect Sensor	1	5.62	5.62	Digikey.co m	NA
U3	MCP6002 Dual Op- Amp	1	0.35	0.35	Digikey.co m	NA
NA	3-D Printed enclosure	1	\$0.40	\$0.40	In House	PLA
			Total:	\$18.25		

4.6 Build Instructions

All designs are made such that they can be milled on a low cost CNC mill [52] (or even a converted multi-material additive and subtractive system [53]), on a single layer board. The mill used is the D3D circuit mill[54]. The specific mill is not necessary, and the methods used for fabrication can be applied to any CNC router or mill.

The circuit boards are exported to Gerber files in KiCAD, and then are turned to G-Code in an open source computer aided manufacturing program (CAM) called FlatCAM [55]. Multiple g-code files are generated in order to produce an accurate high density board, which is easy to assemble. The first pass uses a 1 mm carbide end mill to remove a bulk of the material around traces and pads. Any areas slimmer than 1 mm will not be touched by this mill. In the next pass, a 0.1 mm V-shaped engraving bit will finish the isolation routing, by going over the 1mm end mill's path, as well as any of the traces untouched by the 1 mm end mill. Then a drilling pass is used to cut all holes smaller than a diameter of 1 mm. All holes large than 1 mm are cut in the next pass with the 1 mm carbide end mill. Finally the rectangular board outline is generated with a margin of 1 mm from all traces, and cut out with a 3.16mm carbide end mill. For isolation routing, the engrave depth is 0.125 mm. A feed rate of 100 mm/min is used for all V-mill cutting, and 50 mm/min for all end mill cutting. The final overlay of G-code layers is generated in Figure 41.

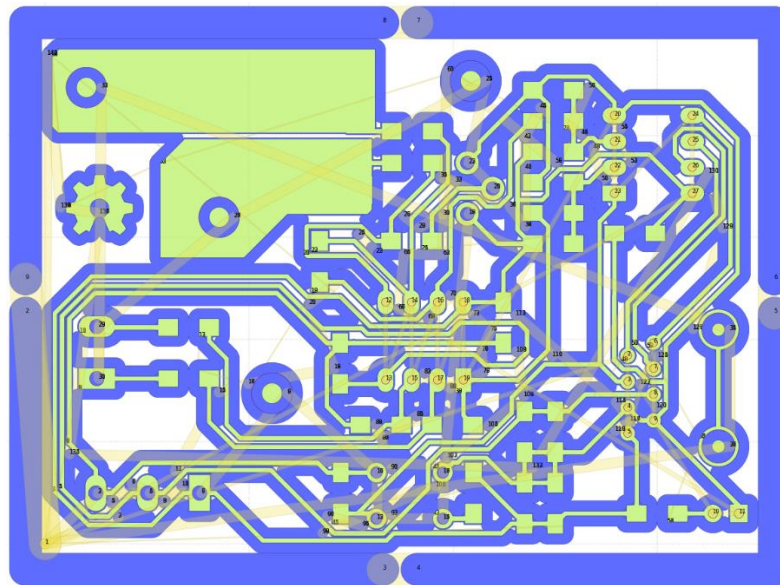


Figure 41: The final output from FlatCAM

A common issue faced with most inexpensive circuit board mills is surface leveling. The raw copper clad fiberglass is not a uniformly flat along the surface and may vary much further than the engraving depth of 0.125mm. An example surface contour can be seen in

Figure 42. Because of this, it is highly likely that the board will be defective, due to missed cuts in the engraving cycle.

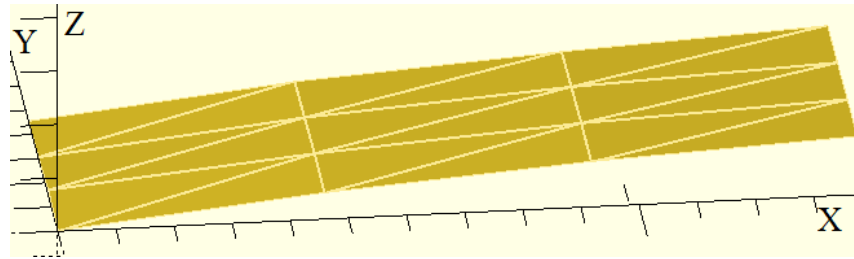


Figure 42: An example uneven 3-D height map of raw PCB material

The uneven height of the PCB raw material can be compensated by automatically moving the Z-axis to compensate for any curvature. The CNC control software, Copper Carve [56], has a feature which measures and compensates for this distortion. This software takes in a variable grid of evenly spaced height points, and adjusts each g-code command to follow an approximate contour based on the measurements. The height can simply be probed by connecting an alligator clamp from ground to the copper material, and another alligator clamp from the engraving bit to the Z-axis limit switch. When the cutting tool makes contact with the copper, the motion will be halted, and the Z-height can be manually input into the leveling software. It is recommended that 1 data point is collected for each square cm.

The DUEL node takes a total of 2 hours to mill from start to finish. The edges of all freshly cut traces are rough, and highly prone to causing short-circuits. 320 grit sand paper (or any very fine equivalent) is used to sand the surface, making sure to stroke in all directions for a full smoothing effect. The finalized board in Figure 43 is now ready to be cleaned, and assembled.

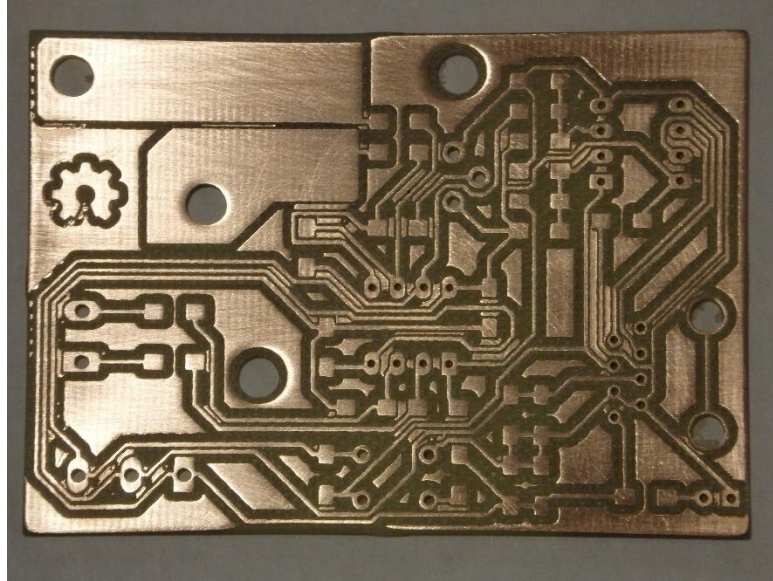


Figure 43: The DUEL node after the smoothing process

The board must be thoroughly cleaned with cotton swabs and isopropyl alcohol in order to remove the coating of copper and fiberglass dust that is left in the channels of the board. By exposing the board to UV light, the residue can be viewed in Figure 44. The cleaned board can be viewed in Figure 45.

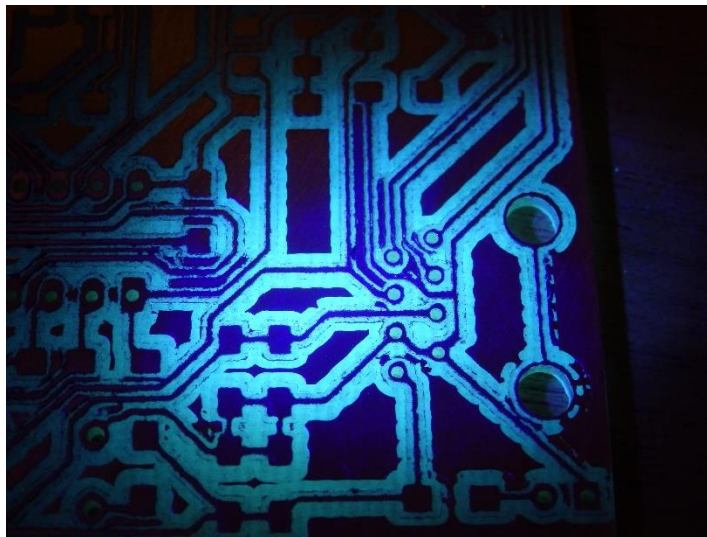


Figure 44: The illuminated circuit board before cleaning

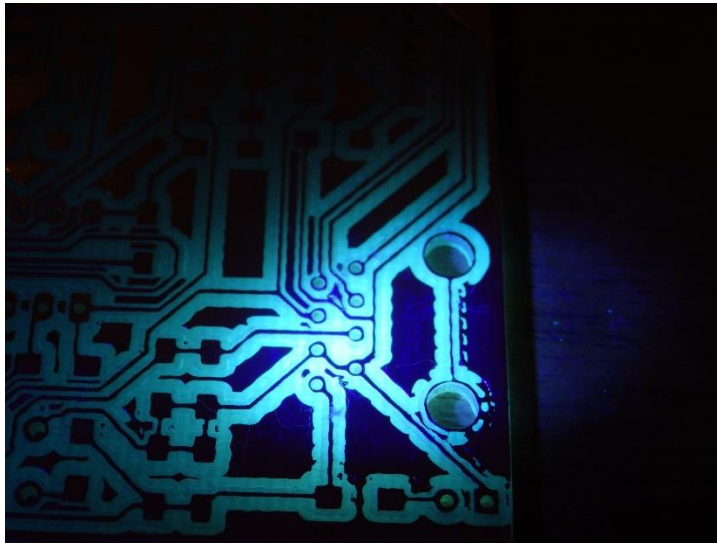


Figure 45: The board after being completely cleaned

Lastly, the components can be soldered onto the circuit board. It is recommended that surface mount devices are soldered first. Do so by first wiping flux over all pads to help prevent solder bridges. Then apply a small amount of solder to each pad before soldering the component. Using forceps, the component is placed and soldered 1 pad at a time. Soldering in this fashion will cause the components to “hover” about any traces that may be passing under them, thereby reducing risks for short-circuits. The final soldered bottom of the board can be viewed in Figure 46, and the top side in Figure 47. Lastly, a multimeter set on the continuity setting should be used to verify no short circuits are present in the board. The board is then placed in the 3-D printed case as shown in Figure 48.

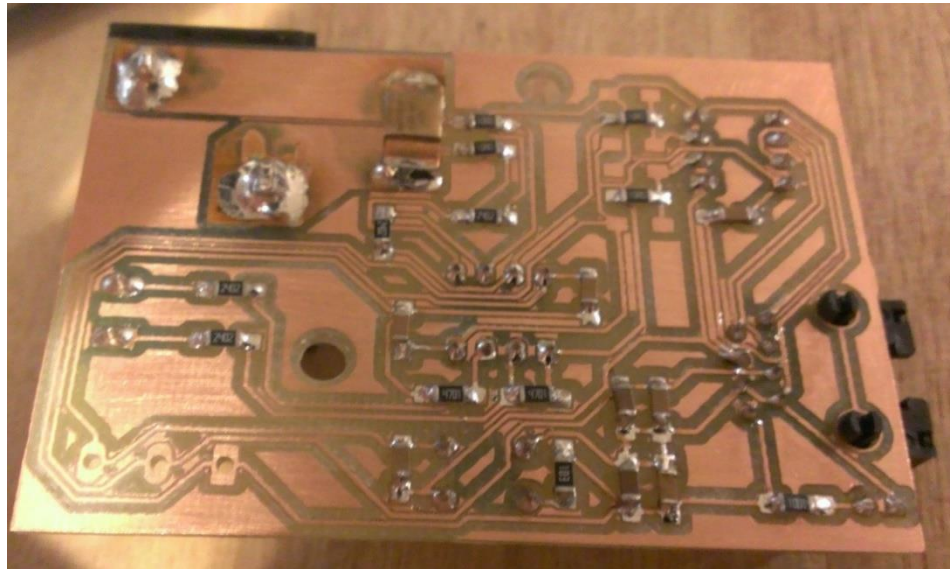


Figure 46: The bottom side of the DUEL node prototype after assembly

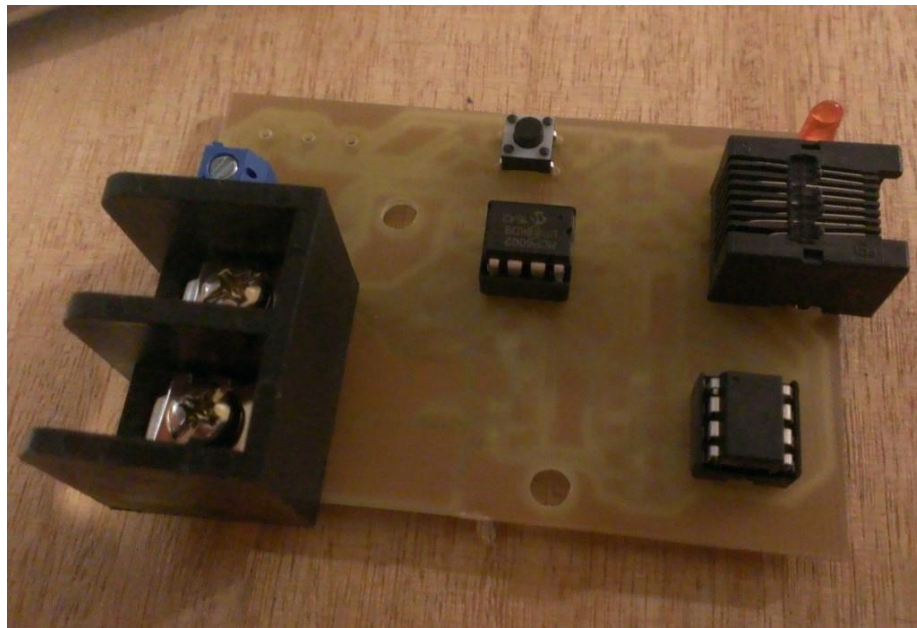


Figure 47: The completed DUEL node prototype

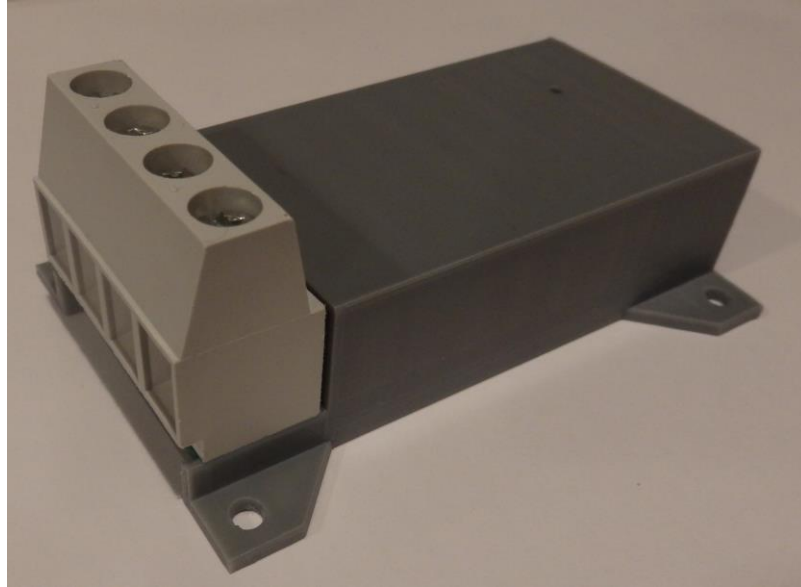


Figure 48: The completed DUEL node

4.7 Operation Instructions

Each DUEL node is calibrated individually. The node is pre-programmed with either firmware for DC measurements or AC measurements. Regardless of configuration, the node will send raw ADC readings via I2C when a request is made of it. In order to calibrate the voltage measurements, the node is wired according to the configuration in Figure 49. Figure 50 is used for calibrating current. For this procedure a Lavolta (BPS-305) DC power supply, a 10A 0-130VAC Variac, and a Fluke 187 True RMS multimeter (to verify supply output) are used, however other equivalent devices may be substituted.

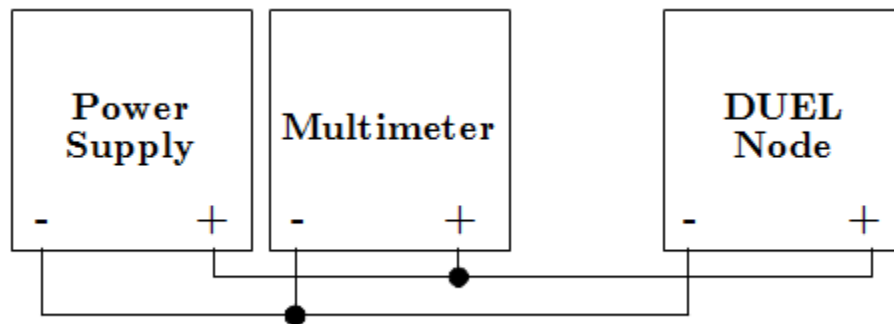


Figure 49: The configuration for calibrating the voltage input of the DUEL node

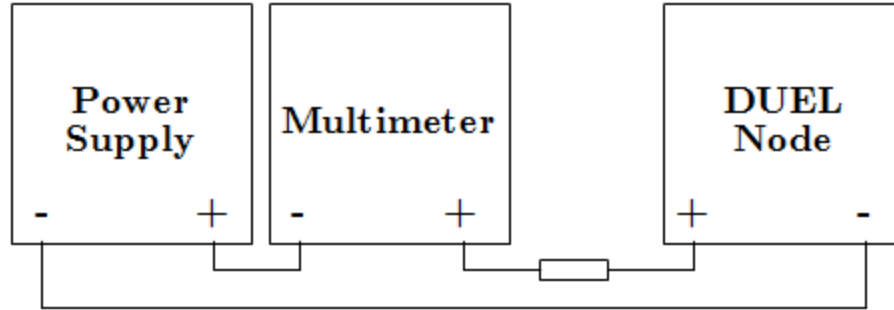


Figure 50: The configuration for calibrating the current input of the DUEL node (10 ohm 100W resistance used)

The DUEL node must be hooked up to an Arduino (or the Main Hub) such that there is a valid I2C connection between the two. Then “Calibration Utility” firmware must be installed onto the Arduino. This procedure is made to automatically walk the user through the calibration process, and generate scaling coefficients. The utility goes through the following steps:

1. Input the I2C address of the node
2. Select type of calibration (Current, Voltage, or Both)
3. Readings from the node will now start streaming. Using the supply, set the voltage and/or current to a known value. Type the known values into the serial interface to create calibration points. Repeat step 3 a max of 16 times.
4. Once complete, the linear scaling coefficients, and calibration point data may be displayed
5. The scaled data is streamed – allowing for a validation step

Using this process, a single node can be characterized in less than 5 minutes.

4.8 Validation and Characterization

The testing procedure uses the same circuit configurations as the calibration feature (namely Figures 49 and 50). It is important that points other than the values used for calibration are measured, in order to gauge the effectiveness of the linear scaling.

4.8.1 Validation by Simulation

The current measurement scaling circuit is validated first through simulation in the Quite Universal Circuit Simulator (QUCS) [57]. The configuration is shown below in Figure 51. For this simulation a simulated input voltage is created, representing a 10A AC

current wave. The simulation is configured for both an AC frequency sweep, to verify the filter effectiveness, as well as a transient simulation to verify proper gain and offset functionality.

Though it is not in the physical circuit, an ideal diode is added to the output of the circuit. This is due to a limitation in QUCS that assumes an op-amp always has a positive and negative supply. The physical circuit only has access to a +5V source, and will therefore saturate at 0V for all input voltages below 0V.

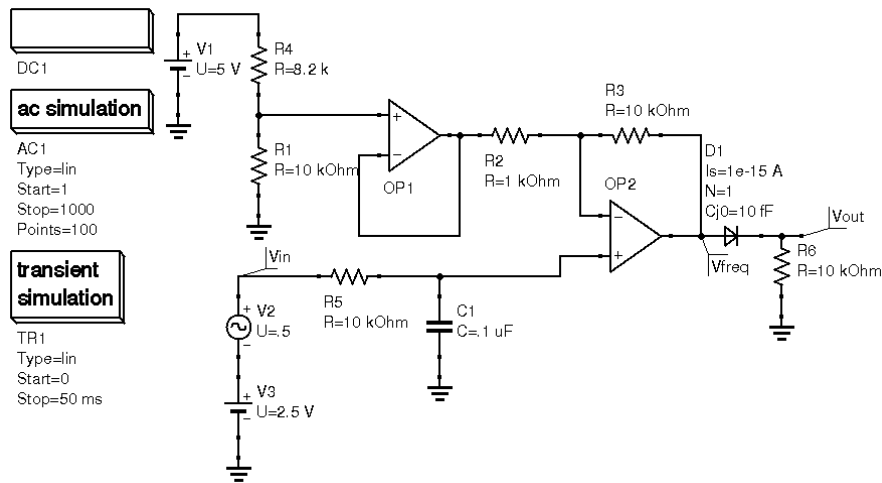


Figure 51: The circuit used to simulate an AC current measurement

The simulation in QUCS has shown that the conditioning circuit is capable of applying both a controllable gain and offset. Some minor effects of the filter are observed in Figure 52, such as the slight lag in voltage V_{out} compared to V_{in} . This lag will not cause a measurement error. Additionally, the frequency response of the circuit is generated in a Bode plot. It shows that the designed cutout frequency of 160Hz is indeed present.

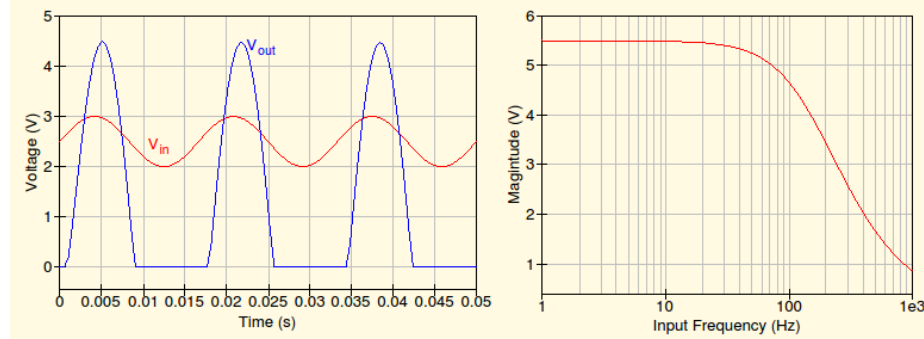


Figure 52: The results of placing a simulated 10A AC input to the sensor. Additionally, a frequency response is generated

4.8.2 Results from Calibration Procedure

The DUEL node under test is configured to accept a maximum of 130V and 25A inputs. First, the firmware for DC measurement is uploaded, and the calibration procedure is carried out. Previous iterations of the DUEL node showed indications of a slight voltage dependence on the current sensing circuit. Because of this, two calibration curves are generated, one made by varying applied voltages, and the other by varying the load.

Figures 53 and 54 show the results from recording and calibrating off of nine points ranging from 0.5A to 4.5A and 3V to 28V respectively.

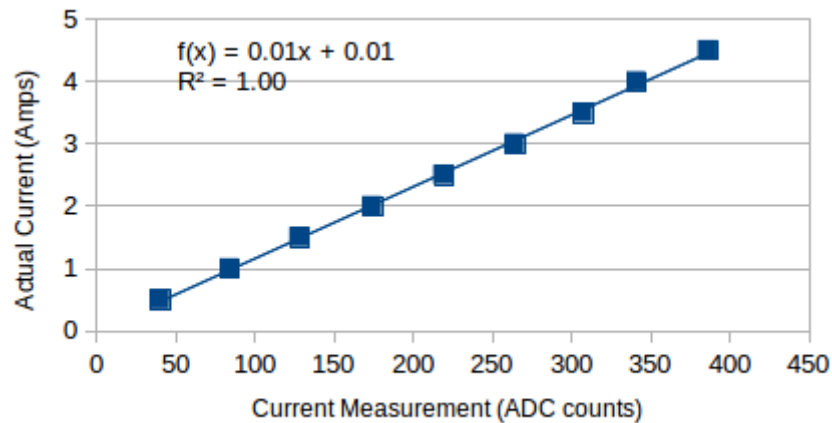


Figure 53: The DUEL node calibration curve for DC current measurement

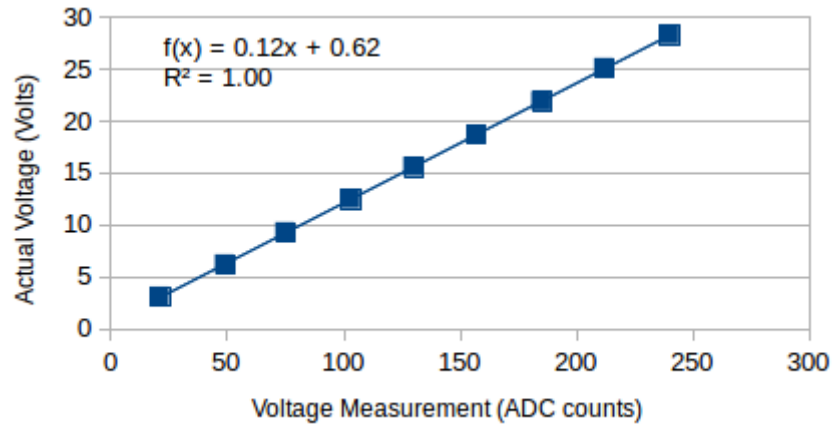


Figure 54: The DUEL node calibration curve for DC voltage measurement

For the second part of this comparison, the voltage is kept at a constant 5V, and the load is varied from 1 to 9 Ohms, generating the calibration curve in Figure 55. The voltage calibration curve in Figure 56 is generated by keeping the supply current constant at 1 A, and varying the load from 1 to 9 Ohms.

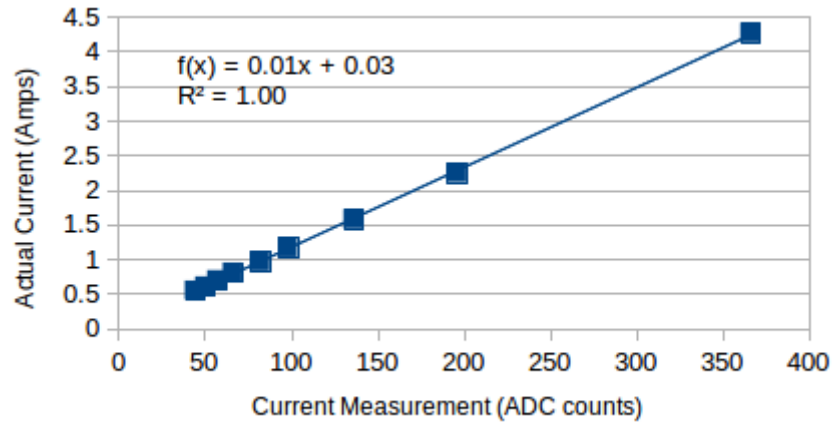


Figure 55: The DUEL node calibration curve for DC current measurement (created by varying load)

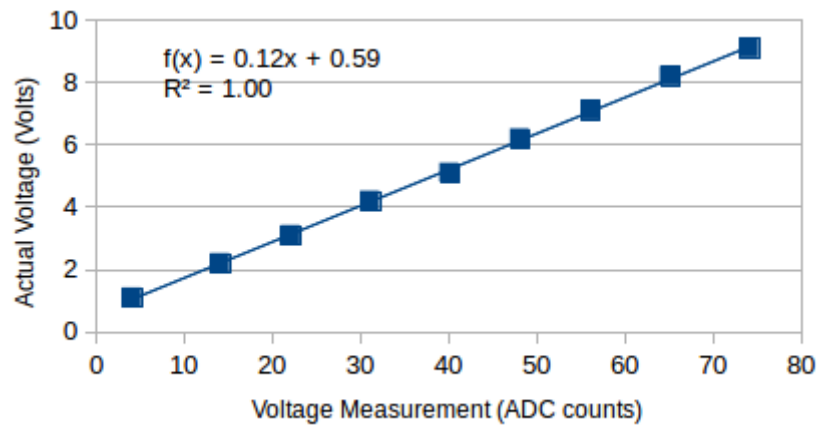


Figure 56: The DUEL node calibration curve for DC voltage measurement (created by varying load)

Comparing Figures 53 and 54, and Figures 55 and 56, specifically the generated equations, it is clear that the measurement circuit is entirely independent of the voltage applied across the device's terminals.

The DUEL node is then programmed to measure AC sources and calibrated using the standard calibration process. For the current calibration, a range of 0.25A to 2.25A are used. The voltage calibration uses a range of 10V to 90V. The resultant calibration curves are generated and plotted in Figures 57 and 58.

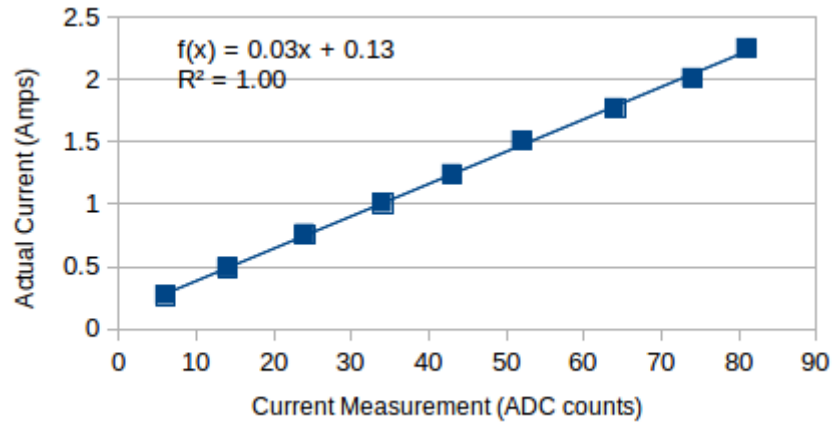


Figure 57: The DUEL node calibration curve for AC current measurement

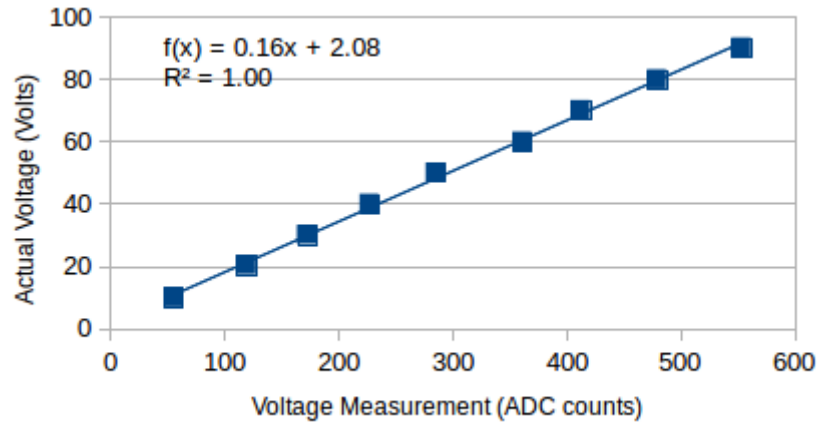


Figure 58: The DUEL node calibration curve for AC voltage measurement

For both DC and AC configurations the DUEL node proves to follow the expected linear relationship and operates in a completely predictable fashion. The linear scaling coefficients found in this process can be recorded and used later to scale the raw ADC readings of the node.

4.8.3 Validation from physical implementation

Given the linear scaling coefficients found in the previous section, the overall device is now tested for accuracy. This is carried out by subjecting the DUEL node to incrementing supply voltages and or currents and measuring the scaled response. First the node is tested for a DC configuration, and then an AC configuration. The results for both voltage and current (AC and DC) are shown in Figures 59 to 62.

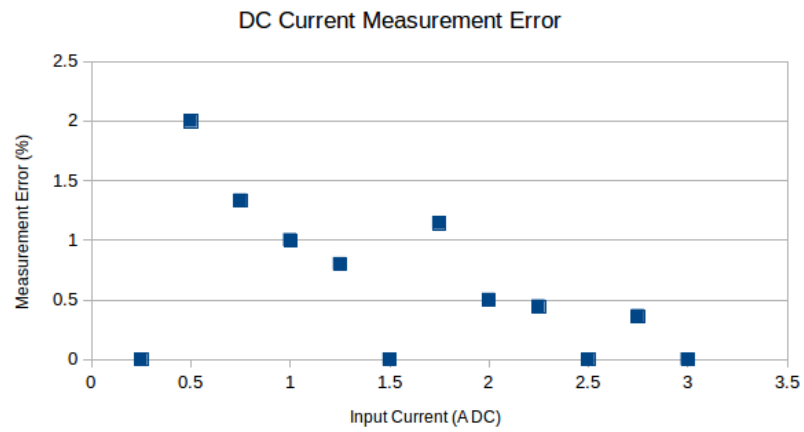


Figure 59: DC Current Measurement Error

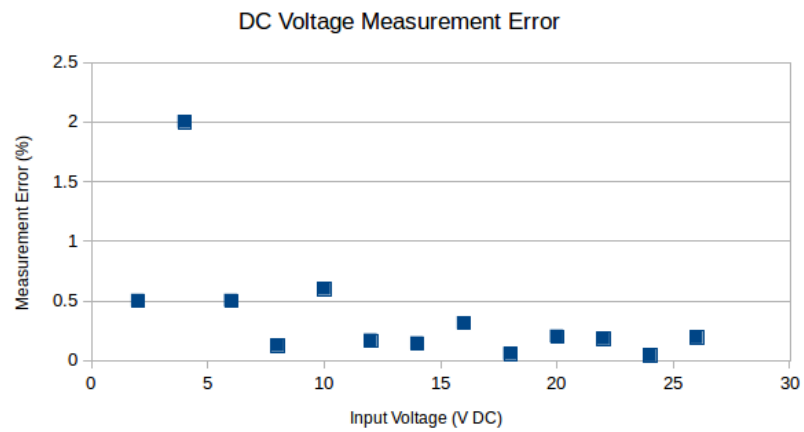


Figure 60: DC Voltage Measurement Error

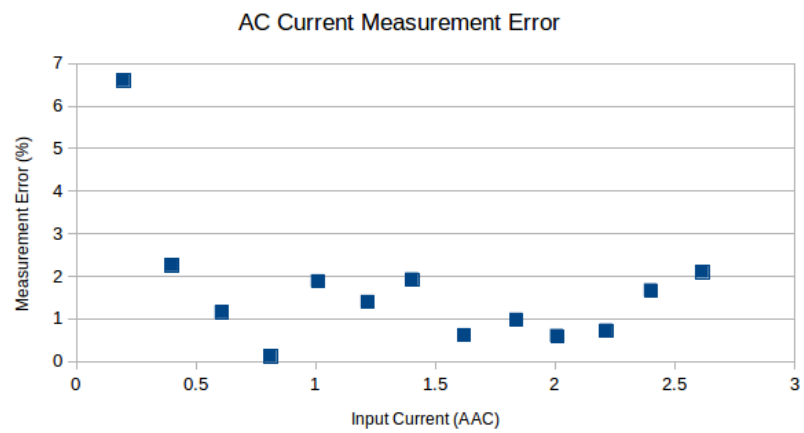


Figure 61: AC Current Measurement Error

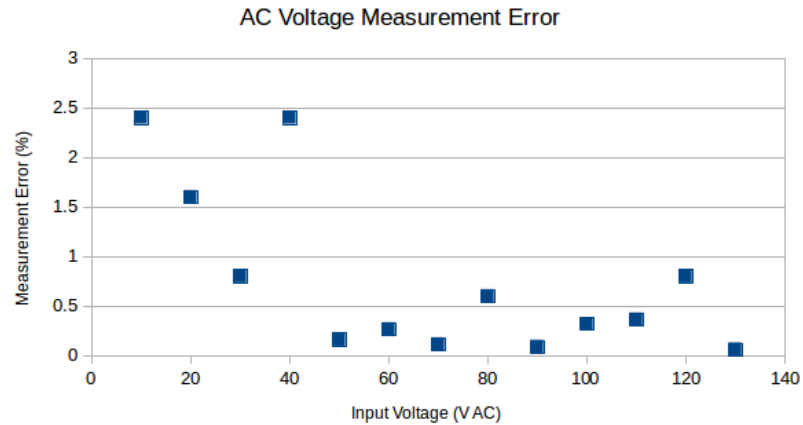


Figure 62: AC Voltage Measurement Error

Averaging the acquired errors, it is found that DC voltage measurement has a mean error of 0.4%. DC Current measurement has a mean error of 0.6%. AC voltage measurement has a mean error of 0.76%, and AC current measurement has a mean error of 1.69%.

4.9 Conclusions

The open source power monitoring system has validated as a low cost and flexible system, which can be used to measure various loads and sources. The system is capable of being fabricated using standard distributed manufacturing techniques, furthering its utility. The serial communication feature allows for an expansive configuration, which is capable of making a substantially larger number of measurements than competing tools.

4.10 References:

- [1] Weber, S. (2004). The success of open source. Cambridge, MA: Harvard University Press.
- [2] Pearce, J. (2014). Open-source lab: how to build your own hardware and reduce research costs. Amsterdam: Elsevier.
- [3] Coakley, M. and Hurt, D.E., 2016. 3D Printing in the Laboratory Maximize Time and Funds with Customized and Open-Source Labware. Journal of laboratory automation, p.2211068216649578.
- [4] Pearce, Joshua M. 2012. Building Research Equipment with Free, Open-Source Hardware. Science 337 (6100): 1303–1304. DOI: 10.1126/science.1228183

- [5] Harnett, C. (2011). Open source hardware for instrumentation and measurement. *IEEE Instrumentation & Measurement Magazine*,14(3), 34-38. doi:10.1109/mim.2011.5773535
- [6] Dhankani, K. C., & Pearce, J. M. (2017). Open source laboratory sample rotator mixer and shaker. *HardwareX*,1, 1-12. doi:10.1016/j.ohx.2016.07.001
- [7] McMunn, M. S. (2017). A time-sorting pitfall trap and temperature datalogger for the sampling of surface-active arthropods. *HardwareX*,1, 38-45. doi:10.1016/j.ohx.2017.02.001
- [8] Pocero, L., Amaxilatis, D., Mylonas, G., & Chatzigiannakis, I. (2017). Open source IoT meter devices for smart and energy-efficient school buildings. *HardwareX*,1, 54-67. doi:10.1016/j.ohx.2017.02.002
- [9] Birtchnell, T. and Hoyle, W., 2014. 3D printing for development in the global south: The 3D4D challenge. Palgrave Macmillan.
- [10] Hazeltine, B. and Bull, C., 1998. *Appropriate Technology; Tools, Choices, and Implications*. Academic Press, Inc.
- [11] Pearce, J.M., 2012. The case for open source appropriate technology. *Environment, Development and Sustainability*, 14(3), pp.425-431.
- [12] Thomson, C. C., & Jakubowski, M. (2012). Toward an Open Source Civilization: (Innovations Case Narrative: Open Source Ecology). *Innovations: Technology, Governance, Globalization*,7(3), 53-70. doi:10.1162/inov_a_00139
- [13] Jakubowski, M., 2011. Global Village Construction Set. Recuperado a partir de <https://www.kickstarter.com/projects/622508883/global-village-construction-set>.
- [14] Mota, C. (2011). The rise of personal fabrication. *Proceedings of the 8th ACM conference on Creativity and cognition - C&C '11*. doi:10.1145/2069618.2069665
- [15] Gwamuri, J., Wittbrodt, B.T., Anzalone, N.C. and Pearce, J.M., 2014. Reversing the trend of large scale and centralization in manufacturing: The case of distributed manufacturing of customizable 3-D-printable self-adjustable glasses. *Challenges in Sustainability*, 2(1), pp.30-40.
- [16] Open Building Institute. About: Who We Are. (2017). Retrieved May 05, 2017, from <http://openbuildinginstitute.org/about-who-we-are/>
- [17] Pearce, J. M. (2002). Photovoltaics — a path to sustainable futures. *Futures*,34(7), 663-674. doi:10.1016/s0016-3287(02)00008-3

- [18] Keoleian, G. A., & Lewis, G. M. (2003). Modeling the life cycle energy and environmental performance of amorphous silicon BIPV roofing in the US. *Renewable Energy*, 28(2), 271-293. doi:10.1016/s0960-1481(02)00022-8
- [19] Pearce, J., & Lau, A. (2002). Net Energy Analysis for Sustainable Energy Production From Silicon Based Solar Cells. *Solar Energy*. doi:10.1115/sed2002-1051
- [20] Prasad, D. and Snow, M., 2014. Designing with solar power: a source book for building integrated photovoltaics (BiPV). Routledge.
- [21] Mohan, N. (2012). Power electronics: a first course. Hoboken, N.J: Wiley.
- [22] Neurio. There is money being wasted in your home. Let Neurio find it. (2017). Retrieved May 05, 2017, from <http://neur.io/>
- [23] Eyedro. Home Electricity Monitors. (2017). Retrieved May 05, 2017, from <http://eyedro.com/home-electricity-monitors/>
- [24] Smappee. A gift for your home. (2017). Retrieved May 05, 2017, from <http://www.smappee.com/us/energy-monitor-home>
- [25] Energy CURB. Power Your Life. Smarter. (2017). Retrieved May 05, 2017, from <http://energycurb.com/>
- [26] Blanchard, R., & Little, M. (2016). Developing an open access monitoring device for off-grid renewables. 2016 4th International Conference on the Development in the Renewable Energy Technology (ICDRET). doi:10.1109/icdret.2016.7421511
- [27] Torres, M., Muñoz, F. J., Muñoz, J. V., & Rus, C. (2012). Online Monitoring System for Stand-Alone Photovoltaic Applications—Analysis of System Performance From Monitored Data. *Journal of Solar Energy Engineering*, 134(3), 034502. doi:10.1115/1.4005448
- [28] Forero, N., Hernández, J., & Gordillo, G. (2006). Development of a monitoring system for a PV solar plant. *Energy Conversion and Management*, 47(15-16), 2329-2336. doi:10.1016/j.enconman.2005.11.012
- [29] H., Khuwaja, A. A., & Sattar, A. (2015). Solar power remote monitoring and controlling using Arduino, LabVIEW and web browser. 2015 Power Generation System and Renewable Energy Technologies (PGSRET). doi:10.1109/pgsret.2015.7312240
- [30] Makonin, S., Popowich, F., Moon, T., & Gill, B. (2013). Inspiring energy conservation through open source power monitoring and in-home display. 2013 IEEE Power & Energy Society General Meeting. doi:10.1109/pesmg.2013.6672619

- [31] Han, J., Lee, I., & Kim, S. (2015). User-friendly monitoring system for residential PV system based on low-cost power line communication. 2015 IEEE International Conference on Consumer Electronics (ICCE). doi:10.1109/icce.2015.7066554
- [32] Riggio, R., Sengul, C., Gomez, K. M., & Rasheed, T. (2012). Energino. ACM SIGCOMM Computer Communication Review, 42(4), 273. doi:10.1145/2377677.2377727
- [33] OpenEnergyMonitor (2017). Retrieved May 05, 2017, from <https://openenergymonitor.org/>
- [34] NXP. UM10204 I2C-bus specification and user manual (2014). <https://www.nxp.com/docs/en/user-guide/UM10204.pdf>
- [35] AKM. CQ-2334 High-Speed Small Current Sensor. <https://www.akm.com/akm/en/file/datasheet/CQ-2334.pdf>
- [36] Non-Invasive Current Sensor – 30A. Retrieved May 05 2017, from <https://www.sparkfun.com/products/11005>
- [37] KiCAD EDA (2017). Retrieved May 05, 2017, from <http://kicad-pcb.org/>
- [38] Oberloier, S. and Pearce, J.M., 2017. General Design Procedure for Free and Open-Source Hardware for Scientific Equipment. Designs, 2(1), p.2. doi:[10.3390/designs2010002](https://doi.org/10.3390/designs2010002)
- [39] Project Ideas. (2017). Retrieved May 05, 2017, from <http://playground.arduino.cc/Projects/Ideas>
- [40] Z. (2017, March 18). Arduino Projects. Retrieved May 05, 2017, from <http://www.instructables.com/id/Arduino-Projects/>
- [41] CEB Press/Manufacturing Instructions/Controller Box/Arduino Control of CEB Prototype 2. (2017). Retrieved May 05, 2017, from http://opensourceecology.org/wiki/CEB_Press/Manufacturing_Instructions/Controller_Box/Arduino_Control_of_CEB_Prototype_2
- [42] Inverter. (2017). Retrieved May 05, 2017, from <http://opensourceecology.org/wiki/Inverter>
- [43] Leon-Garcia, A., & Leon-Garcia, A. (2008). Probability, statistics, and random processes for electrical engineering. Harlow: Prentice Hall.

- [44] Paul, C. R. (2004). Electromagnetics for engineers: with applications to digital systems and electromagnetic interference. Hoboken, NJ: John Wiley & Sons.
- [45] Adafruit Industries, (2017). Adafruit 1.44" Color TFT LCD Display with MicroSD Card breakout. Retrieved May 05, 2017, from <https://www.adafruit.com/product/2088>
- [46] Arduino (2017). Retrieved May 05, 2017, from <https://www.arduino.cc/en/main/software>
- [47] Peterson, L. L., & Davie, B. S. (2012). Computer networks: a systems approach. Amsterdam: Morgan Kaufmann is an imprint of Elsevier.
- [48] Atmel. Atmel 8-bit AVR Microcontroller with 2/4/8K Bytes In-System Programmable Flash (2013). docs-europe.electrocomponents.com/webdocs/15fe/0900766b815fed70.pdf
- [49] Neamen, D. A. (2010). Microelectronics circuit analysis and design. New York: McGraw-Hill Education.
- [50] Programming ATtiny85 with Arduino Uno. (2017). Retrieved May 05, 2017, from <https://create.arduino.cc/projecthub/arjun/programming-attiny85-with-arduino-uno-afb829>
- [51] <https://osf.io/8keau/> 7.23.2018
- [52] Oberloier, S. Belt Driven Open Source circuit Mill Using Low Cost 3-D Printer Components (to be published).
- [53] Anzalone, G. C., Wijnen, B., & Pearce, J. M. (2015). Multi-material additive and subtractive prosumer digital fabrication with a free and open-source convertible delta RepRap 3-D printer. Rapid Prototyping Journal, 21(5), 506-519. doi:10.1108/rpj-09-2014-0113
- [54] "Manufacturing Hardware." Manufacturing Hardware Open Circuit Institute. Retrieved April 04, 2018. <http://opencircuitinstitute.org/content/manufacturing-hardware>
- [55] PCB Prototyping (2017). Retrieved May 05, 2017, from <http://flatcam.org/>
- [56] "OCI Copper Carve." OCI Copper Carve Open Circuit Institute. Retrieved April 04, 2018. <http://opencircuitinstitute.org/content/oci-copper-carve>.
- [57] Jahn, S. Quite Universal Circuit Simulator (QUCS) (2017). Retrieved May 05, 2017, from <http://qucs.sourceforge.net/>

5 Conclusions and Future Work

5.1 Overview

The work in this thesis has detailed the process of designing and implementing processes for designing open source electronics using distributed manufacturing methods. The prescribed open source hardware design methodology in Chapter 2 has acted as a powerful charter to ensure the success of designs. The circuit mill detailed in Chapter 3 can be implemented to make a multitude of mid-level-complexity circuit boards, which enable rapid prototyping of designs, and ease of design sharing. The power meter designed in Chapter 4 is a strong case to show the capability of the circuit mill.

5.2 Future Work

5.2.1 General Design Procedure for Free and Open Source Hardware for Scientific Equipment

- This method is well defined – future work includes further utilizing the prescribed procedure to gauge its effectiveness.

5.2.2 Belt Driven Open Source Circuit Mill Using Low Cost 3-D Printer Components

- Boards with increased complexity may require 2 layers. This can be accomplished with the mill by creating a precision fixture for the board material.
- Further increase visuals on Copper Carve which indicate the tool-path, and display a height map from probing data
- Create a detailed language-agnostic set of instructions for assembling the mill so that it can be widely shared and utilized.
- Using the mill, fabricate circuitry for open source welding supplies for metal 3-D printing

5.2.3 Open Source Low-Cost Power Monitoring System

- Implement the design in a field deployment to verify system longevity.
- Adapt the system to be utilized for measurements in other applications including in metal 3-D printing processes

5.3 Conclusions

5.3.1 General Design Procedure for Free and Open Source Hardware for Scientific Equipment

- A well-defined ten step process for designing open source hardware was provided.
- The process provides for highly customizable designs that are competitive to market alternatives for scientific hardware.
- A case study implementing the given methods was used, which yields a low cost and parametric slide drying rack.

5.3.2 Belt Driven Open Source Circuit Mill Using Low Cost 3-D Printer Components

- A low-cost circuit board mill, made using reconfigurable 3-D-printable parts and belt drive systems was designed, manufactured and tested.
- The system is capable of milling with 0.1mm resolution, which can manufacture most typically occurring feature geometries.

5.3.3 Open Source Low-Cost Power Monitoring System

- A highly scalable power monitoring system capable of measuring voltages and currents on varying ranges was designed, manufactured and validated.
- I2C communication allows for up to 127 Nodes.
- The system is capable of measuring both AC and DC voltages and currents with an accuracy of 1.6%
- The cost is \$17.85 per DUEL measurement node.
- Designs are easily sharable and manufacturable using distributed manufacturing techniques.